9.5

Rijkswaterstaat
Road and Hydraulic Engineering Division

Overtopping on vertical structures
part of research T.A.W.

by A. Popescu

Supervisor:
Ir. W. Leeuwestein

August 1997

1089

Rijkswaterstaat
Road and Hydraulic Engineering Division

Overtopping on vertical structures
part of research T.A.W.

Supervisor:
Ir. W. Leeuwestein
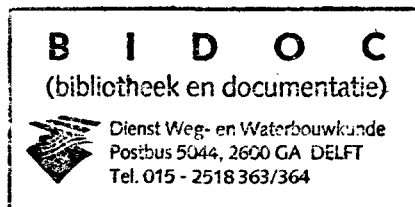
Research fellow:
Ir.A. Popescu

August,1997

Table of contents

List of figures

List of tables

List of symbols and achronims

B	berm width	(m)
D	diameter of the rockfill relative to SWL	(m)
d_h	berm depth relative to SWL	(m)
f_b	width of a roughness element (perpendicular to dike axis)	(m)
f_h	height of a roughness element	(m)
f_L	centre-to-centre distance between roughness elements	(m)
f_l	length of a roughness element (parallel with dike axis)	(m)
g	acceleration due to gravity	(m/s^2)
H	wave height	(m)
H_{m0}	significant wave height based on the spectrum $4\sqrt{m_0}$	(m)
H_s	significant wave height, average of the highest 1/3 part	(m)
h	water depth	(m)
h_d	final crest height	(m)
R_c	crest height relative to SWL	(m)
h_m	water depth at the position of the toe of the structure	(m)
L_{op}	wave length at deep water based on T_p ($L_{op} = (g/2\pi) * T_p^2$)	(m)
m_0	area of energy-density spectrum	(m^2)
$m_0(1)$	m_0 for the first peak in a double-peaked spectrum	(m^2)
$m_0(2)$	m_0 for the second peak in a double-peaked spectrum	(m^2)
N_w	number of incoming waves	(-)
N_{ow}	number of overtopping waves	(-)
P_V	$= P(\underline{V} \leq V)$ probability of the overtopping volume $\underline{V}$ being smaller or greater than V	(-)
P_{ow}	probability of overtopping per wave	
Q_b	dimensionless overtopping discharge with breaking waves $\xi_{op} < 2$	(-)
Q_n	dimensionless overtopping discharge with non-breaking waves $\xi_{op} > 2$	(-)
q	average overtopping discharge per unit crest length	$(m^3/s$ per m)
R	wave runup, measured vertically with respect to the still water line	(m)
$R_{u2\%}$	height of wave runup exceeded by 2% of the incoming waves	(m)
R_b	dimensionless crest height with breaking waves $\xi_{op} < 2$	(-)
R_n	dimensionless crest height with non-breaking waves $\xi_{op} > 2$	(-)
r_B	reduction factor for the berm width	(-)
r_{dh}	reduction factor for the berm location	(-)
s_{op}	wave steepness with L_0 based on T_p ($s_{op} = H_s/L_{op}$)	(-)
T	wave period	(s)
T_m	mean period	(s)
T_p	peak period	(s)
T_{peq}	equivalent peak period with double-peaked spectra	(s)
T_s	significant period, average of the highest 1/3 part	(s)
V	volume of overtopping wave per unit crest width	$(m^3$ per m)

List of symbols (continued)

α	slope gradient	(°)
α_{eq}	equivalent slope gradient for a slope with a berm	(°)
β	angle of wave attack	(°)
γ_b	reduction factor for a berm	(-)
γ_f	reduction factor for the roughness	(-)
γ_h	reduction factor for a shallow foreland	(-)
γ_β	reduction factor for the angle of wave attack	(-)
ξ_{op}	surf similarity parameter based on T_p ($\xi_{op} = \tan\alpha/\sqrt{s_{op}}$)	(-)
ξ_{eq}	equivalent surf similarity parameter ($\xi_{eq} = \gamma_b \, \xi_{op}$)	(-)

1. Introduction

1.1 General

Increasing population pressures in developing countries and the desire for water front living in developed countries are causing development to take place near the high water mark in the coastal zone. Such development is not limited to the coastal zone but extends to the foreshore areas of lagoons and lake systems. This has resulted in development which is increasingly vulnerable to wave inundation. The approval of foreshore developments within councils requires information on water levels and wave inundation through the waterway to assist in the assessment of development proposals.

The problem of wave overtopping by oscillatory waves has been studied by various researchers since 1960's. The initial investigations were basically based on laboratory experiments. In recent years, following advances on mathematical treatment on wave propagation some researchers concentrated on numerical modelling of wave deformation on the dike slope and the subsegment overtopping (i.e. Kobayashi and Wurjanto 1989).

The primary function of sea defences in general, and sea dikes and dikes in particular is the flood prevention of the (low) interland. Under storm conditions, these structures should withstand the combined action of storm surges, waves and strong winds. On the other hand they should fulfill the assigned functional requirements, i.e. protection of hinterland from adverse effects of high water and waves. For dikes, since the hight water protection is required, the structure's height H_s in relation to the design storm surge level or to the maximum level of wave run-up during design storms is one of the *most important structural parameters to be determined*. This directly depends on the character of hinterland to be protected. In general, some amount of wave overtopping q may be allowed under design conditions.
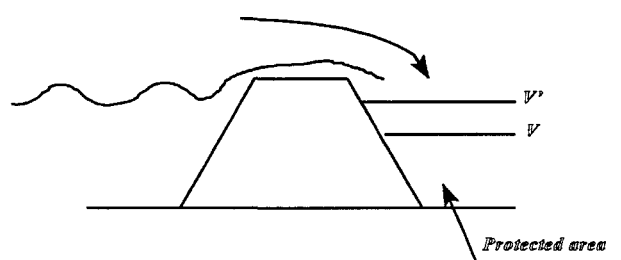
For analysis, the wave overtopping criterion is used. That is during the design storms, the discharge over the structure's crest should be less that some specified quantity, q liters/second per running meter of a structure. The allowable value of q primarily depends on the quality of the inner slope.

Figure 1.1. Definition of problem

The above mention criterion can be stated in terms of formula as:

$$Pr(\overline{q} > q_{cr}) \leq pv$$
$$Pr(\overline{V_q} > V_{cr}) \leq pv$$

(1.1)

in which:

Pr(x)   - probability of the occurance of event x;

pv   - prescribed value of the probability which should not be exceeded;

q, q_{cr} - values of the normal and critical overtopped discharge on the structure;

V, V_{cr} - values of the normal and critical volume of the water which is allow in hinterland.
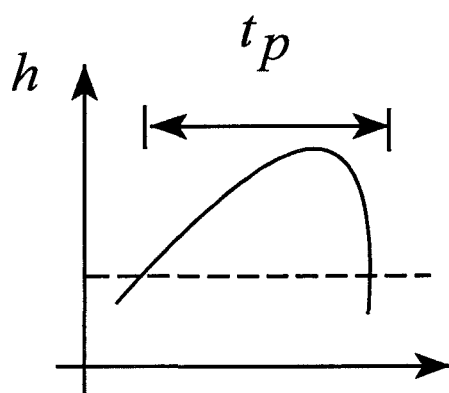
Figure 1.2. Flow hydrograph

Overtopped discharge and the volume of the water inside the protection area are functions of the crest of the structure, peak of the flow hydrograph and time of the hydrograph:

$$q = f_1(h, H_s, t_p) \quad and \quad V_q = f_2(h, H_s, t_p) \quad (1.2)$$

1.2   Objective of the study

The main objective of the study is to add to the understanding of overtopping over structures computation. This is an important part of a design of sea structures and dikes.

With this main objective in view specific tasks developed in the study are:

-       to make a review Of the existing formula in the literature, formula for computing discharges due to overtopping;

-       assessment of duration and time development of water levels with purpose of introducing them in computer program;

-       writing computer code based on formula which are design and set-up of the existing design graphs;

1.3   Outline of the thesis

The summary presentation of the study is done in this section. Thesis has seven chapters in which the statement of the problem and the available formulas are presented.

Formulas found in literature are presented in two chapters (i.e. chapter 3 and chapter 4). The reason for this was to group the formulas based on both mathematical and experimental approach in one chapter and that ones based mainly on experimental study were grouped together in chapter 4. The importance of them is not to be neglected because of this experimental part which adds a lot to the understanding of the complex phenomena of wave overtopping for a given structure in a certain environment.

The contents of the report is as follows:

❑ Chapter 1.   Introduction - in which the reason and objective of the thesis is presented.

❑ Chapter 2.   Statement of the problem - is identifying the major parameters used for determining the overtopping rates over structures in general and over vertical structure in particular. A review of geometries of existing types of structures is also presented together with the references to the authors which researched them.

❑ Chapter 3.   Analysis of different overtopping formula - is presenting 11 most important used formula for computing overtopping. The reference method for computing the formula remains Goda's graphs. Formulas are presented in order of time publication of them.

❑ Chapter 4.   Experiments and test in literature - is presenting the most significant 7 experiments which can be found in the literature.

❑ Chapter 5.   Comparison of the formula - is comparing the difference in values of overtopping obtained for a given set of data. The reference point for this comparatione are Goda's graphs. Also in the frame of this chapter expression for run-up needed for each overtopping formula is presented. Analysis of various formula is only supportive and ment to take a selection of most promising and reliable overtopping models to be connected to the final probabilistic approach for safety of dikes and vertical structures and of polders, design described in chapter 6.

❑ Chapter 6.   Procedure for design of flood defense - the basic principles of risk and safety acceptance are presented together with probabilistic determination of the crest height of a structure. Inundation level and speed flooding are commented. However in a given design situation a clear cost analysis is required, analysis which is only mention as a principle in this chapter.

❑ Chapter 7.   Computer programs - As a final outcome of this study a Pascal computer programme and spreadsheet were built. The use of them are presented in this chapter.

The choice of three most promising different formulas of overtopping is available via the programme. The researcher using these computer tools has to decide which formula he should use for preliminary design and for final design as well.

2. Statement of the problem

2.1. Introduction

Wave overtopping is one of the most important hydraulic responses of a breakwater and the definition of tolerable limits for the overtopping discharge is still an open question, given the high stochasticity of the phenomenon and the difficulty in measuring it and recording its consequences.

Usually, in order to estimate the wave overtopping rate, the Goda`s diagrams (Goda 1987) are used. This diagrams illustrates the relationship between a mean overtopping and a crown height. It has been pointed out that short term overtopping rate is important for the design of drainage facilities behind the seawall (Kimura and Seyama, 1984). More over it is suggested that the short term overtopping rate become several ten times of mean wave overtopping rate and large amount of water comes into the drainage facilities (Inoue et al, 1989)

It can be pointed out that overtopping discharges are estimated from empirical equations that were developed from physical model studies on scale models (Weggel 1976, Ahrens and Martin 1985, Ahrens And Heimbaugh 1988, Saville 1955, Jensen and Sorensen 1979, Jensen and Juhl 1987, Aminti & Franco 1988, Bradbury and Allsop 1988, De Waal and Van der Meer 1992, Van der Meer and Stam 1991, Schulz and Fuhrboter 1992, Ward 1992, Yamamoto and Horikawa 1992) while only few data from full scale observation (Goda 1985, De Gerloni 1991) are available.

Numerical models have been developed by Kobayashi and Wurjanto 1989, 1991, Kobayashi and Poff 1994, Peregrine 1995, models which needs to be calibrated with physical model test results. Empirical formulas are limited to the structural geometry and wave conditions examined in the model tests and are not versatile enough to deal with various combinations of different coastal structures and incident wave characteristics. As a results it is desirable to develop numerical models (to fill the gap between empirical formulas and site specific hydraulic model tests).

Numerical models have been developed by Kobayashy and Wurjanto 1989, 1991, Kobayashi and Poff 1994, Peregrine 1995, models which needs to be calibrated with physical model test results.

2.2. Basic formula

Wave overtopping can be described by the following formula:

$$Q = a \ \exp\left(b\frac{R}{\gamma} \right) \qquad\qquad (2.1)$$

in which:

Q	- dimensionless discharge	[-]
a, b	- coefficients	[-]
R	- dimensionless freeboard	
γ	- reductio coefficient for different influence as berms, roughness, depth limitation, wave attack, etc.	[-]

The above a and b coefficients are used in two different approaches depending on the author. The approaches are as follows:

1)   values of coefficients a and b are computed as an *average values* from carried out experiments';

2)   values of coefficients a and b are computed as an *average standard deviation* from carried out experiments.

From design point of view the second approach is situated more in the safety part so this is the reason why it is more preferred by the designers.

2.3. Relevant parameters

2.3.1. Basic parameters

The scheme below presents the relation between the basic parameters and the parameter of interest: the wave overtopping.
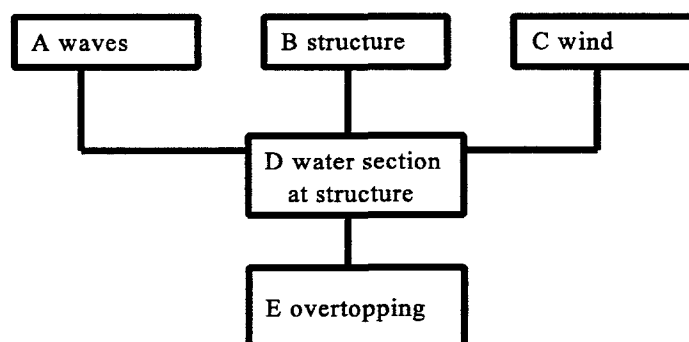
The parameters A, B and C are regarded to be independent. The five parameters may be subdivided as follows:

A   Waves (incident, undisturbed)
          A_1 significant wave height
          A_2 peak period
          A_3 (mean) angle of wave attack
          A_4 directional spreading
          A_5 spectrum shape
          A_6 wave height probability of exceedance curve

B   Structure
          B_1 shape below SWL
                B_{11} water depth at toe
                B_{12} structure shape between toe and SWL
                B_{13} slope of foreshore
          B_2 shape above SWL
                B_{21} crest height
                B_{22} structure shape between SWL and crest
          B_3 roughness
          B_4 permeability

C Wind
          C_1 wind speed according to standard definition
          C_2 spray density profile
          C_3 time average velocity field
          C_4 time variation in velocity field

D Water motion at structure
          D_1 time average velocity field and average density in vertical plane

E Overtopping
          E_1 time average discharge
          E_2 volume per wave
          E_3 distribution of water volume over the height above the crest and distance from the crest

A) The water is characterized by the mass density ρ_w, the dynamic viscosity μ and the surface tension σ. The compressibility is not taken into consideration.

A first approximation to a description of irregular waves is obtain by assuming that the wave phenomenon is linear, in which case the wave patten may be interpret as the sum of a large

number of waves each with a given frequency, propagation direction and energy, behaving independently of each other. This approximation may only be used if the steepness is sufficiently low. The otherwise arbitrary wave pattern is then statistically determined if the energy per unit of area is known as a function of the propagation direction and frequency. This function is known as the two dimensional energy density spectrum. This spectrum is difficult to measure because it is necessary not only to know the wave pattern at a fixed point but also the correlation between the latter and the wave pattern in the environment.

If we confine ourselves to the wave pattern at a fixed point, the direction in space ceases to be independent variable; the wave pattern is considered solely as a function of time. All energies which are associated with components of a given frequency but of different directions are added together. The total is considered solely as a function of frequency and the two dimensional energy density spectrum reduces to a one dimensional energy density spectrum, known simply as the energy spectrum.

The energy spectrum for an arbitrary irregular wave pattern of sufficiently low steepness therefore indicates the quantity of energy which must be attributed to respective component waves for the statistical characteristics of the sum of the components to be identical to those of the wave pattern, as a function of time. To describe a wave pattern of this kind statistically. It is therefore sufficient to know the energy spectrum. In practice this may give difficulties because the spectrum cannot be determined precisely in a finite measuring time but only estimated. In such cases it is useful to measure in addition a number of other characteristic parameters of the wave level, wave height and periods and the correlation between height and period.

Waves which are relevant for design purposes are generally so steep that a linear theory is not adequate to describe then. The energy spectrum can then be determined but the component waves are not completely independent because they are partly coupled by non-linear influences.

Both the energy spectrum and the distributions of wave height, period etc. are completely determined by a length scale and their shape. In general, a characteristic wave height H_k may be chosen for the length scale and a characteristic period T_k for the time scale.

The above considerations indicate how the wave movement at a particular point may be described as a function of time. The wave length can be approximately determined from this, provided that g, the gravitational acceleration, and d, the depth, are known.

B) It is assumed that the slope is completely rigid and stationary. For the consideration of wave run-up (and also overtopping) this assumption seems reasonable so that the dynamic characteristics of the slope are not taken into account. The slope is then determined entirely by its geometry. It is also assumed that this geometry and that of the foreshore are entirely determined by the form and a characteristic length λ of the cross-section.

C) The wind is partly characterized by ρ_a, the air density, $\overline{w}_{10}$, the time-average velocity at 10 m above the water level, $\overline{\beta}$, and $\overline{\varphi}_w$, the average wind direction. If necessary a number of parameters may be added giving a more detailed description of the variation of the mean wind speed as a function of height and the instantaneous wind speed as a function of time. The dependent variable is the run-up height z, the maximum height above the water level reached by a wave tongue running up against the slope. The run-up height is a stochastic variable. If n is the exceedance frequency, then $z_{(n)}$ is the dependent variable for a given or chosen n value, $\overline{\beta}$, an average direction of incidence in relation to the dike, $\overline{\rho}_a$, mass density of air, $\overline{\rho}_w$, mass density of water, σ, surface tension at air-water interface, and d, water depth, the above may be summarized as follows:

$$z = f(\rho_w, \ \mu, \ \sigma, \ H_k, \ T_k, \ g, \ d, \ \overline{\beta}, \ \rho_a, \ \overline{w}_{10}, \ \overline{\varphi}_w, \ formfactors, \ n, \ \lambda) \tag{2.2}$$

or

$$\frac{z}{H_k} = f\left(\frac{H_k}{d}, \ \frac{H_k}{gT_k^2}, \ Re_k, \ We_k, \frac{\rho_a}{\rho_w}, \ \frac{\overline{w}^2_{10}}{gH_k}, \ \overline{\beta}, \ \overline{\varphi}_w, \ form \ factor, \ n, \ \frac{H_k}{\lambda} \right) \tag{2.3}$$

where:

Re_k = Reynolds number   [-]
We_k = Weber number   [-]

2.3.2. Discussion on different parameters find in literature

2.3.2.1. Run -up and dimensionless overtopping

Run up is a major parameter need to compute overtopping rate and the formula of computing it differs from author to another depending on the range of geometric and hydraulic condition considered for experiments.

Dimensionless overtopping is the main parameter defining overtopping computation. Two different approaches can be found in the literature:

$$Q^* = \frac{q}{\sqrt{2gH_s^3}} \qquad - \ Goda \tag{2.3}$$

$$Q = \frac{q}{\sqrt{gH_s^3}} \qquad - \ van \ der \ Meer \ and \ others \tag{2.4}$$

Formulas on overtopping and related parameter are given in detail in chapter 5 for different authors.

2.3.2.2. Admissible overtopping rates

The definition of tolerable limits for overtopping is still an open question, given the high irregularity of the phenomenon and the difficulty of measuring it and its consequences. Many factors, not only technical ones, should be taken into account to define the safety of the increasing number of breakwater users such as psychology, age and clothing of a person surprised by an overtopping wave.

Still the current admissible rates (expressed in m^3/sec per m length) are those proposed by the Japanese guidelines, based on impressions of experts observing prototype overtopping (Fukuda et al, 1974; Goda, 1985).
They are included in CIRIA/CUR - manual (1991), and in British Standards (1991). The lower limit of inconvenience to pedestrians may correspond to safe working conditions on the breakwater, while the upper limits of danger to personnel may correspond to safe ship stay at berth.

2.3.2.3. Spray transport

Due to strong winds the phenomena of spray transport occur. This is a volume of water which should be added to the overtopping values. Few experimental formulas for computing quantity of spray transport are available (N. Matsunga et al, 1994). Further studies should be done.

2.3.2.4. Personnel danger on a promenade

Public access to breakwater areas is usually prohibited due to safety reasons, yet many people nevertheless enter these areas to enjoy the comfortable sea environment. On the other hand because breakwater are typically the low - crown type, wave overtopping sometimes occurs, and therefore, it is essential for the design of a breakwater to consider maintaining safety.

Various studies were done for this. The main research was done in Japan and main formulas can be found in "Numerically modeling personnel danger on a promenade breakwater due to overtopping waves" (Kimihiko Endoh and Siego Takahashi 1994). The basic concluding remarks are:
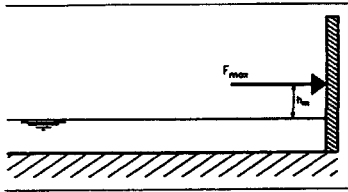
1)   Based on prototype experiments, was developed a loss of balance model to calculate the critical water depth at a breakwater's seaward edge. If a person is 152 cm tall and has a standard body physique, the critical water depth is 0.5 m which causes a person to their balance.
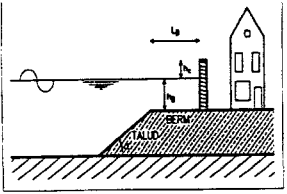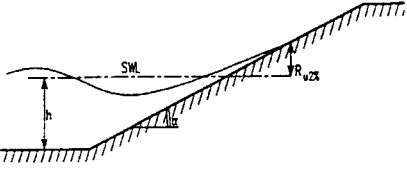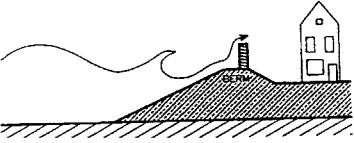
2)   The proposed carry model can calculate the critical water depth at the breakwater's seaward edge which will carry a person into the sea. This depth is dependent on the opening ratios of handrails installed at the breakwater's seaward and landward edge. If fence-type handrails having a 0.7 opening ratio are installed at the both edges, the critical water depth is 2.1 m for a 152 cm tall person.

3)   When no handrails are present, the calculated critical water depth which carries a person into the sea is only 0.7 m for a 152 cm tall person, thus handrails are demonstrated to be a very effective measure for preventing a person from being carried into the sea by overtopping waves.

4)   The proposed breakwater formula for evaluating the wave height at which personnel dangers will occur during successive stages of wave overtopping should be employed in the design of promenade breakwaters.

2.4. Types of structures

The most varied parameter in studying of overtopping is the structure geometry.

Therefore, an initial distinction is made between certain "basic" types of structures. The two most basic types are a vertical wall and a plane slope. Many variants of these two types of structures commonly occur. In the table below, common types of structures are identified and references pertaining to each type are given. A few references vary also the loading conditions: accounting for oblique wave attack and/or the influence of wind. These are also noted in the table below.

Table 2.1. Types of structures

Structure	References	Comments
1.Vertical wall	Goda et.al. (1975)	Foreshore slopes 1:10,1 :30; parapet wall present, with nose
	Ahrens et.al. (1986)	Vertical wall with crest nose and 1:100 foreshore.
	Juhl (1992)	3 different caisson structures tested.
	Report Taw-A1	Max. possible contribution by wind measured by mechanical transport device.

Structure	References	Comments
2. Vertical wall fronted by a berm	Goda et.al. (1975)	Foreshore slopes 1: 10,1:30; parapet wall present; berm width varied.
	Ahrens et.al. (1986)	3 berm/wall configurations tested
3. Plane slope (impermeable)	Goda & Kishira (1976)	Smooth, stepped slope. 1:10 & 1:30 foreshores.
	v.d. Meer (1987) TAW	Afsluitdijk section. Measured average overtopping, volume per wave, % overtopping waves, thickness & speed of overtopping water.
	Jensen and Juhl (1989)	Long and short crested wave attack; oblique wave attack Influence of wind
4. Plane slope (permeable)	Jensen and Juhl (1989)	Influence of wind
5. Slope with a berm	Szmytkiewicz	(*) data not yet available
6. Slope fronted by offshore reef	Goda and Kishira (1976)	1:30 foreshore slope
	Takayama et.al. (1982)	Same structure as Goda and Kishira (1976). Additional tests for low crests.

3.   Analysis of different overtopping formula

3.1.   Nagai and Takada's formulas (1972)

The figure shows a plot with $\frac{H_0}{L_0}$ on the vertical axis (from 10^{-3} to 1) and $\mathrm{Cot}\,\theta$ on the horizontal axis (from 0 to 6), with curves labeled BREAKING WAVES and SURGING WAVES, and annotations:

$$h_1/L_1 = 0.097\sim0.171$$
$$h_1/H'_0 = 2.66\sim4.05$$
$$H_0/H'_0 = 0.526\sim1.27$$
$$\tan\alpha = 0.0$$

$$\frac{H_0}{L_0} = \sqrt{\frac{2\theta}{\pi}\ \frac{\sin^2\theta}{\pi}}$$
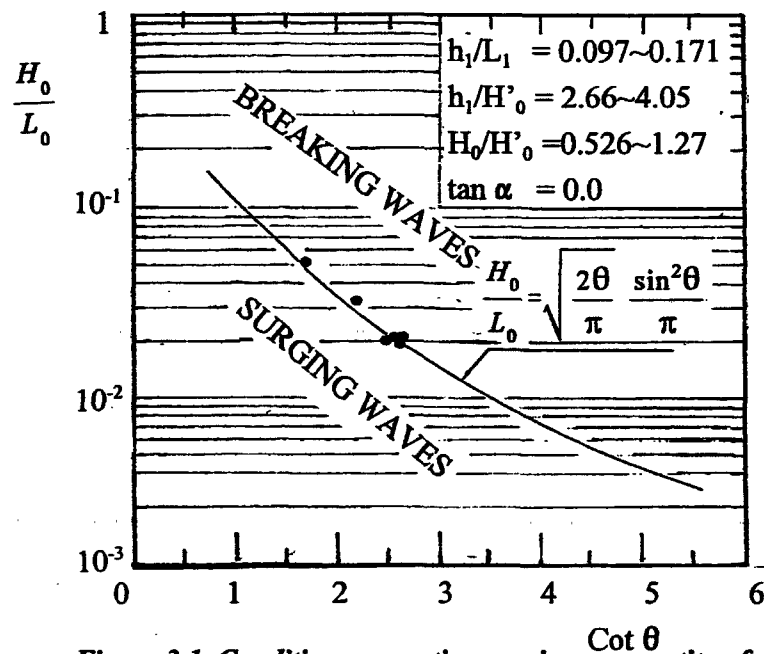
Figure 3.1. Condition generating maximum quantity of wave overtopping

Shoshiro Nagai and Akira Takada deduced formulas for the maximum quantity of overtopping The relationships between the slope angle of the sea-wall and the deep-water-wave steepness were studied by experiments. Figure 3.1 shows the results which they obtained. According to figure 3.1, the maximum overtopping of waves occurs at the critical region between surging waves and breaking waves.

There are two methods to relate the height of wave run-up to the quantity of overtopping. One is the method which uses the profile of wave run-up (Takada, 1970), and the other uses the surface elevation of wave run-up on the front of the sea-wall (Shigai, 1970; Takada, 1972).

The study of the authors is concerned with the former ones, but whichever method is used, it is thought to be of practical importance to find out a response function against the incident waves. The formulas are specific for each geometry of a structure. These formulas are presented bellow.

3.1.1. For the Vertical Wall
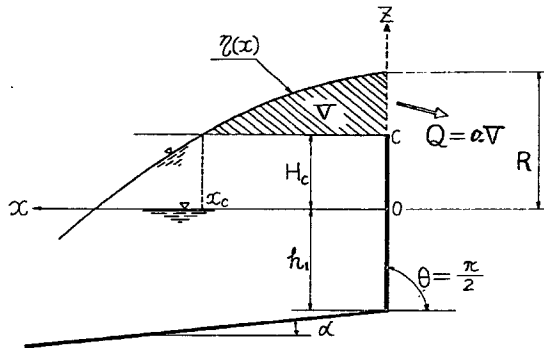
Figure 3.2. Relation between wave run-up and wave overtopping over a vertical wall

It was assumed that the quantity of overtopping for a constant wave period, Q is proportional to the water volume of the run-up wave above the crown height of the sea-wall, (from fig.3.2),

$$Q = aBv \tag{3.1}$$

in which:

a   = the coefficient for quantity of overtopping;   [-]

B   = the width of overtopping, perpendicular on plane xOz.   [m]

If the wave profile obtained from the second-order approximation is used of finite amplitude standing wave theory without overtopping, the water quantity of overtopping can be calculated as:

$$Q = a_{II} B \int_{0}^{x_c} \{ n_{II}(x) - H_c \} dx =$$

$$a_{II} B [(H_1/k_1) \sin k_1 x_c + (H_1^2/16)(3 \coth^3 k_1 h_1 + \tanh k_1 h_1) \sin 2k_1 x_c - H_c x_c] \tag{3.2}$$

in which:

H_c = crown height of a sea-wall from the still water level   [m]

H_1 = wave height at the toe of the sea wall   [m]

H_0' = wave height in deep water   [m]

θ = angle of inclination of sea wall to the horizontal plane   [rad]

$n_{II}(x)$ = profile of wave run-up of the second order solution of
finite amplitude standing wave theory   [m]

$x_c(<L_{1/4})$ = can be obtained by $n_{II}(x) = H_c$ [m]

$L_{1/4}$ = one quarter of the length of the wave   [m]

$$\cos k_1 x_c = \frac{1}{4d} \left(\sqrt{H_1^2 + 8d(d + H_c)} - H_1 \right) \tag{3.3}$$

in which:

$$d = \frac{1}{8} k_1 H_1^2 (3 \coth^3 k_1 h_1 + \tanh h k_1 h_1) \tag{3.4}$$

➡ *when $h_1 \geq (h_b)_s$:*

    $(h_b)_s$ = water depth of breaking of standing waves   [m]

    a_{II} = given by the following equation, which was obtained by the experiments:

$$a_{II}=9.3\frac{H'_0}{L_0}\left(\frac{R_{II}-H_c}{H_1}\right)^{1/2} \tag{3.5}$$

in which, R_{II} shows the height of wave run-up of the second-order approximation of finite amplitude standing wave theory.

The quantities of overtopping obtained by the experiments were compared with the calculated ones, as shown in figure 3.3.
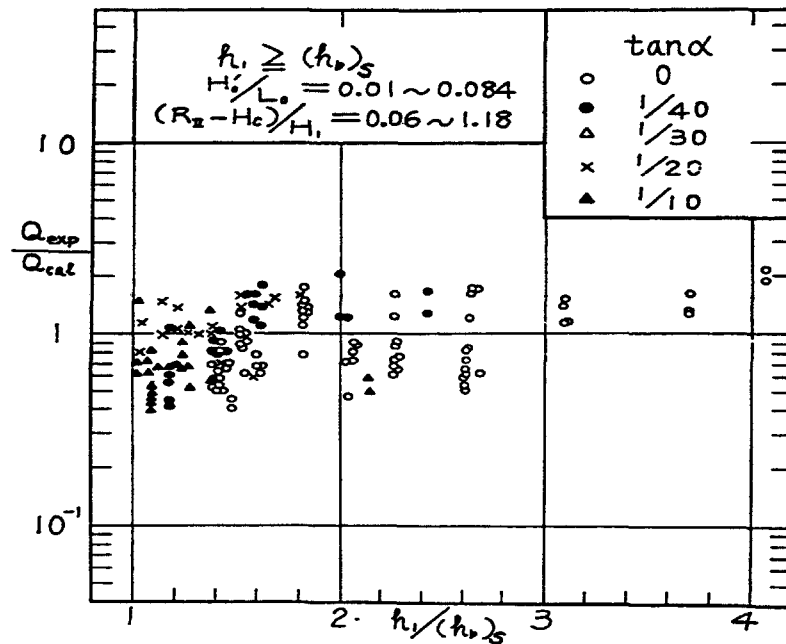
Figure 3.3. Calculated and measured values for wave overtopping

Figure 3.3 shows that eq.(3.2) may be adapted to be in a fairly good agreemental values. The mean value of Q_{exp}/Q_{cal}, $\overline{(Q_{exp}/Q_{cal})}$ and the standard deviation, σ, are given by:

$$\overline{(Q_{exp}/Q_{cal})}=0.98 \tag{3.6}$$

and:

$$\sigma=\sqrt{\frac{1}{N}\sum_{i=1}^{N}\left\{\frac{Q_{exp}}{Q_{cal}}-\left(\overline{\frac{Q_{exp}}{Q_{cal}}}\right)^2\right\}}=0.28 \tag{3.7}$$

➡**when $h_1 = (h_b)_p \sim (h_b)_s$** and tan$\alpha$ =1/10, in which $(h_b)_p$ denotes the water depth of breaking of progressive wave and tanα is the slope, a_{II} is given by:

$$a_{II}=5.5\left[\frac{h_1}{(h_b)_s}\right]^{2/3}\left(\frac{H_0'}{L_0}\right)\left(\frac{R_{II}-H_c}{H_1}\right)^{1/2} \tag{3.8}$$

Values of $\overline{(Q_{exp}/Q_{cal})}$ and σ for eq. (3.8) are given by:

$$\overline{(Q_{exp}/Q_{cal})}=1.1 \tag{3.9}$$

and

$$\sigma=0.40 \tag{3.10}$$

Further investigations are needed to get higher accuracy.

3.1.2. For the Sloping Wall

If the wave profile running up on the slope of the sea-wall in the case of non-overtopping of waves can be approximated by a trapezoid, as shown in figure 3.4.
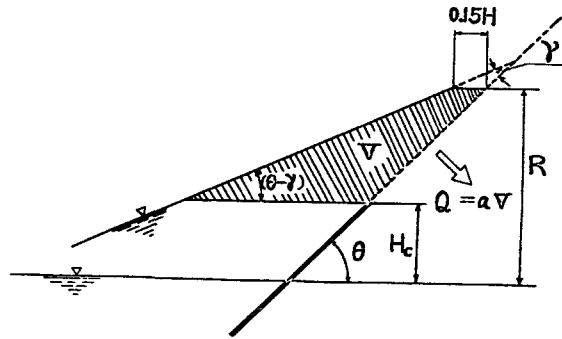
Figure 3.4. Relation between wave run-up and wave overtopping for sloping wall

The quantity of overtopping is obtained by the following equation:

$$Q=a_\theta BV=(a_\theta)_{II}B\left[\frac{(1+\cot^2\theta)(R_{II}-H_c)^2}{2(\cot\gamma-\cot\theta)}+0.15H_1(R_{II}-H_C)\right] \tag{3.11}$$

in which:

$\quad (a_\theta)_0 \quad =$ denotes the coefficient for quantity of overtopping $\qquad [-]$

γ = is an angle at the edge of the profile of run-up wave [rad]

$\cot\gamma$ = is given by the following equations, obtained by the experiments,

when: $\cot\theta \geq 1$,
$$\cot\gamma = 67 \ (H_1/L_1)(\cot\theta)^{1.6}$$

when: $\cot\theta = 0\sim1$,

$$\cot\gamma = \left[n + \frac{n(n-1)}{2}\cot^2\theta\right]^{1/2}\cot\theta \tag{3.12}$$

in which:

$$n = -3.224\log_{10}\left\{\frac{1}{1+(67H_1/L_1)^2}\right\} \tag{3.13}$$

Figure 3.5 shows that the comparison between the experimental and calculated values may be stated to be in a fairly good agreement.
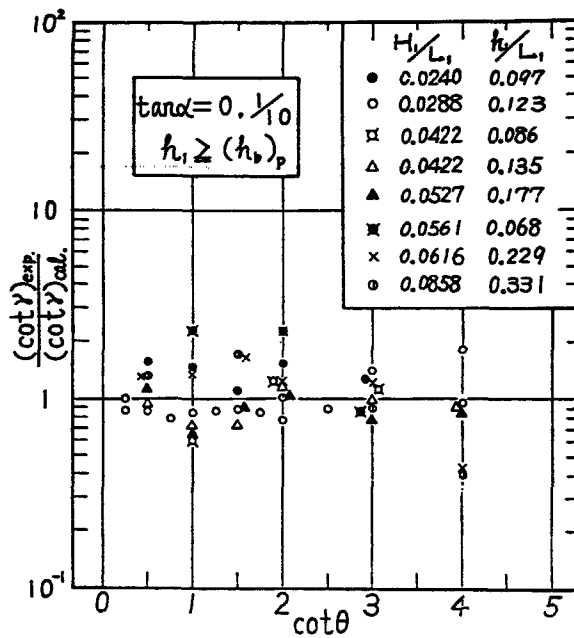
Figure 3.5. Comparison between experimental and analytical approaches

When $h_1 \geq (h_b)_s$, $(a_\theta)_{II}$ is given by the following equation obtained by the experiments:

$$(a_\theta)_{II} = 7.6(\cot\theta)^{0.37}(H_0'/L_0)^{0.83} \tag{3.14}$$

Figure 3.6 shows that the comparison between the experimental and calculated values may be stated to be in a fairly good agreement.

Figure 3.6. Calculated and measured values of
wave overtopping for $h_1 \geq (h_b)_s$
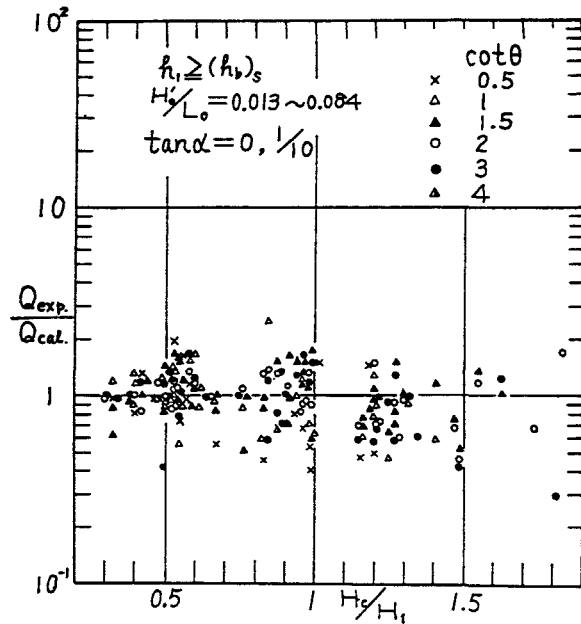
Values of $\overline{(Q_{exp}/Q_{cal})}$ and σ calculated by eq.(3.14) are:

$$\overline{(Q_{exp}/Q_{cal})} = 1.0 \qquad\qquad (3.15)$$

and:

$$\sigma = 0.35 \qquad\qquad (3.16)$$

When $h_1=(h_b)_p \sim (h_b)_s$ and $\tan\alpha = 1/10$, $(a_\theta)_{II}$ is given by the following equation:

$$\log_{10}(a_\theta)_{II} = \log_{10}\left[6.6 + 1.8\log_{10}\left\{\frac{h_1}{(h_b)_s}\right\}\right.$$

$$+2\left\{\frac{(h_b)_s - h_1}{(h_b)_s - (h_b)_p}\right\}\log_{10}\left\{\frac{R_{II} - H_c}{H_1}\right\} \qquad (3.17)$$

$$\left. +0.73\log_{10}\cot\theta + 0.83\log_{10}\frac{H_0'}{L_0}\right]$$

Values of $\overline{(Q_{exp}/Q_{cal})}$ and σ calculated by eq.(3.17) are:

$$\overline{(Q_{exp}/Q_{cal})} = 1.0 \qquad\qquad (3.18)$$

and:

$$\sigma = 0.51 \qquad\qquad (3.19)$$

Further experiments are needed to get higher accuracy. In the previous studies, the maximum overtopping of waves arise generally in the critical region between surging waves and breaking waves. The calculation formulae for the quantity of overtopping proved to give fairly good values to the experimental values. It is clear that the slope which produces the highest run-up of waves is nearly in agreement with the slope which produces the maximum overtopping.

3.2.   Akira Takada formula (1974)

The author investigated the problem by the "Calculation method for discharge of overflow weirs" i.e. the method of Fukui et al. (1963) and Shi-igai et al. (1970).

The quantity of wave overtopping Q of width B per a wave period is represented by eq. (3.20) by using the method of Shi-igai et al. (1970):

$$Q = \int_{t_u}^{t_d} q(t)dt = \frac{2}{3}\sqrt{2g} \ B\int_{t_U}^{t_d} c(t) \ [\{\eta^*(t) + h_a - H_c\}^{3/2} - (h_a)^{3/2}]dt \qquad (3.20)$$

where:

q(t)	= discharge of wave overtopping per a unit time at time t	[m³/sec]
H_c	= crown height of a sea-wall from the still water level	[m]
C(t)	= discharge coefficient of overtopping wave at time t	[-]
$\eta^*(t)$	= time history of the surface elevation for a vertical sea-wall at the wave overtopping time	[-]
(h_a)	= water head of approach velocity	[m]
(t_u)	= time when a wave of a given period start overtopping	[sec]
(t_d)	= time when the overtopping is terminated	[sec]
g	= acceleration of gravity	[m/sec²]

For practical use, (h_a) is disregarded and the time history of surface elevation $\eta(t)$ on a vertical sea-wall for non-overtopping wave is used instead of $\eta^*(t)$, and errors caused from above assumptions are considered to be included in C(t).

On the other hand, assuming that an average value of times is used for C(t) which is defined by a constant K, Q is given by eq.(3.21), as proposed by Shi-igai et al. (1970).

$$Q = \frac{2}{3}\sqrt{2g} \ BK\int_{t_u}^{t_d} \{\eta(t) - H_c\}^{3/2}dt \qquad (3.21)$$

where:

K	= average coefficient of wave overtopping discharge	[-]

As shown in figure 3.7 $\eta(t)$ is assumed to have approximately a trapezoidal profile, then Q is further given by follows, as proposed by the author (1972):
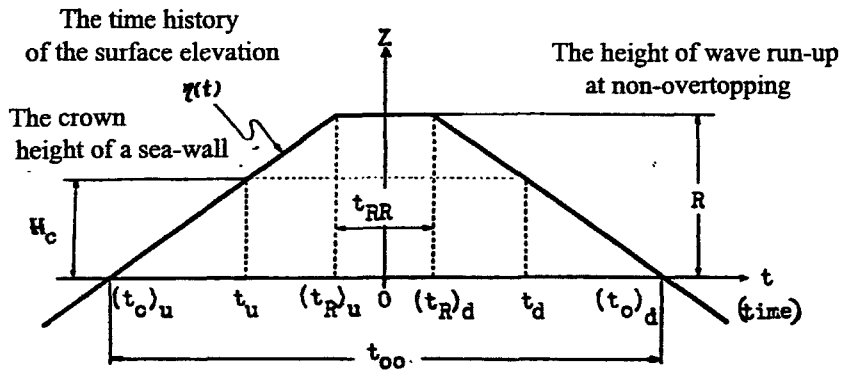
Figure 3.7. The assumption of the time history of the surface elevation.

$$Q=\frac{2}{3}\sqrt{2g}\ BK\ \left[2\int_{t_u}^{t_d}\left\{\frac{(t-t_u)R}{(t_R)_u-t_u}-H_c\right\}^{3/2}dt+\int_{(t_R)_u}^{(t_R)_d}(R-H_c)^{3/2}dt\right] \tag{3.22}$$

$$Q=\frac{4}{15}\sqrt{2g}\ BK\ (R-H_c)^{3/2}\left\{\left(1-\frac{H_c}{R}\right)(t_{00}-t_{RR})+\frac{5}{2}t_{RR}\right\} \tag{3.23}$$

where (t_{RR}) varies with H/L and h/L. Here the values of (t_{RR}) are assumed to have approximately 0.05T. Therefore, the calculational formula of Q is expressed by eq. (3.24):

$$Q=\frac{4}{15}\sqrt{2g}\ BK\ (R-H_c)^{3/2}\left\{\left(1-\frac{H_c}{R}\right)\left(\frac{t_{00}}{T}-0.05\right)+0.125\right\}T \tag{3.24}$$

where:

T   = wave period   [sec]

(t_{00})   = is shown in figure 3.7.   [sec]

The (t_{00}) values are expressed by follows:
-for h>0:

$$t_{00}/T=(t_0/T)_d-(t_0/T)_u \tag{3.25}$$

-for 1/8 < t_0/T<1/4:

$$t_{00}/T=2(t_0/T) \tag{3.26}$$

Here, the values of t_{00}/T are calculated from η(t). Eq (3.27) is η(t) by the second-order approximation solution of finite amplitude standing wave.

$$\eta(t)=H\cos2\pi\frac{t}{T}+\frac{\pi}{4}\frac{H}{L}\ H(3\coth^3 2\pi\frac{h}{L}-\coth2\pi\frac{h}{L})\ \cos4\pi\frac{t}{T}+\frac{\pi}{4}\ \frac{H}{L}H\coth4\pi\frac{h}{L} \qquad (3.27)$$

With $\eta(t) = 0$ in eq. (3.27), the values of t_{00}/T are calculated from eq(3.28):

$$\cos(2\pi\frac{t_0}{T})=\frac{1}{\pi\dfrac{H}{L}}\left[\left\{1+\frac{\pi^2}{2}\left(\frac{H}{L}\right)^2 MN\ \tanh2\pi\frac{h}{L}\right\}^{1/2}-1\right] \qquad (3.28)$$

where:

$$M=\{3\coth^2(2\pi\frac{h}{L})-1\}\coth(2\pi\frac{h}{L})$$

$$N=3\coth^4(2\pi\frac{h}{L})-2\coth^2(\frac{h}{L})-1 \qquad (3.29)$$

The (t_{00}) value for beach line (h=0) are:

$$t_{00}=0.25\ \ \sec \qquad (3.30)$$

Fig.3.8. shows the comparison between calculated values and experimental values. It is thus seen that, though the scattering in experimental values are fairly large, the calculated values indicate fairly accurately the tendency of the experimental values.

Relative water depth at the toe of sea-walls
(a) Results for H'$_0$/L$_0$ = 0.018 and the bottom slope of 1.10

Relative water depth at the toe of sea-walls
(b) Results for H'$_0$/L$_0$ = 0.038 and the bottom slope of 1.10
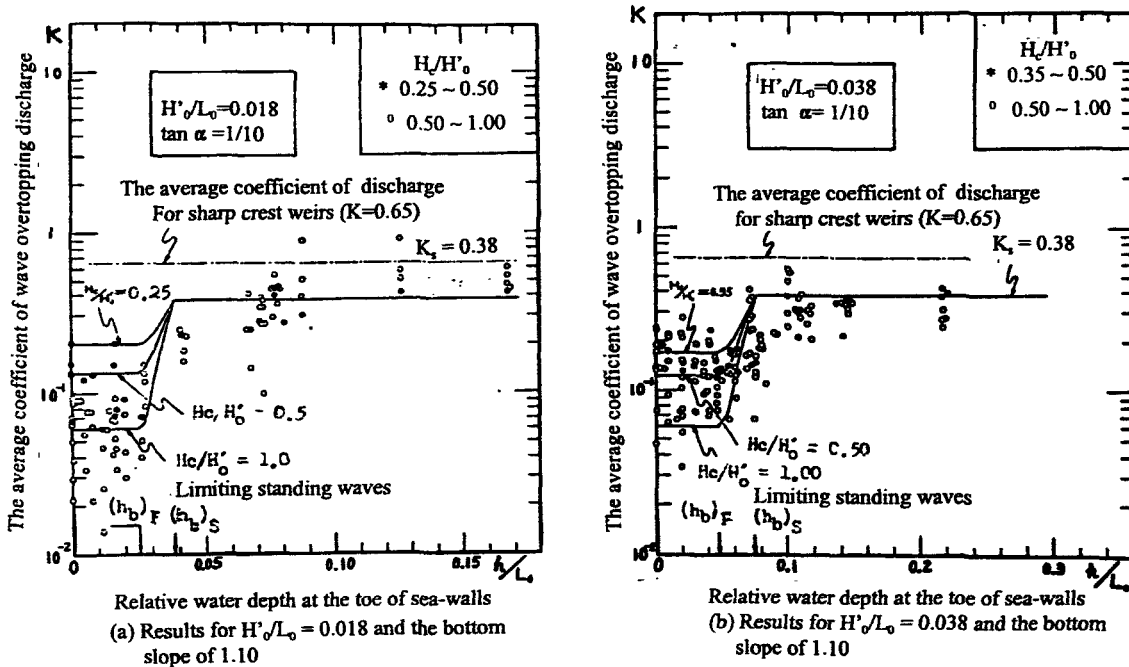
Figure 3.8. Comparison between calculated and measured values of the average coefficient of wave overtopping discharge for vertical walls

3.3. Richard Weggel formula (1976)

The overtopping data was reanalyzed and an empirical expression derived. A broad range of model scales were used in the overtopping experiences. The variables describing the overtopping of a given structure are depicted on figure 3.9.
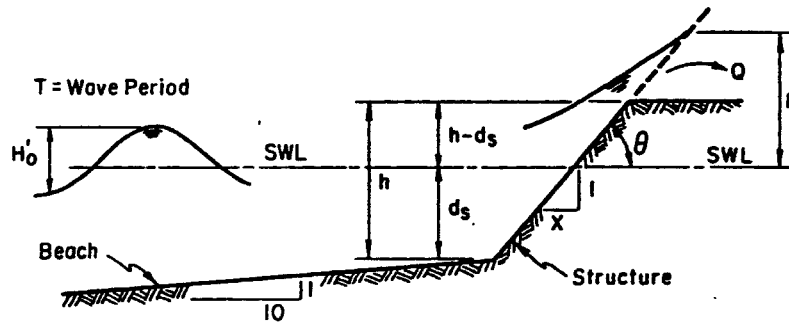
Figure 3.9. Definition of terms

Variables are:

H'_0	= deepwater wave height	[m]
T	= wave period	[sec]
g	= gravitational acceleration	[m/sec^2]
Q	= overtopping rate	[-]
R	= run-up height measured vertically from the still water level	[m]
d_s	= water depth of the structure toe	[m]
h	= height of the structure crest above the bottom	[m]
v	= kinematic viscosity	[sec/m^2]
θ	= structure slope	[rad]

A dimensional analysis of the precedent 9 variables having 2 dimensions gives the following dimensionless terms:

d_s/H'_0	= relative water depth at the structure toe	[-]
H'_0/gT^2	= wave steepness parameter	[-]
$F=(h-d_s)/H'_0$	= relative height of structure or height of structure crest required to preclude overtopping	[-]
$Q^*=Q^2/gH'^3_0$	= relative overtopping rate	[-]
θ	= structure slope	[rad]
$R_e = \dfrac{H_0'^2}{vT}$	= a Reynolds' number	[-]

The phenomenon is scaled primarily according to Froude similarity. However, the Reynolds' number serves as a measure of any scale effects. Other formulations of R_e are possible, the present one having been adopted for its simplicity.

Generally it is not permissible to eliminate dimensionless terms by combining them unless an analytic or empirical relations between two of the variables is known. If it is assumed that such a satisfactory relationship is available for the run-up R, the overtopping rate can be expressed in terms of R and the ratio $F/F=(h-d_s)/R$ can be substituted for F and F_0. The preceding dimensionless terms are obviously not the only combinations of terms possible; however, they were selected after considerable trial and error because they provided the greatest possibility for keeping dimensionless variables constant and investigating the variation of Q^* with individual parameters.
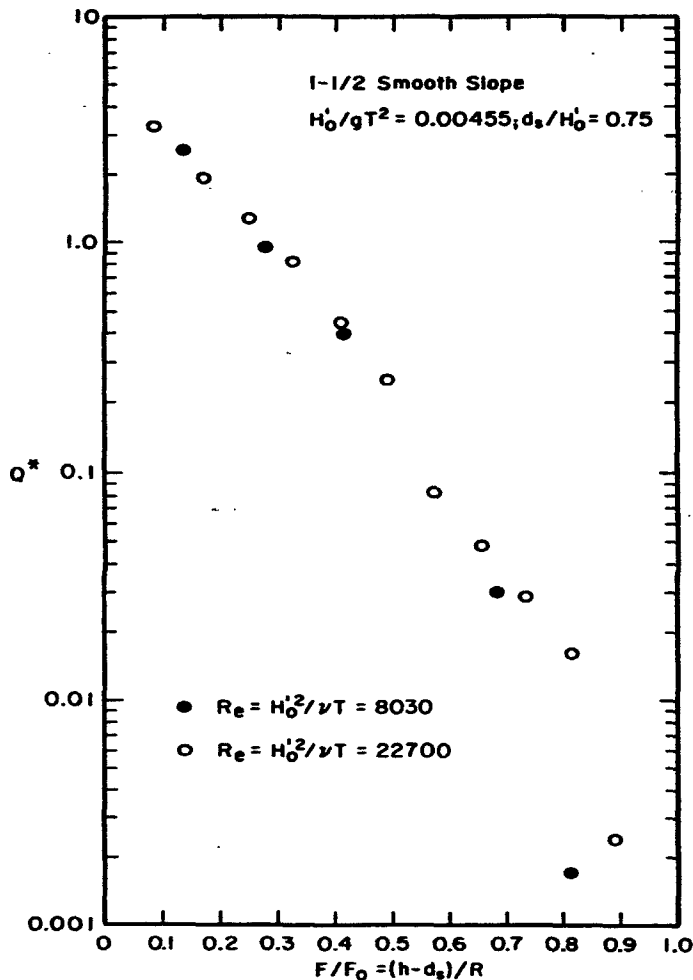
Figure 3.10. Typical data plot

For a given structure and set of incident wave conditions (e.g. constant d_s/H'_0, H'_0/gT^2 and θ), the dimensionless overtopping rate, Q^* was plotted against the dimensionless crest height, $F/F_0=(h-d_s)/R$. A typical plot showing two data sets differing only in model scale, is shown in figure 3.10. Generally, all data sets when plotted semi-logarithmically exhibited a linear variation of Q^* with F/F_0 for small values of F/F_0; also, the values of Q^* must approach zero as the relative crest height, F/F_0 approaches 1.0 (i.e. as the crest of the structure approaches the limit of wave run-up).

The curve therefore approaches $F/F_0=1.0$ asymptotically on the semi-logarithmic plot.

The hyperbolic tangent function exhibits identical behavior; hence, an equation of the form,

$$\frac{F}{F_0} = \alpha \ \tanh \left[\log \frac{Q*}{Q_o*} \right] \tag{3.31}$$

was used to approximate the data. Here α and Q_0* are empirical coefficients to be established by comparing the equation with the data.

The values of α generally establishes the shape of the curve since it is the slope of the curve at $F/F_0 = o$. $Q*_0$ represents the value of $Q*$ for a structure with its crest elevation at the SWL. By substituting the dimensionless variables into equation (3.31) and solving for Q, one finds:

$$Q = \sqrt{g Q_0^* H'^3_0} \exp \left\{ -\frac{0.217}{\alpha} \tanh^{-1} \left[\left(\frac{h - d_s}{R} \right) \right] \right\} \tag{3.32}$$

or equivalently, since $\tanh^{-1} \left(\frac{a}{b} \right) = \frac{1}{2} \log_e \left(\frac{b+a}{b-a} \right)$,

$$Q = \sqrt{g Q_0^* H'^3_0} \exp \left\{ -\frac{0.217}{\alpha} \log_e \left[\left(\frac{R + h - d_s}{R - h + d_s} \right) \right] \right\} \tag{3.33}$$

Either equation (3.32) or (3.33) can be used in conjunction with figures such as those from annex 4 to determine overtopping rates.

Table 3.2.

AGREEMENT BETWEEN MEASURED AND CALCULATED OVERTOPPING RATES
(Using SPM published values of d and Q_0^*, based on 1 to 17 scale data)

Structure Type	Number of Points	Correlation Coefficient
Smooth Face		
Vertical	56	0.980
1 on 1-1/2 slope	93	0.996
1 on 3 slope	83	0.992
Riprap Face		
1 on 1-1/2	43	0.998
Stepped Face		
1 on 1-1/2	60	0.990
Galveston Curved Wall		
on 1 on 10 beach	33	0.995
on 1 on 25 beach	33	0.998
Recurved Wall		
on 1 on 10 beach	5	0.999

To evaluate the ability of equation (3.32) or (3.33) to predict the overtopping rates measured in the experiments, the values of α and $Q*_0$ as published in the SPM, were used with equation

(3.32) and computed overtopping values compared with measured values. Tables 3.1 presents the correlation coefficients found in the analysis. In general, agreement was excellent; the worst case was for the vertical wall data with r=0.98. The small number of data points for the recurved wall make the correlation analysis for that structure inconclusive.

3.4. Saville formulas (1984)

Saville provides formulas for wave overtopping for two kind of waves: regular and irregular. Bellow are given these formulas.

3.4.1. Regular waves

Saville and Caldwell (1953) and Saville (1955) investigated overtopping rates and run-up heights on small-scale laboratory models of structures. Larger scale model tests have also been conducted for Lake Okeechobee levee section (U.S. Army Corp of Eng, 1984). A re analysis of Saville's data indicates that the overtopping rate per unit length of structure can be expressed by:

$$Q = \sqrt{gQ_0^* H_0^{*3}} \; e^{-\left[\frac{0.217}{\alpha} \tanh^{-1}\left(\frac{h-d_s}{R}\right)\right]} \tag{3.34}$$

in which:

$$0 \le \frac{h-d_s}{R} < 1.0 \tag{3.35}$$

or equivalently by:

$$Q = \sqrt{gQ_0^* H_0^{*3}} \; e^{-\left[\frac{0.1085}{\alpha} \log_e\left(\frac{R+h-d_s}{R-h+d_s}\right)\right]} \tag{3.36}$$

in which:

$$0 \le \frac{h-d_s}{R} < 1.0 \tag{3.37}$$

where:

Q	= overtopping rate (volume/unit time) per unit structure length	[-]
g	= gravitational acceleration	[m/sec²]
H_o^*	= equivalent deepwater wave height	[m]
h	= height of the structure crest above the bottom	[m]
d_s	= depth at the structure toe	[m]

R   = run-up on the structure   [m]

Q_0^*, α = empirically determined coefficients that depend on incident
            wave characteristics and structure geometry   [-]

Approximate values of Q_0^*, α are given as functions of wave steepness and relative height for
various slopes and structure types as:

- smooth vertical wall on a 1:10 nearshore slope   (annex 1);
- smooth 1:1,5 structure slope on a 1:10 nearshore slope   (annex 2);
- smooth 1:3 structure slope on a 1:10 nearshore slope   (annex 3);
- smooth 1:6 structure slope on a 1:10 nearshore slope   (annex 4);
- riprapped 1:1,5 structure slope on a 1:10 nearshore slope (annex 5);
- stepped 1:1,5 structure slope on a 1:10 nearshore slope   (annex 6);
- curved wall on a 1:10 nearshore slope   (annex 7);
- curved wall on a 1:25 nearshore slope   (annex 8);
- recurved wall on a 1:10 nearshore slope   (annex 9).

Equations (3.24) and (3.25) are valid only for $0 \leq (h-d_s) < R$. When $(h-d_s) \geq R$ the overtopping rate
is taken as zero. Calculated overtopping rates may be multiplied by a wind correction factor
given by:

$$k' = 1.0 + W_f \left(\frac{h - d_s}{R} + 0.1 \right) \sin\theta \qquad (3.38)$$

where W_f is a coefficient depending on wind speed, and θ is the structure slope ($\theta = 90^0$ for
Galveston walls). For onshore wind speeds of 60 mi/hr, or greater, $W_f=2.0$ should be used. For
a wind speed of 30 mi/hr, $W_f=0.5$; when no onshore winds exists, $W_f=0$. Equation (3.38) is
unverified, but is believed to give a reasonable estimate of the effects of onshore winds of
significant magnitude. For a wind speed of 30 mi/hr, the correction factor k' varies between 1.0
and 1.55, depending on the values of $(h-d_s)/R$ and sin. Values of Q_0^*, α larger that those should
be used if a more conservative (higher) estimate of overtopping rates is required.

3.4.2. Irregular wave.

Irregular wave run-up on coastal structures is assumed to have a Rayleigh distribution, and the
effect of this assumption is applied to the regular wave overtopping equation.
In applying this equation to irregular waves and the resulting run-up and overtopping, certain
modifications are made and the following equation results:

$$Q = \left[\sqrt{g Q_0^* H_0^3} \right] \cdot e^{- \left[\frac{0.217}{\alpha} * \tanh^{-1} \left(\frac{h - d_s}{R} \right) \right]} \qquad (3.39)$$

in which:

$$0 \leq \left(\frac{h-d_s}{R_s} \right) \frac{R_s}{R_p} < 1.0 \qquad (3.40)$$

where:

Q_p = overtopping rate associated with R_p [m²/sec]

R_p = wave run-up with a particular probability of exceedance   [m]

R_s = wave run-up of the equivalent deepwater significant wave height.[m]

The relationship between R_p, R_s and P is given by:

$$\frac{R_p}{R_s} = \sqrt{\frac{-LnR}{2}} \qquad (3.41)$$

Equation (3.39) provides the rate of overtopping for a particular wave height. In analysing the rate of overtopping of a structure subjected to irregular waves and the capacity for handling the overtopping water, it is generally more important to determine the extreme (low probability) rate and the average rate Q of overtopping based on a specified design storm wave condition.

3.5. Goda's graphs (1985)

Goda (1985) presents six separate graphs for wave overtopping of a vertical wall at specific combinations of the foreshore slope and the wave steepness. Compared with other information on wave overtopping in literature these graphs have proven to be very well applicable. These graphs are presented in Annex 10 for two different slopes of the bottom . The dimensionless overtopping discharge is plotted on a logarithmic scale against the relative local water depth,

identifying lines for constant values of the relative crest height. In order to make the information in the graphs more accessible, the information was tabulated for $h_t/H_{os} \geq 1.0$

In the six graphs of Goda (1985), the vertical distance between the lines for successive relative crest height values is fairly constant. This implies that the relation between the dimensionless overtopping discharge and the relative crest height is well approximated by an exponential relation, for constant values of the foreshore slope, the wave steepness and the local water depth. An example of the relationship

Figure 3.11. Overtopping discharge of regular waves

between the dimensionless overtopping discharge and the relative crest height according to Goda is presented in figure 3.11. Although the presented lines are slightly curved an approximation with a straight line is very well possible. Figure 3.11 shows the overtopping discharges of regular waves, q (cm^3/ cm sec), against the incident wave height, H (cm).
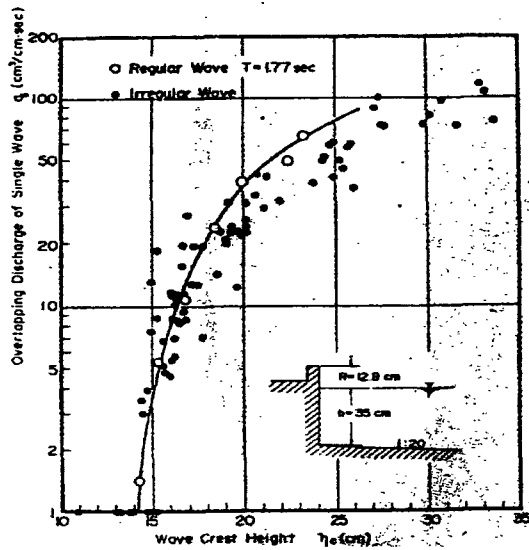
Figure 3.12. Overtopping discharge of individual waves in irregular wave train

The overtopping discharge of individual wave in irregular wave train, on the other hand, does not show much difference with that of regular waves as shown in figure 3.12, where the rate of individual wave overtopping on the vertical wall of R = 12.8 cm (where R stands for crest height) is plotted against the wave crest height η_c in front of the vertical wall. Although the data of irregular waves show some scatter, they almost agree with those of regular waves. The scatter is partly due to the difficulty in accurate determination of individual wave overtopping quantity. The interference of preceding waves may have caused additional scatter of the overtopping data, but the tendency

of figure 3.12. indicates that the irregular wave overtopping if expressed in terms of wave crest height does not differ much from that of regular waves. All these results are the outcome of an experiment carried out by Tsurta and Goda . With the experimental data of regular wave overtopping shown in figures 3.12. and the histograms of wave height of incident waves, the expected discharge of irregular wave overtopping was calculated. The results of calculation are compared with the experimental discharge in figure 3.13. for R = 9.4 cm and for R = 12.8 cm.
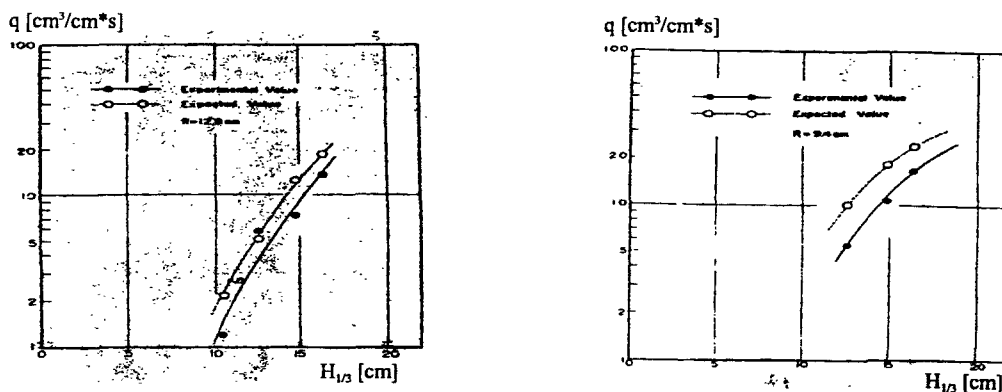
Figure 3.13. Comparison of expected and experimental discharge for R=9.4 cm and R=12.8 cm

The expected values are generally larger than the experimental ones: about 50 to 80% up for R = 9.4 cm and about 30 to 50% up for R = 12.8 cm. The difference is partly attributed to the effect of interference by preceding waves and to the effect of wave period, but the difficulty in maintaining the same statistical characteristics of irregular waves is another cause of the difference. In spite of these differences, the tendency of expected overtopping discharge agrees with that of experimental data.

The non-dimensional calculation of expected overtopping discharge has been carried out for predetermined values of R (crest height). Along one q-H curve with the parameter of R/h, $q_{EXP}/\sqrt{2gh^3}$ was calculated .The result was converted into the form of $q_{EXP}/\sqrt{2gH_{so}^3}$ with the ratio of H_{so}/h, which is obtained by dividing R/h with R/H_{so}. For the asymptotic case of $H_{so}/h \rightarrow 0$, equation of Kikkawa et al. (1967) was utilized after rewriting it as follows:

$$\frac{q}{\sqrt{2gH_{so}^3}} = 0.1\beta^{3/2}\eta^{3/2}\left[1 - \beta\frac{R}{H_{so}}\frac{1}{\eta}\right]^{5/2}$$

(3.42)

with $\beta = H_{so}/H = 1.60$ and $\eta = H/\overline{H}$ (Rayleigh distribution).

The parameter k for η_c/H was taken as 1 since at the limit of $H_{so}/h \rightarrow 0$ the sinusoidal wave gives a good approximation to the wave profile. Also the discharge coefficient, m, was given a little over-estimated value of 0.5 in order to cover the difference between the sinusoidal wave and triangular wave profiles, the latter having been employed in the derivation of eq. 3.42.

The result of calculation are combined in figures 3.14 for vertical walls and in figures 3.15 for block mound type sea walls, These figures reveal several characteristics of expected overtopping discharge. First, it does not respond sharply to the variation of H_{so}/h. This is clearly observed for the small value of R/H_{so}. Second, even with a high parapet of R/H_{so} = 2.0, the average discharge of overtopping may amount to $0.0004\sqrt{2gH_{so}^3}$ for vertical walls.

The figure yields the discharge of 0,02 m³/sec per every one metre of the sea wall for the wave height of H_{so}=5 m.

If a pumping station for drainage is constructed for every thousand metres of the sea wall, the station must have the capacity greater than 20 ton/sec. Third, the maximum overtopping discharge appears at relatively low wave height: i.e. , H_{so}/h = 0.8 for vertical walls and H_{so}/h =0.6 for block mounds. The shift of peak position toward smaller height for block mounds is explained as the result of the promotion of wave breaking by presence of block mounds and of the absorption of after- breaking waves.
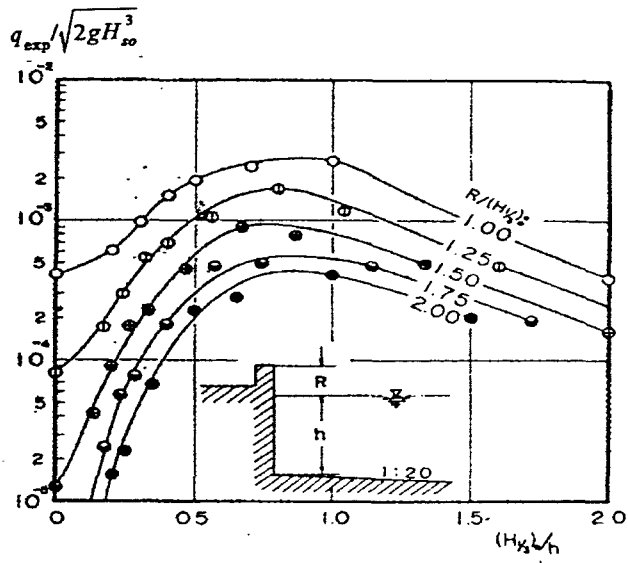
Figure 3.14. Dimensionless overtopping for vertical walls
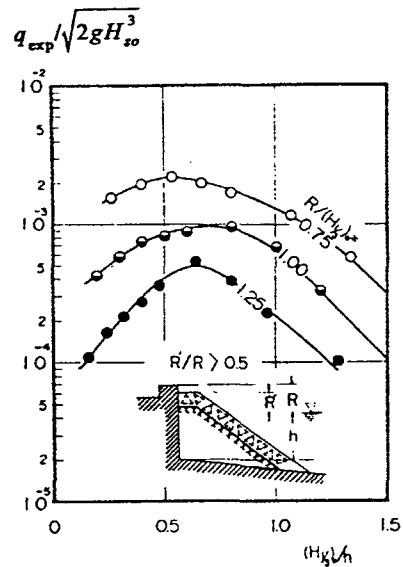
Figure 3.15. Dimensionless overtopping for block mound sea walls

Annexes 10 a ÷ f are design diagrams compiled by the author for the estimation of wave overtopping rate of vertical revetments. They were prepared on the basis of irregular wave tests and calculation of wave deformation in the surf zone. Annex 10.b. is for a sea bottom slope of 1/10, and annexes 10a is for a slope of 1/30. The symbol H_o' in the figures denotes the equivalent deepwater wave height, h the water depth, h_c the crest elevation of the seawall above the still water level, and g the acceleration of gravity (g = 9.8 m/s^2). As seen in the insets of the figures, a simple wall with no recurved parapet and no foot-protection rubble mound is being considered. If either the wave steepness or the bottom slope differs from those in annexes 10, interpolation or extrapolation becomes necessary. If the bottom slope is gentler than 1/30, the wave overtopping rate in water shallower than $2H_o$' becomes less than that given by annexes 10 in general. The rate of reduction in overtopping rate increases as the relative crest elevation h_c/H_o' increases.

Seawalls made of sloping mounds of rubble stones and concrete blocks of the energy-dissipating type are more popular than vertical revetments. In Japan, block mound seawalls of relatively steep slope backed by a vertical retaining wall are quite common, especially along coasts facing rough seas. The wave overtopping rate of block mound seawalls is governed not only by the characteristics of the incident waves, water depth and crest elevation, but also by the size and shape of the mound. Therefore, the compilation of generalized design diagrams for the overtopping rate of block mound seawalls is more difficult than for the case of vertical revetments.

3.6.   Juul Jensen and Jorgen Juhl formula (1986)

The study presents the J. Jensen and J. Juhl experience from studies of wave overtopping on breakwater and sea dikes. The studies wave were all made by use of irregular waves. Based on model investigations is discusses the influence of the various physical parameters on wave overtopping, such as wave height, wave period, water level, wind speed, type of armour unit, distribution of overtopping, discharges for individual waves and as function of the distance from the breakwater.

The wave run-up, R_u on a rubble mound breakwater armour layer is for a fixed wave period almost proportional to the wave height, H, which means: $R_u = \alpha H$. If for simplicity all waves in an irregular wave train are considered having the same wave period, T, i.e. the parameter α is independent of T, the overtopping discharge as function of H_s can be calculated. The height crest is quoted as Δh.

The Rayleigh wave height distribution is assumed valid:

$$p(E) = \frac{\pi}{2\overline{H^2}}\, H\, \exp\left(-\frac{H^2}{\overline{H^2}}\frac{\pi}{4}\right) \tag{3.43}$$

The volume of water passing the crest per unit length of the breakwater is equal to (figure 3.16):

$$A = \left(\frac{V}{2\pi}\right) Nl^2 = \frac{V}{2}l^2 \tag{3.44}$$

$$l = \left(R_n - \Delta h\right)/\sin\theta \tag{3.45}$$

By introducing $R_u = \alpha H$, the volume per unit length of overtopping for a single wave is given by:

$$q = \frac{V}{2}\frac{(\alpha H - \Delta h)^2}{\sin^2\theta} = \alpha^2 \frac{V}{2(H - \Delta h/\alpha)^2/\sin^2\theta} \tag{3.46}$$

The total volume of overtopping can be as:

$$Q = \int_{H=\frac{\Delta}{\alpha}}^{\infty} q\; p(H)dh = \int_{H=\frac{\Delta}{\alpha}}^{\infty} \alpha^2\frac{V}{2}\frac{1}{\sin^2\theta}\left(H^2 - \frac{2H\Delta h}{\alpha} + \left(\frac{\Delta h}{\alpha}\right)^2\right)\frac{\pi}{2\overline{H^2}}H\; e^{\frac{-\pi H^2}{4\overline{H^2}}}\, dh \tag{3.47}$$

$$\eta = \frac{\Delta h}{\alpha}, \qquad \zeta = \frac{\alpha^2 V}{2\sin^2\theta}, \qquad \gamma^2 = \frac{(\Delta h/\alpha)^2}{\overline{H^2}}\frac{\pi}{4}$$

The equation can hereafter be solved and written as:

$$Q = 2\zeta\overline{H}\left(\frac{2\overline{H}}{\pi}\ e^{-\gamma^2} - \eta(1 - erf(\gamma)) \right) \tag{3.48}$$

In figure 3.16 the calculated overtopping per wave is shown as function of $H_s/\Delta h$. It appears that the parameter, $H_s/\Delta h$, is not giving completely dimensionless values of Q. It is further of interest to notice that the curves for Q is not exactly linear, but tends to curve especially for larger values of $H_s/\Delta h$. All the tests were performed with the DHI method of direct reproduction of natural wave records. All tests were performed in a flume of 0.6m width and about 22m long. Most tests had a prototype duration of about one hour.

The results show that the overtopping varies from structure to structure, but some general conclusions may be derived:

- the amount of overtopping increases rapidly with the parameter $H_s/\Delta h$. The logarithm of Q is an almost linear function of $H_s/\Delta h$;

- the influence of the wave period is very different from structure to structure;

- in the presentation of the results, no sharp limit exists between wind-carried spray and mass overtopping where solid masses of water are passing the crest of the breakwater ("green water").

The intensity of overtopping behind a breakwater decreases very rapidly with the distance from the breakwater. In all the tests performed as well as in the available prototype measurements, it has been experienced that on the average the intensity of overspill decreases exponentially with the distance, x, from the breakwater. This means :

$$q(x) = q_0 10^{(x/\beta)} \tag{3.49}$$

where:

q - intensity at a distance x $[m^2/sec]$

q_0 - intensity for x=0 $[m^2/sec]$

Figure 3.16. Calculation of wave overtopping

The parameter β is a constant and equal to the distance for which the overspill intensity decreases by a factor of 10.Now the total amount of overtopping, Q, may be calculated by integration:

$$Q = \int_0^\infty q_0 10^{-(x/\beta)} dx \qquad\qquad (3.50)$$

resulting in the following formula:

$$Q = q_0 \frac{\beta}{\ln 10} \qquad\qquad (3.51)$$

knowing Q and β, the intensity, q_0 for x=0 may be calculated, and thus the intensity, q(x), for a distance x can be estimated.Besides the horizontal distribution of wave overtopping behind a breakwater, the distribution of the wave overtopping discharge of individual waves is highly important. Since the overtopping discharge is an nonlinear physical phenomenon, it is not so much the average intensity that determines the level of inconvenience or danger, although average intensities can be used as criteria for acceptable overtopping.

The authors have made model tests in scale 1:30 with measurements of both the average overtopping volume and the volume of overtopping in the 5-10 waves causing the largest overtopping. These tests were made without wind. The breakwater used for theses experiments appears in figure 3.17, where the results are also shown.
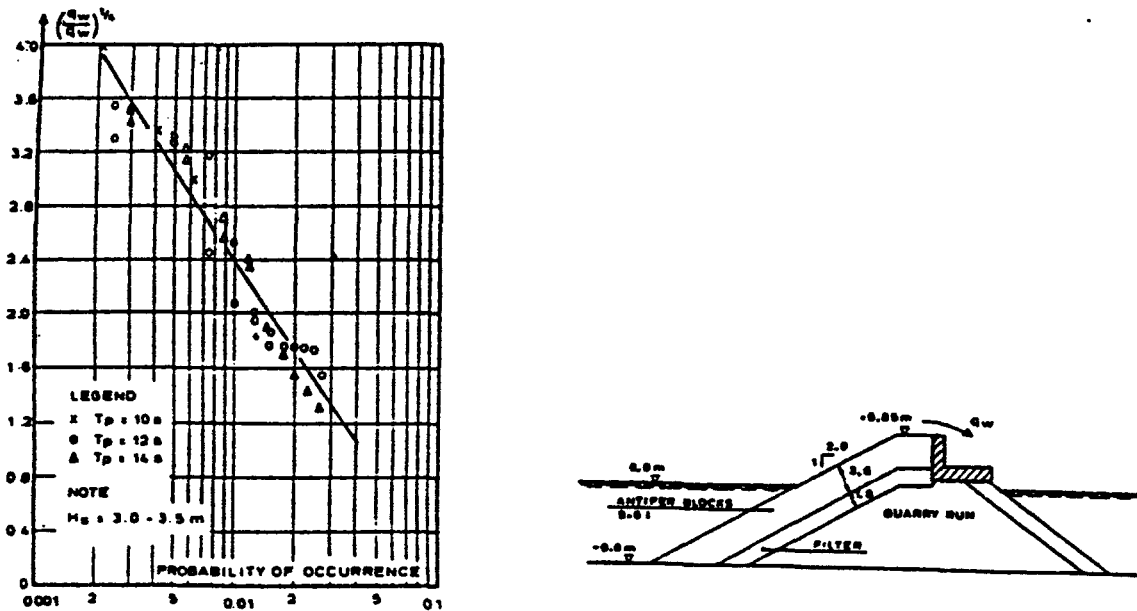
Figure 3.17. Results of overtopping measurements

In the following, q_w, is the overtopping for one single wave and $\overline{q_w}$, the average value of overtopping, i.e.

$$\overline{q_w}=\frac{1}{N}\sum_{1}^{N}q_w \qquad (3.52)$$

where N is the theoretical number of zero-crossing waves. Note q_w may be zero for many of the smaller waves. It appears from the study that the following distribution applies as an approximation:

$$p(q_w)=\exp\{-(q_w/A)^{\gamma}\} \qquad (3.53)$$

A and γ are constants. The results show that for this specific case that γ is in the order of 0.25. The wind velocity has an important influence on the quantity of wave overtopping especially for small overtopping quantities, i.e. "Spray carry over" conditions. In situation with extreme " green water" overtopping the effect of the wind is almost negligible.

From the results it appear clearly that the wind velocity is an important factor for the overtopping discharge for small overtopping discharges, i.e. "Spray-carry-over" conditions.

3.7. Dutch guidelines (1989)

In the following section formulas for wave overtopping according to Dutch guidelines (D.G.), edition 1989 are presented. At the end of the section there are presented modification done to this in June 1997 by van der Meer in report H 2458/H3051.

3.7.1. D.G.- 1989
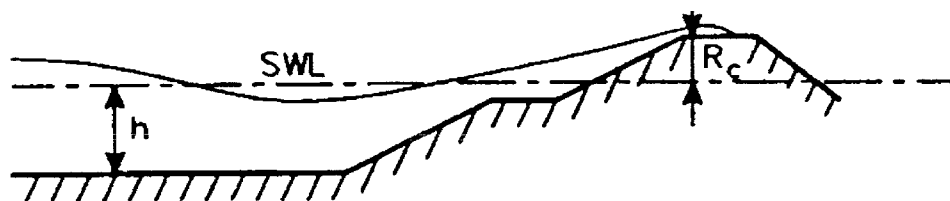
Figure 3.18. Free crest height with wave overtopping

With wave overtopping, the crest height is lower than the run up levels of the highest waves. The parameter to be considered here is the free crest height R_c (Figure 3.18). This is the difference in level between SWL and the crest height. The crest height itself can be given as an absolute crest height h_d, for example determined with respect to NAP (Amsterdam ordnance datum). If the crest height is reduced by the water level (also with respect to NAP) then yields the free crest height R_c.

Wave overtopping is mostly given as an average discharge q per metre width, for example in m³/s per m or in l/s per m. The Guideline (TAW, 1989) indicates that for relatively heavy seas and with wave heights of up to a few metres the 2%-wave run up criterion yields an overtopping discharge of the order of 1 l/s per m. It becomes 0.1 l/s/m with lower waves such as those occurring in rivers. An overtopping of 1 l/s per m in the river area can lead to a reduction of the freeboard of the dike (taking into account the minimum freeboard of 0.5 m). The Guideline further quotes "Which criterion applies depends of course also on the design of the dike and the possible presence of buildings. In certain cases, such as a covered crest and inner slopes, sometimes 10 l/s per m can be tolerated".

In the Guidelines it is assumed that the following average overtopping rates are allowable for the inner slope:

* 0.1 l/s per m for sandy soil with a poor turf;
* 1.0 l/s per m for clayey soil with relatively good grass;
* 10 l/s per m with a clay protective layer and grass according to the standards for an outer slope or with a revetment construction.

At the moment studies are being carried out to better explain the relation 0.1, 1.0 and 10 l/s per m overtopping as well as the condition of the inner slope.

Wave overtopping can be expressed in two formulas: one for breaking waves (ξ_{op} <2) and one for non-breaking waves (ξ_{op} >2).

The dimensionless overtopping discharge Q_b (b for *breaking waves*) is given on the ordinate :

$$Q_b = \frac{q}{\sqrt{gH_s^3}}\sqrt{\frac{S_{op}}{\tan\alpha}}$$
(3.54)

and the dimensionless crest height R_b (application area 0.3<R_b<2) with:

$$R_b = \frac{R_c}{H_s}\frac{\sqrt{S_{op}}}{\tan\alpha}\frac{1}{\gamma_b\gamma_h\gamma_f\gamma_\beta}$$
(3.55)

The formula using first approach (average value) presented in section 2.2. is:
$$Q_b = 0.06\exp(-5.2R) \quad \text{For } \xi_{op} <2$$
(3.56)

The dimensionless overtopping discharge for *non-breaking waves* (ξ_{op}>2) is:

$$Q_n = \frac{q}{\sqrt{gH_s^3}}$$
(3.57)

and the dimensionless crest height R_n:

$$R_n = \frac{R_c}{H_s} \frac{1}{\gamma_b \gamma_h \gamma_f \gamma_\beta} \qquad (3.58)$$

The formula is:

$$Q_n = 0.2\exp(-2.6\,R_n) \qquad (3.59)$$

By TAW , a somewhat more conservative formula with build in safety factor should be applied for design purposes rather than the average value. The two recommended formulas based on mean average values (second approach from section 2.2.) for overtopping are:

* for breaking waves with $\xi_{po} < 2$:

$$Q_b = 0.06\exp(-4.7R) \qquad (3.60)$$

* and for non-breaking waves with $\xi_{op} > 2$:

$$Q_n = 0.2\exp(-2.3R_n) \qquad (3.61)$$

The used quotation in above formulas are:

Q_b	= dimensionless overtopping discharge for breaking waves ($\xi_{op} < 2$)	[-]
Q_n	= dimensionless overtopping discharge for non-breaking waves ($\xi_{op} > 2$)	[-]
q	= average overtopping discharge (in m^3/s per m width)	[m^2/sec]
g	= acceleration due to gravity	[m/sec^2]
H_s	= significant wave height (average of highest 1/3 part)	[-]
S_{op}	= wave steepness $= 2\pi H_s/(gT^2_p)$	[-]
T_p	= peak period, with a double peaked spectrum T_{peq}	[sec]
R_b	= dimensionless crest height with breaking waves ($\xi_{op} < 2$)	[-]
R_c	= free crest height above still water line	[m]

$\gamma_b, \gamma_h, \gamma_f, \gamma_\beta$ = reduction factors for influence of a berm, shallow foreshore, roughness and angle of wave attack. Minimum value using a combination of factors is 0.5. 　　　　　　　　　　　　　[-]

Both the dimensionless overtopping discharge and the dimensionless crest height are function of the significant wave height, the wave steepness and the slope gradient. To account for the varying conditions, the dimensionless crest height is virtually increased through division by the reduction factors $\gamma_b, \gamma_h, \gamma_f, \gamma_\beta$ ($\leftrightarrow \gamma < 0.1$), which are also given by the Dutch Guidelines .

Both design formulas are graphically shown in figures 3.19 and 3.20. In these figures the recommended lines, the mean and the 95% confidence limits are. Also, in figure 3.19 the formula from the Guideline, part two, is drawn and is practically the same as the recommended line (figure 3.19, 3.20).
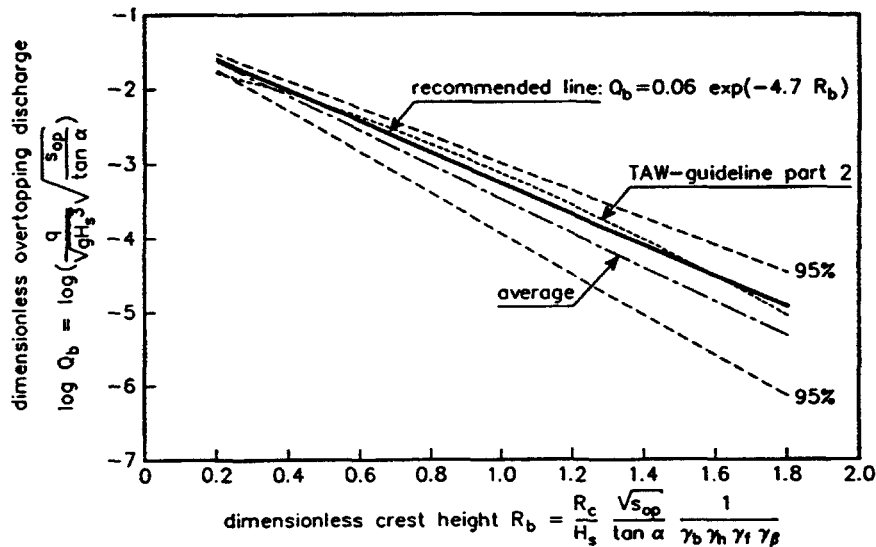
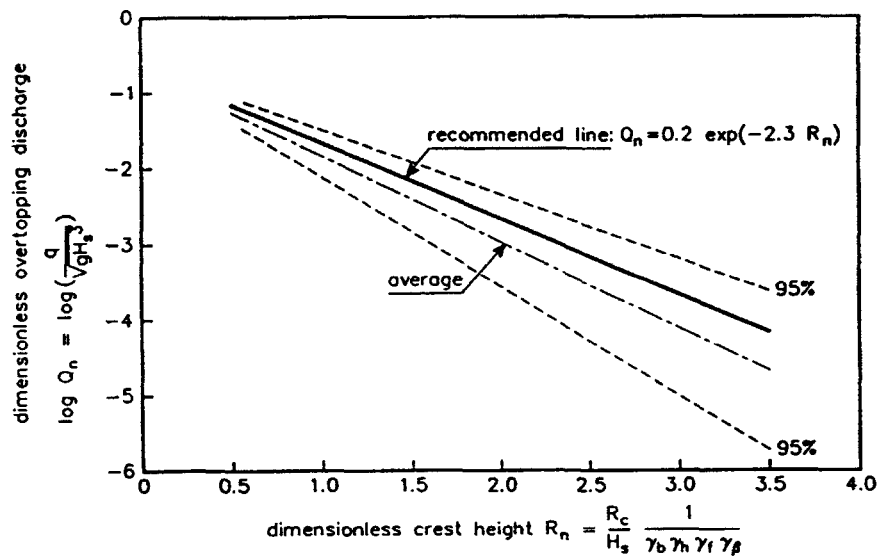*Figure 3.19. Wave overtopping with breaking waves*

Figure 3.20. Wave overtopping with non-breaking waves

With the presented formulas steep slopes are accounted for by considering non-breaking waves separately. The improvement is mainly the description of the reliability of the formulas and a better description of the influence of berms, a shallow foreshore, roughness and the angle of wave attack.

The recommended line for the overtopping discharge q, according with the Dutch guidelines, is described in the above section by the equations (3.60) and (3.61.). However, the average overtopping discharge does not say much about the amount of water of a certain overtopping wave passing the crest. The volumes of individual waves deviate considerably from the average discharge. By means of the average overtopping discharge the probability distribution function of the overtopping volumes can be computed. This probability distribution function is a Weibull distribution with a form factor of 0.75 and a scale factor a which is independent of the average overtopping discharge per wave and the overtopping probability. The probability distribution function is given by (Report H638, Delft Hydraulics, 1994):

$$P_v = P(\bar{V} \le V) = 1 - \exp\left(-\left(\frac{V}{a}\right)^{0.75}\right) \tag{3.62}$$

$$a = 0.84 \frac{T_m q}{P_{ow}} \tag{3.63}$$

with:

P_v = probability of the overtopping volume per wave V being
less than or similar to V   [-]

V = overtopping volume per wave   [m³/m]

T_m = average wave period (NT_m is the storm duration or
time interval considered)   [sec]

q = average overtopping volume   [m³/m]

P_{ow} = N_{ow}/N_w = probability of overtopping per wave   [-]

N_w = number of incoming waves during the time the storm lasts   [-]

The probability of overtopping can be computed by:

$$P_{ow} = \exp\left(-\left(\frac{R_c/H_s}{c}\right)^2\right) \tag{3.64}$$

The value of the reduction factor c follows from the assumption that the run up distribution is similar to the Rayleigh distribution.

3.7.2. 1997 modifications

According to report H 2458/H3051 of Delft Hydraulics new values for reduction factors have been found as follows:

γ_h = 1

$\tan \alpha$ = 3 H_s/(L_{slope}-B) - were α is the equivalent angle of the slope   [$^\circ$]

L_{slope} = the length of slope in front of the structure measured between 1.5 H_s depth in the water and 1.5 H_s above the water level.   [m]

B   = is the length of the berm (if this exist)   [m]

γ_v = new coefficient for influence of vertical wall on the top of the sloping structure.   [-]

3.8. Yoshimichi and Kiyoshi formulas (1992)

The proposed formula by the above authors presents a new methods for calculating the wave overtopping rate over a seawall located on a complicated bottom profile of sea coast. It was assumed that the influence of the complicated coastal profile on the wave run-up height can be evaluated by introducing a hypothetical single slope angle α proposed by Nakamura et al.(1972) as follows:

$$\alpha = \tan^{-1}(R + h_b)^2/2A \qquad\qquad (3.65)$$
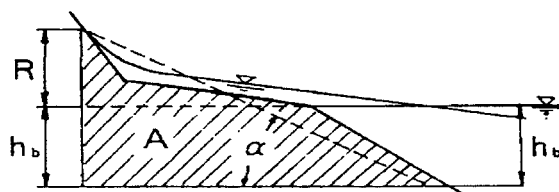
Figure 3.21.   Hypothetical single slope angle (Nakamura et al. 1972).

where:

R   = wave run-up height   [m]

h_b = breaking water depth   [m]

A   = the shade area from the depth at the breaking point to the extreme of maximum wave run-up, as shown in figure 3.21.   [m^2]

The predicted results coincide well with the available data.

3.8.1. Breaking Waves

The actual shape of wave run-up profile is presented in figure 3.22 (a). Takada (1977) assumed that it could be approximated by the one presented in figure 3.22 (b) and studied the wave overtopping rate over one wave period T. He found that this value is proportional to the shade area A in figure 3.22 (b). That is,

$$q \ :: \ A \tag{3.66}$$

where:

   q   = wave rate overtopping over one wave period   [m³/sec/m]

   A   = hypothetical area above the seawall crown in a wave run-up profile   [m²]

$$A = (R - H_c)[(X_0/R) - \cot\alpha](R - H_c)/2 \tag{3.67}$$

            where:

   H_c = freeboard above SWL   [m]

   X_0 = horizontal length of the shape of the wave run-up profile.   [m]
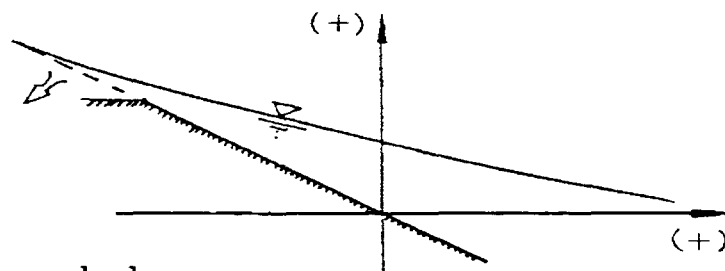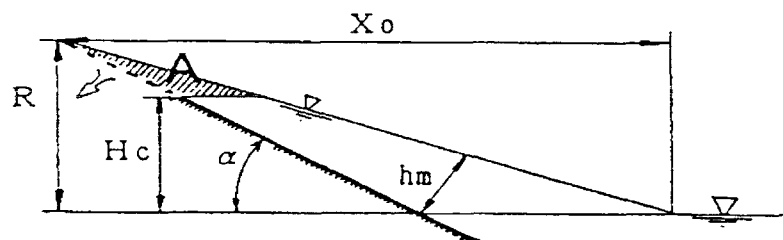
Figure 3.22. Actual shape and assumed shape of wave run-up profile.

From eq. (3.65) and (3.66) , the overtopping rate q can be predicted by the following equation:

$$q = c[(X_0/R) - \cot\alpha](R - H_c)^2/2 \tag{3.68}$$

where c is the overtopping coefficient which can be determined from experiment

In figure 3.22 , the upper part of the actual shape of the wave run-up is thinner than that of assumed shape, and the value of X_0 in the actual shape is longer than that of the assumed shape. Thus if the value of X_0 of the actual shape is used, the resultant evaluation of the area A will be extremely exaggerated. Therefore the value of X_0 of assumed shape is used. It is calculated by using the following equation obtained from geometrical relationship.

$$X_0/R = \cot[\alpha - \tan^{-1}(h_m/R/\sin\alpha)] \tag{3.69.}$$

where h_m is the maximum thickness of the water tongue shown in figure 3.22 (b).
The expression for h_m can be found by the following formula:

$$\frac{h_m}{H_b} = \frac{1}{2} \frac{H_a}{H_b} J_0\left(\frac{4\pi\sqrt{H_b}}{\sqrt{g}\ Ti}\sqrt{\frac{h_m}{H_b}}\right) + 0.8\ i^{0.6} \tag{3.70}$$

where:

H_a	= wave height at the point where is no energy loss by breaking waves	[m]
H_b	= breaking wave height	[m]
J_0	= Bessel function of the zero order	[-]
i	= bottom slope (cotg α)	[-]
T	= wave period	[sec]

R is calculated using the system given by equations (3.68) - (3.70).
The results of the calculation by using Eq.(3.70) are shown as the dotted lines in figure 3.23.
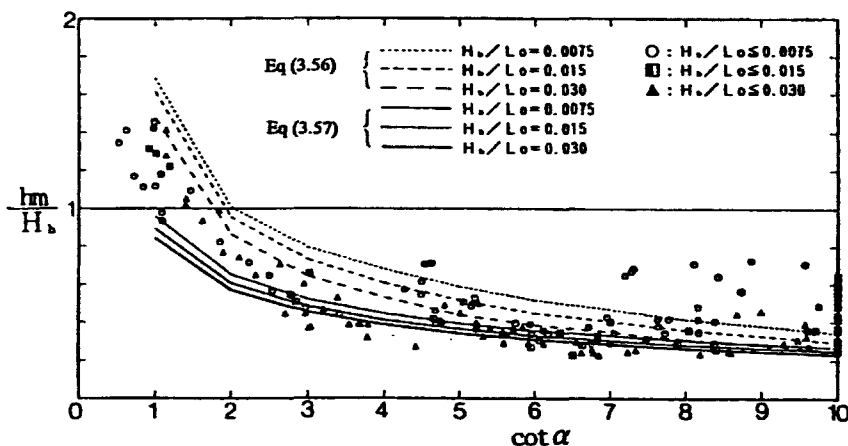
Figure 3.23 Relation between the maximum thickness of the water tongue and the bottom slope.

It takes long time to calculate the Bessel function J_0 in eq. (3.70) . Therefore the use of the approximate expression of the Bessel function and the substitution of realistic values for h_m induce the following equation:

$$\frac{h_m}{H_b} = 0.7 \left[\frac{0.375}{\pi^{3/4}} \left(\frac{i}{\sqrt{0.8 H_b/L_0}} \right)^{1/2} + 0.8 \; i^{0.6} \right]$$

(3.71)

The results of the calculations by using eq.(3.71) are shown as the solid lines in figure 3.23. Finally the overtopping coefficient c, can be obtained, by substituting experimental data into eq (3.68) and (3.68):

$$c = 0.1 (L_0/H_b)^{1/2} (\cos\theta + \cos\alpha)/2$$

(3.72)

3.8.2. Non-breaking waves

It can be assumed that the effect of the seabed profile on the wave overtopping rate is small for non-breaking waves. Therefore the following experimental equation by Takada (1977) was used.

$$q = 0.65 (R - H_C)^2$$

(3.73)

where:

$$R = [1.0 + \pi(H/L)\coth(2\pi h/L)]H_0$$

3.8.3. Irregular waves

The wave overtopping rate for irregular waves can be calculated by the following equation:

$$Q = \int_0^\infty \int_0^\infty q \; p \; dH \; dT$$

(3.74)

where:

Q	= overtopping rate of irregular waves	[m³/sec/m]
p	= joint distribution function of wave period and height of the wave	[-]
q	= overtopping rate of the component waves	[m³/sec/m]
H,T	= wave height and wave period of the component waves respectively.	[m,sec]

The term p proposed by Watanabe et al. (1984) can be expressed as follows:

$$p = p(\tau)p(\chi_f|\tau)/\chi_m(\tau)$$

$$p(\tau) = \frac{\sqrt{1+v^2}}{1+\sqrt{1+v^2}} \frac{v^2}{[v^2+(\tau-1)^2]^{1.5}}$$

$$v = \sqrt{(m_0 m_2/m_1^2) - 1}$$

$$p(\chi_f|\tau) = (32/\pi^2)\chi_f^2 \exp[-4\chi_f^2/\pi]$$

$$\chi_f = \chi/\chi_m(\tau)$$

$$\chi_m(\tau) = \sqrt{S(f)}\,f\,/\int_0^\infty \sqrt{S(f)}\,f\,p(\tau)d\tau$$

(3.75)

where:

$\chi = H/\bar{H}$, $\tau = T/\bar{T}$ (The over bar indicates an average value)   [-]

f   = frequency   [-]

m_k = Kth order moment of the spectrum   [-]

S(f)   = Bretschneider-Mitsuyasu Spectrum.   [-]

The proposed methods have been checked with laboratory data as well as the field data. The agreement between the calculated values and the available data is favorably good.

3.9. Kobayashi formula (1992)

The numerical model developed by Kobayashi et al. (1987) for predicting the up-rush and down-rush of normally incident waves on rough impermeable slopes is expanded to predict wave overtopping over the specified crest geometry of an impermeable coastal structure located on a sloping beach. The related problem of wave overtopping (e.g. Cross and Sollitt 1972; Seelig 1980) and through a porous rubble-mound breakwater (e.g. Madsen and White 1976) is considered herein. Kobayashi et al. (1987) showed that their numerical model was in agreement with available test data on run-up, run-down, and reflection of monochromatic waves plunging and collapsing and surging on uniform and composite riprap slope. This model is presented in annex. Based on this numerical model, for incident monochromatic waves, the normalized average overtopping rate per unit width, Q, is obtained from the computed temporal variation of m=uh at x=x_e

$$Q = \frac{Q'}{H'_0 \sqrt{gH'_0}} = \int_{tp}^{tp+1} m\,dt$$

(3.90)

in which:

Q' = dimensional average overtopping rate per unit width; [m³/sec/m]

t_p = normalized time when the flow at $x=x_e$ becomes periodic. [sec]

For the computation made in this paper, t_p =4 is found to be sufficient as will be shown later. The computed value of Q is hence the average value of m(t) at $x=x_e$ during $4 \le t \le 5$.

The numerical model is compared with the extensive small-scale test data summarized by Seville (1955). The following comparison is limited to the structure geometry shown in figure 3.24 (annex) in which:

B' = crest width [m]

H'_c = crest height above SWL [m]

d'_s = water depth below SWL at the toe of the structure

     fronted by a 1:10 slope [m]

θ'_s = angle of the structure slope [rad]

d'_h = water depth below SWL on the horizontal bottom in a wave flume [m]

The values of Q listed in Table 3.2 are plotted in figure 3.25 where, for each measured value of Q,the numerically computed value of Q and that calculated using SPM are shown. The numerical model yields fairly good agreement with the data but it underestimates Q for the runs in group1
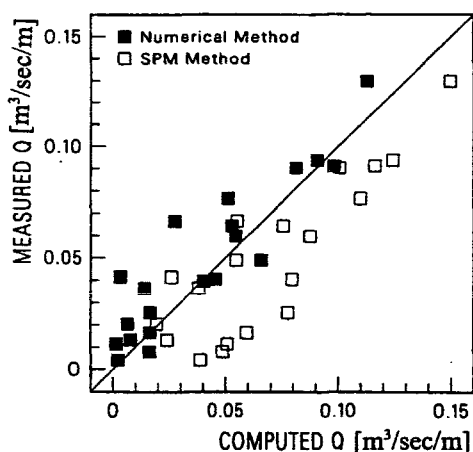

Figure 3.25.Computed and measured values of wave overtopping

TABLE 3.2   Summary of Computed Results for 20 Runs

Run number (1)	d_h (2)	d_s (3)	d_c (4)	H_c (5)	r (6)	Data (7)	Numerical (8)	SPM (9)
						Q × 10²		
1	4.92	3.00	0.75	0.50	0.27	6.6	2.7	5.5
2	4.92	3.00	0.75	1.00	0.30	4.1	0.3	2.6
3	5.67	3.00	1.50	0.50	0.29	6.4	5.3	7.6
4	5.67	3.00	1.50	1.00	0.29	3.6	1.4	3.8
5	7.56	4.00	2.00	0.67	0.49	9.0	8.1	10.0
6	4.92	4.00	0.75	0.50	0.44	6.0	5.4	8.7
7	4.92	4.50	0.75	1.00	0.48	1.7	1.6	5.9
8	4.92	4.00	0.75	1.50	0.49	0.4	0.2	3.9
9	5.67	4.00	1.50	0.50	0.53	9.4	9.1	12.4
10	5.67	4.00	1.50	1.00	0.60	4.0	4.5	8.0
11	5.67	4.00	1.50	1.50	0.65	0.8	1.6	4.9
12	6.56	6.00	1.00	0.67	0.60	9.1	9.8	11.6
13	7.56	6.00	2.00	0.67	0.60	13.0	11.3	14.9
14	7.56	6.00	2.00	1.33	0.70	7.7	5.1	11.0
15	7.56	6.00	2.00	2.00	0.76	2.5	1.6	7.8
16	7.56	6.00	2.00	2.67	0.77	1.1	1.5	5.1
17	4.92	4.92	0.75	0.50	0.45	4.9	6.6	5.5
18	4.92	4.92	0.75	1.50	0.63	1.3	0.8	2.4
19	4.17	4.17	0.00	0.50	0.16	3.9	4.0	4.1
20	4.17	4.17	0.00	1.00	0.28	2.0	0.7	2.0

In addition to the average overtopping rate, the model computes the temporal and spatial variations of the normalized water depth and horizontal velocity in the computation domain $0 \le x \le x_e$.

The numerical model presented herein may be used to predict the fairly detailed hydrodynamics associated with wave overtopping over the crest of a smooth impermeable coastal structure located on a sloping beach. The comparison of the model with the data is limited to the average overtopping rates of monochromatic waves. The numerical model may also be applied to rough impermeable structures by adjusting the friction factor associated with the surface roughness (Kobayashi et al. 1987). In order to apply the model to overtopping rubble- mound breakwaters, the effects of permeability and wave action on the landward side of the breakwater may need to be taken into account. Such an extended numerical model combined with the armor stability model of Kobayashi and Otto (1987) could be used to investigate various design problems associated with rubble-mound breakwater.

3.10. Richard Silvester formula (1992)
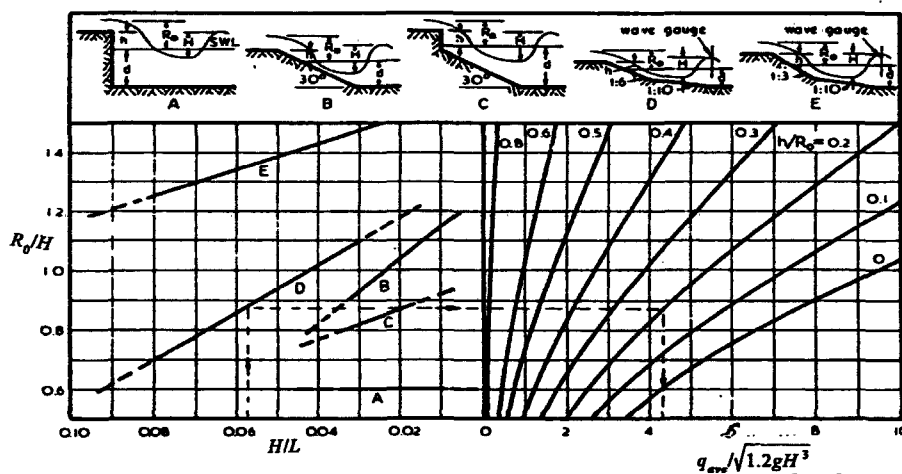
Figure 3.26. Average overtopping discharge q_{ave} per unit length of walls

The definition sketch of figure 3.26 indicates the variety of variables that can enter the problem of overtopping. By the time the wave reaches the crest of a dike it will either be a standing wave or be breaking. In either case the crest shape should be close to triangular. The equation so derived can be put in the form:

$$\frac{q_{ave}}{\sqrt{gH^3}} = \sqrt{2}\frac{2}{15}m\left(\frac{R_0}{H}\right)^{\frac{3}{2}}\left(1-\frac{h}{R_0}\right)^{\frac{5}{2}}$$

(3.91)

where:

q_{ave}	= average discharge over the weir per unit length of dike	[m³/sec/m]
m	= discharge coefficient for flow over the weir	[-]
R_0	= maximum reach of the overtopping wave above SWL	[m]
h	= height of the dike above SWL	[m]

Eq.(3.91) has been plotted in figure 3.26 for m=0.6. also included are curves for R_0/H from the various dikes illustrated. The volume V_T discharging over a length B of the dike in a wave period T is given by:

$$V_T = q_{ave}TB \tag{3.92}$$

with an average velocity $v=2q_{ave}/(R_0-h)$, assuming the discharge to take as a rectangular block for half the wave period. Since the overtopping water body has been considered of triangular cross-section this velocity should be doubled, but verification of such figures should be made in the laboratory.

3.11. Van der Meer formulas (1994)

The following basic dimensionless parameters are to be identified:

Mean overtopping discharge

$$Q = \frac{q}{\sqrt{gH_{os}^3}} \tag{3.93}$$

Relative crest height

$$R = \frac{R_c}{H_{os}} \tag{3.94}$$

Wave steepness

$$S_{op} = \frac{H_{os}}{L_{op}} \tag{3.95}$$

Relative local water depth

$$\frac{h_t}{H_{os}} \tag{3.96}$$

with:

g	= acceleration due to gravity (= 9.81)	[m/sec^2]
h_t	= water depth at the structure	[m]
H_{os}	= significant wave height at deep water	
	(mean of highest one third of the waves)	[m]

L_{op} = wave length in deep water, based on T_p [m]

q = average overtopping discharge per metre structure width [m³/sec/m]

R_c = crest level with respect to SWL [m]

S_{op} = wave steepness in deep water (= H_o'/L_{op}) [-]

T_p = wave period at the peak of the spectrum [sec]

A basic form of overtopping formula proposed by van der Meer is presented bellow.

A generally applicable form of the overtopping formula is the basic relationship between the dimensionless overtopping discharge Q and the relative crest height R:

$$Q = c_1 \exp(-c_2 R) \qquad (3.97)$$

The coefficients c_1 and c_2 are also dimensionless and may be dependent upon all parameters except Q and R. Another way to write the basic formula is:

$$logQ = logc_1 - \frac{c_2}{ln10} R \qquad (3.98)$$

A common way to present a measured relationship between Q and R is a plot of log(Q) (or Q on logarithmic scale) against R. Formula (3.98) implies that this type of presentation yields a straight line. Formula (3.97) is valid for wave overtopping of slopes, but also for overtopping of vertical structures.

An important parameter for slopes is the breaker parameter ξ:

$$\xi_{op} = \frac{\tan\alpha_s}{\sqrt{S_{op}}} \qquad (3.99)$$

With:

ξ_{op} = breaker parameter [-]

α = structure slope [°]

Wave overtopping can be expressed in two formulas: one for breaking waves $\xi_{op} \leq 2$, and one for non-breaking waves $\xi_{op} > 2$. The transition between breaking and non-breaking has been defined as $\xi_{op} = 2$.

For breaking waves:

$$c_1 = 0.06 \sqrt{\frac{\tan\alpha_s}{s_{op}}} \tag{3.100}$$

$$c_2 = 5.2 \frac{\sqrt{s_{op}}}{\tan\alpha} \tag{3.101}$$

For non-breaking waves:

$$c_1 = 0,2 \tag{3.102}$$

$$c_2 = 2.6 \tag{3.103}$$

These values are valid for the average of reference measurements with relatively deep water at the structure ($h_t/H_{os} > 3,0$).

There is a close relation between the wave overtopping and the wave run-up: For nonbreaking waves the wave run-up is proportional to the significant wave-height and independent of the peak period and structure slope. For breaking waves the wave run-up is proportional to the structure slope ($\tan\alpha_s$) and the parameter $\sqrt{H_{os} L_{op}}$ (or $T_p\sqrt{H_{os}}$).

This relationship between wave overtopping and wave run-up is reflected in formulas 3.101 to 3.103 for the coefficients c_1 and c_2.

4. Experiments and tests in literature

4.1. A. Paape experiment (1960)

Information about the overtopping by waves was obtained from model investigations on simple plane slopes with inclinations varying from 1:8 to 1:2 by A.Paape. The experiments were made in a windflume where wind generated waves as well as regular waves were employed. Using wind generated waves, conditions from nature regarding the distribution of wave heights could be reproduced. It appeared that the overtopping depends on the irregularity of the waves and that the same effects cannot be reproduced using regular paddle generated waves.

In this paragraph a description of the model and the results of the A.Paape tests are given. Investigations were done on composite slope, including the reproduction of conditions for a seawall which suffered much overtopping but remained practically undamaged during the flood of 1953 in Holland.

The height of a series of wind waves are often characterized by the value of the significant wave height $H_{1/3}=H_{13}$. The wave period is determined as the mean value of a series of waves. The mean wave length can be found from period and water depth. For wind generated waves in the wind flume the mean period were varying from 0.65 sec with a wind velocity of 4m/sec to 0.85 sec with a wind velocity of 10m/sec. When the wave height and period, using wind only, is too small, a regular paddle generated swell can be applied in combination with a rather high wind velocity to obtain the required period and wave height distribution. In his experiments only wind was used.

The model had a width of 0.5 m and was placed in a glass wall flume, which formed part of a windflume, 4m wide and 50 m long. Before the model was placed, series of tests showed the subdivision of the main flume had no effect on measured wave characteristics.

The overtopping was measured as the volume of water passing the crest during each test. For every height of the crest the overtopping was measured as the volume of water passing the crest during 600 sec, from which an average value per second could be determined. Also the number of overtopping waves, as a percentage of the total number was determined. During each run waves registrated for 120 sec. In this way an average distribution from about 2000 wave heights was obtained for each slope and wind velocity.

An attempt has been made to express the results of these tests in terms of dimensionless parameters as follows.

The height of the crest of the seawall above still water level, h, was expressed as the ratio:

$$h/H_{50} \hspace{4cm} (4.1)$$

It was found that the overtopping could be related to the dimensions of the waves using the ratio.

$$\frac{2\pi QT}{H_{50}L} \hspace{4cm} (4.2)$$

where:

h	= height of the crest of the seawall above still waterlevel	[m]
Q	= overtopping in m³/sec per m length of the seawall	[m³/sec/m]
T	= wave period	[sec]
H_{50}	= wave height exceeded by 50%	[m]
L	= wave length	[m]
$\frac{HL}{2\pi}$	= area, in cross section, of a sinusoidal wave above mean water level.	[m²]

The results obtained are given in figure 4.1 for each slope curves for different average wave steepness were obtained, as various wind velocities were applied. Also the percentage of the waves causing overtopping is indicated. From the tests carried out on a slope of 1:5, the same results were obtained for a water depth of 0.25, 0.30 and 035m. The wave length in deep water, L_o, according to the periods used in these tests was approximately 1.2 m, so no influence of the water depth, d, was found for $d/L_0 \geq 0.21$.

The best results have been obtained using the assumption that the overtopping is proportional to

$(\tan \alpha)^{3/2}$, which is shown in figure 4.2. where, instead of h/H_{50}, $\dfrac{h(cotan\ \alpha)^{3/2}}{H_{50}}$ has been plotted.

It is seen that with slope varying from 1:3 to 1:8 the results can be represented by a single line. But for a slope of 1:2 the results are completely different, possibly due to greatly increased reflection of wave energy for the steeper slopes.

It should be noted that there are probably limitations to the applicability of these results and that the experiments reported here were limited to the ranges:

$$0.03 < \frac{H_{50}}{L_0} < 0.06 \hspace{3cm} (4.3)$$

and

$$d/L_0 \geq 0.21 \hspace{3cm} (4.4)$$

in which:

d	= water depth	[m]
L_0	= wave length in deep water	[m]

The overtopping has been measured for regular and irregular waves with the same mean height. The results are given on figure 4.3. As could be expected, the irregular waves produced more overtopping. It can also be seen from this figure that there is no simple relationship between the height of a regular wave which will give the same overtopping as a given irregular wave, because the height of the seawall crest must also be taken into account
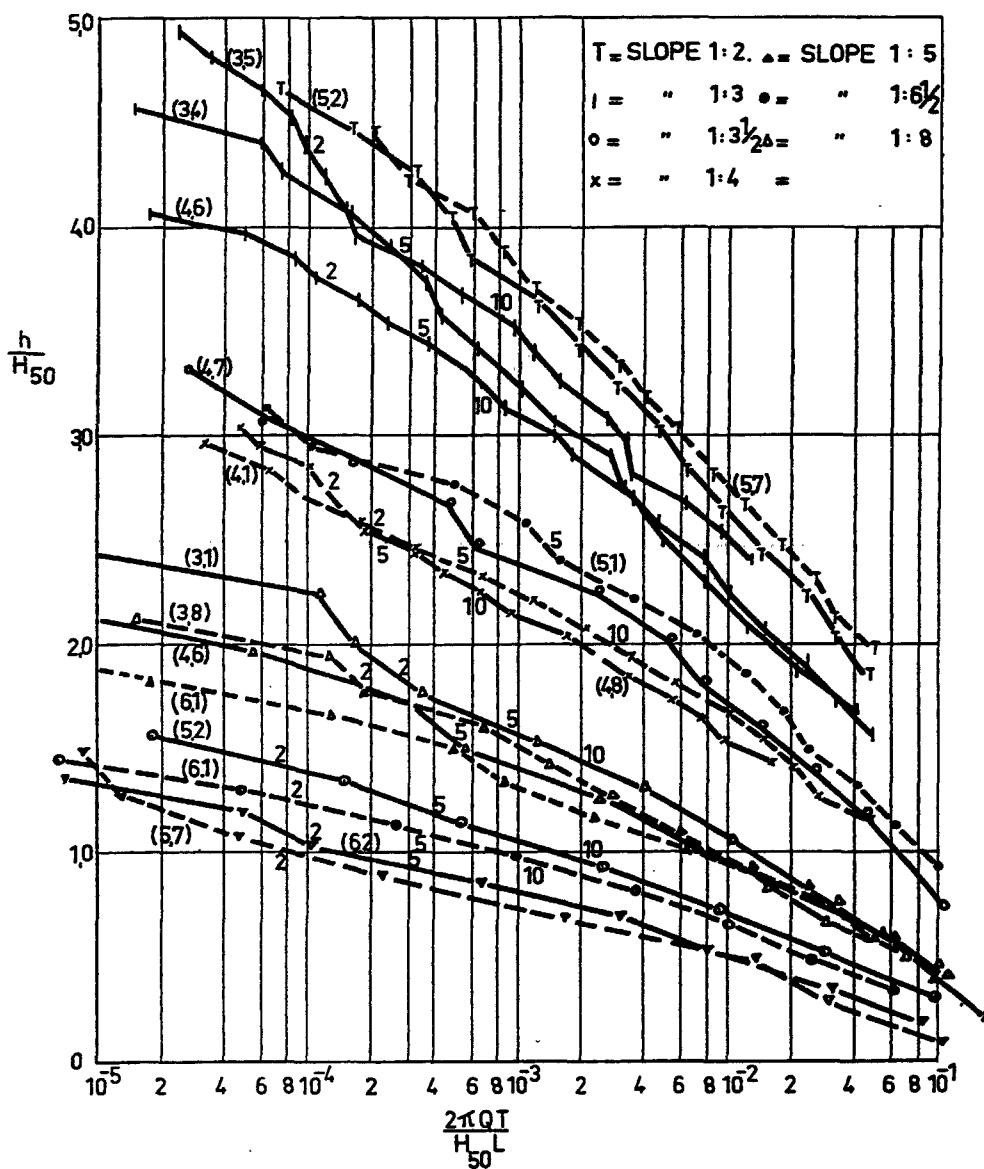
NUMBERS IN BRACKETS INDICATE WAVE STEEPNESS IN %.
PLAIN NUMBERS INDICATE PERCENTAGE OF WAVES OVERTOPPING.

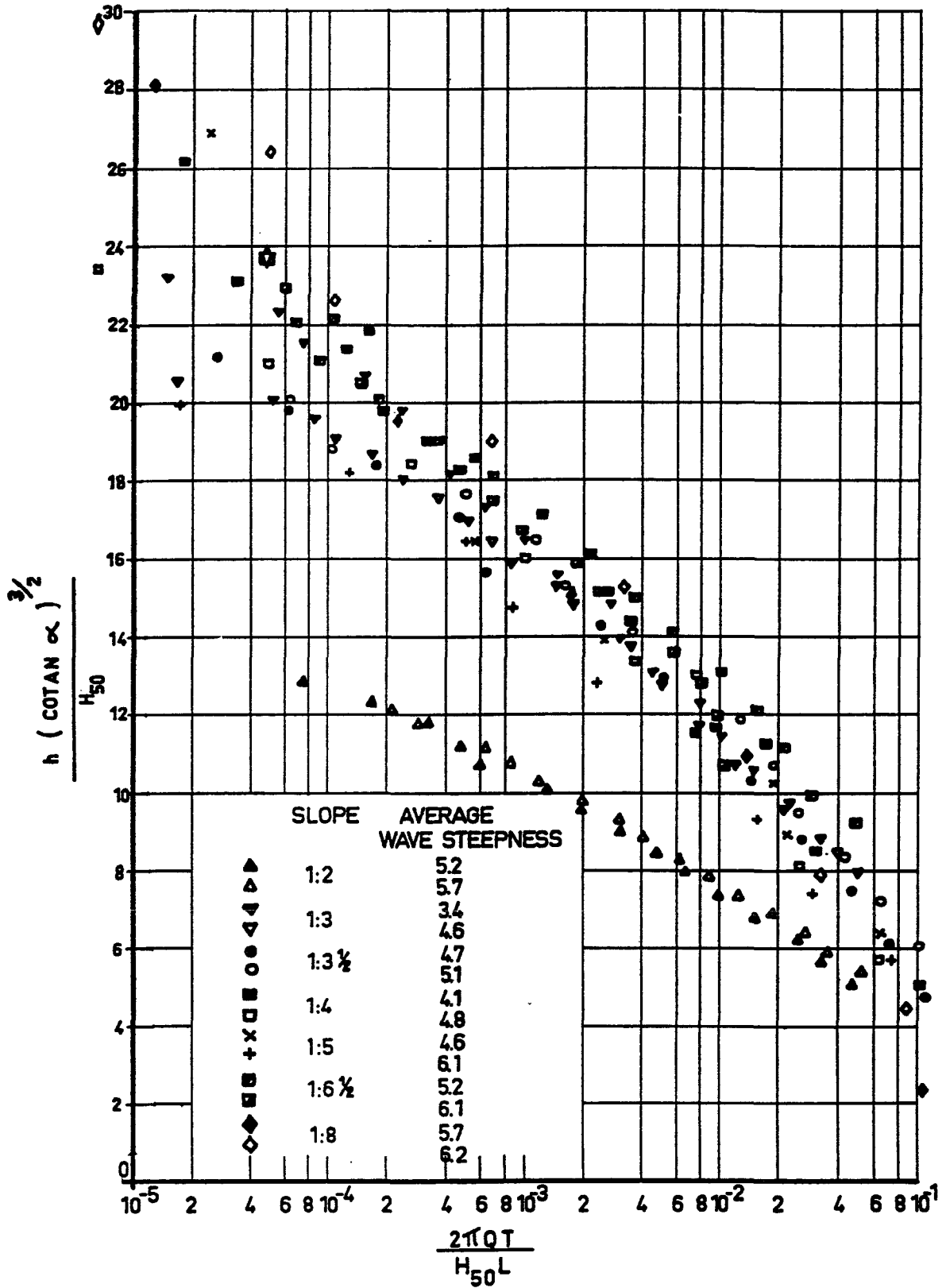*Figure 4.1. Overtopping for diferent average wave steepness for various wind velocities*

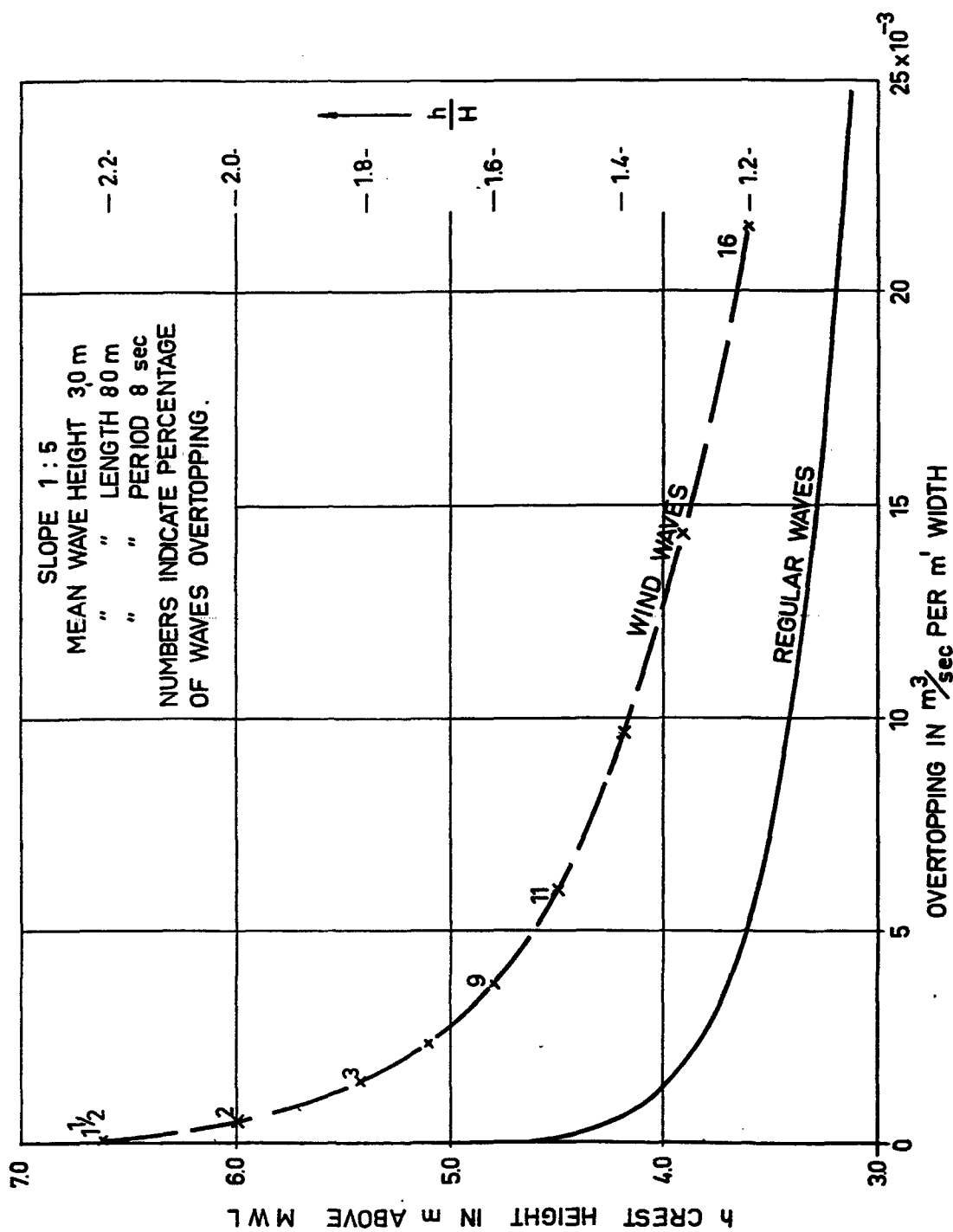*Figure 4.2. Overtopping values for diferent wave steepness*

Figure 4.3. Measured overtopping for regular and irregular waves

4.2.   Oullet and Eubakans experiment (1976)

Yvon Oullet and Pierre Eubakans describes the results of an experimental study on the effect of waves on rubble-mound breakwater, wave transmission subsequent to overtopping, the stability of the three subjected to wave action and the effect of the breakwater on waves. Two different rubble-mount breakwaters were tested, i.e. one with a rigid impermeable crest and other with a flexible permeable crest. Tests were performed with both regular and irregular wave train systems. To obtain the simulated irregular wave trains, four theoretical spectra were chosen: Neumann, Bretschneider, Moskowitz and Scott which are shown in figure 4.4.with the corresponding wind velocities used.

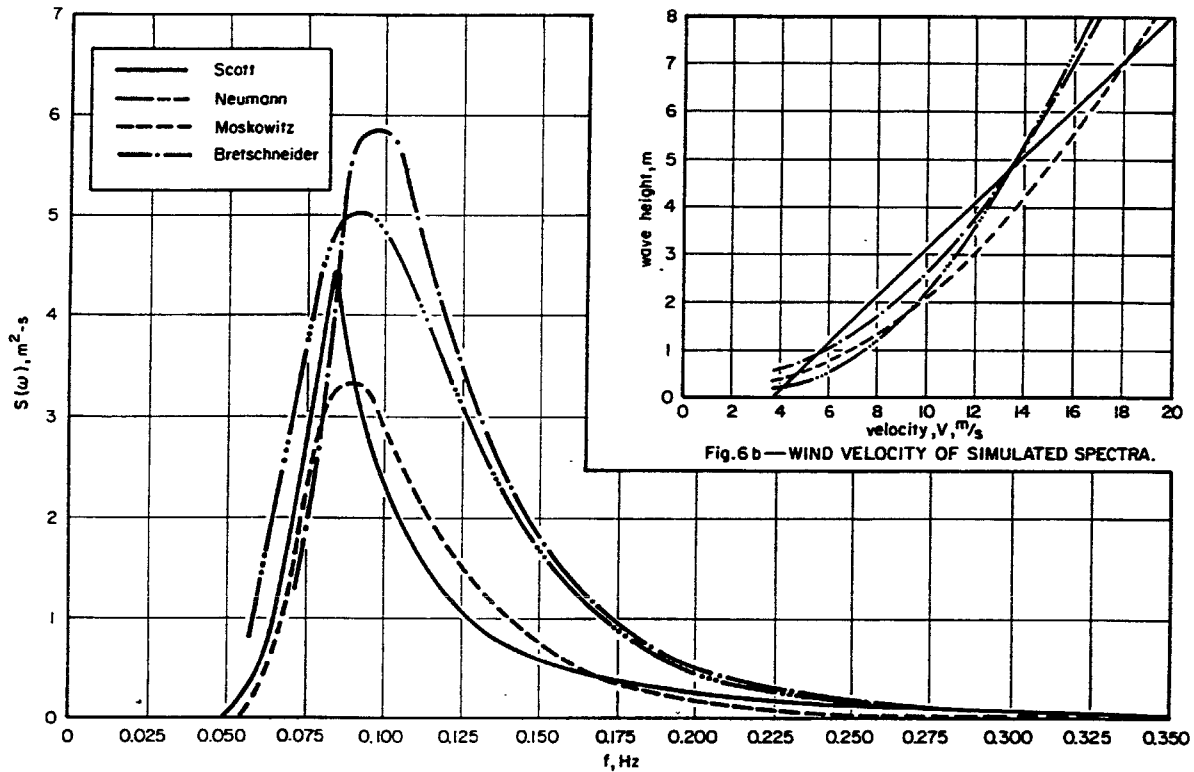

Figure 4.4. Theoretical wave spectra

Wave flume has the following characteristics: a channel 36m long, 1.86m wide and 1.3m deep. The distance between the wave paddle and the model breakwater (center of crest) is about 21m.

Figure 4.5 a) and b) show typical examples of recorded surface profiles of incident and transmitted waves, and the results of the spectral analysis of the above signals in the case of a simulated Neumann spectrum. Figure 4.5 a) corresponds to the concrete cap breakwater with the depth h=60cm and the simulated significant wave height H_s=4.25m. Figure 4.5b), on the other hand, corresponds to the other structure for the same values of h and H_s.

Fig. 8 —IRREGULAR WAVES: NEUMANN SPECTRUM.

(a)

Fig. 9 —IRREGULAR WAVES: NEUMANN SPECTRUM.
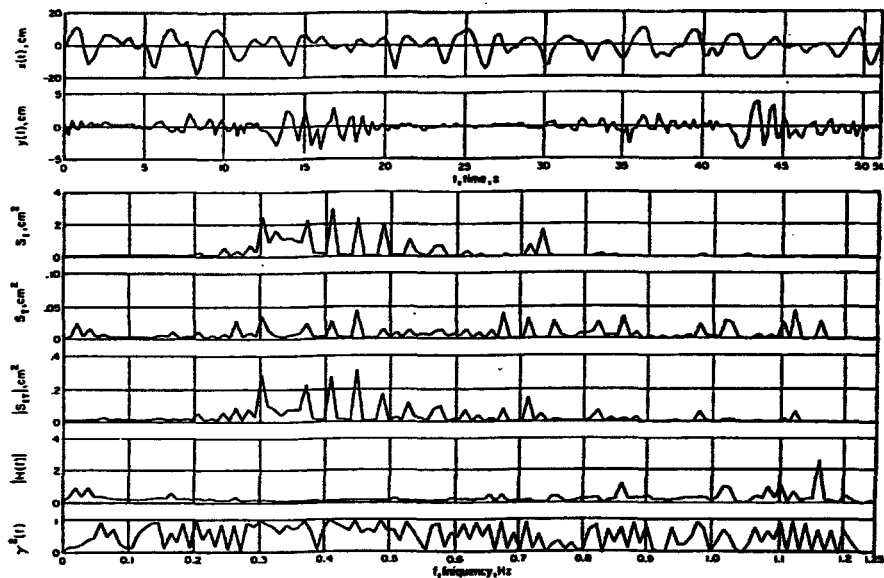
(b)

Figure 4.5. Waves spectrum

Figure 4.6 (a) and (b) show the relationship between height and overtopping wave height for all four spectra respectively for the concrete and dolos crest breakwater in 60 cm depth. The same relationship was also found in the case of regular wave trains as shown in figure 4.7.(a) for the concrete cap and in figure 4.7.(b) for the dolos crest breakwater.
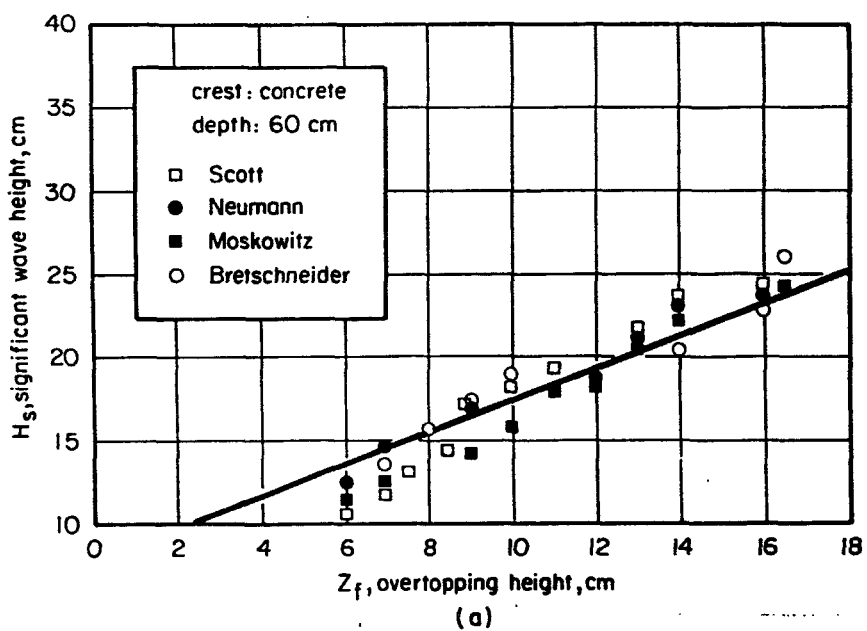
Figure 4.6. *Significant wave height versus overtopping height for irregular waves*

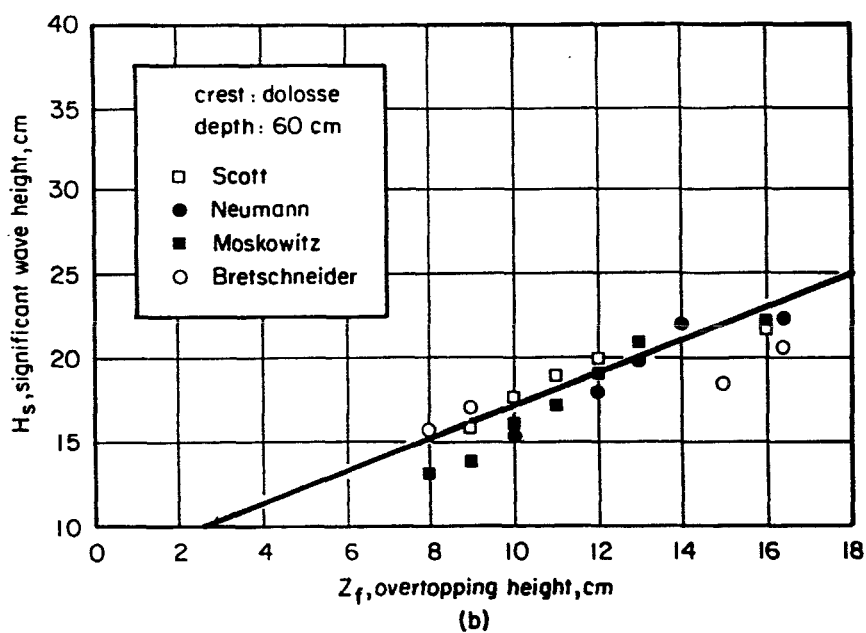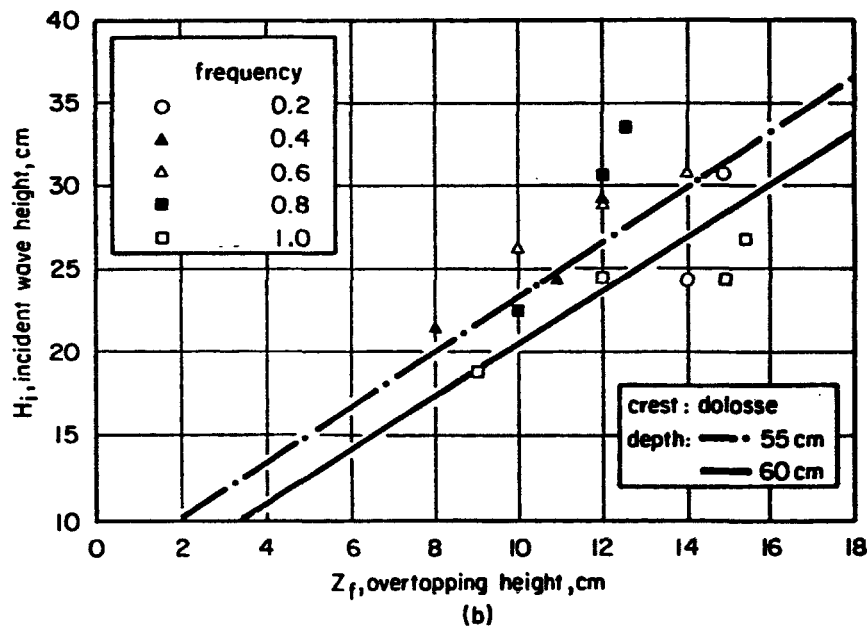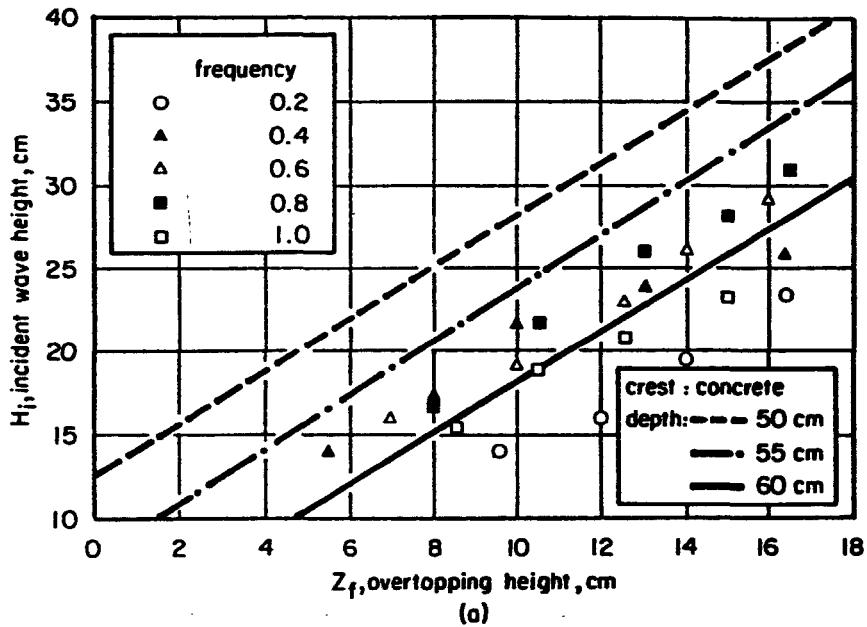*Figure 4.7. Wave height versus overtopping height for regular waves*

Having established that an incident wave height and an equivalent significant wave height have almost identical overtopping heights, it would be possible to predict at which significant wave height structure will be damaged, using only regular wave trains, the main difference being the quantity of damage.

4.3. Ozhan and Yalciner formula (1990)

Erdal Ozhan and Ahmet Cevet Yalciner discusses in the paper ' Overtopping of solitary waves and model sea dikes'- published in Coastal Engineering,1990 for The 22nd International Conference of Coastal Engineering - an analytical model for solitary wave overtopping at sea dikes. The analogy proposed by Kikkawa et al (1968) is extended in their proposal and applied to solitary wave overtopping to derive a closed form analytical model.

By considering analogy with steady flow over a sharp crested weir, wave overtopping rate at a sea dike may be equated to:

$$q(t) = \frac{2}{3} m \sqrt{2g\{z(t) - z_0\}^3} \qquad (4.5)$$

where:

$q(t)$	= unsteady overtopping rate per unit dike width	[m³/sec/m]
$z(t)$	= changing water level elevation measured from still water level	[m]
z_0	= crow elevation of the dike	[m]
g	= gravitational acceleration	[m/sec²]
m	= the weir coefficient which is equal to 0.611 in steady flow	[-]

The change of water level elevation during overtopping is written as:

$$z(t) = Z_{max} F(t) \qquad (4.6)$$

where:

z_{max}	= maximum rise of the water level	[m]
$F(t)$	= a function having the range of 0 and 1	[-]

It is assumed that the maximum water level rise is related to the incident solitary wave height :

$$z_{max} = K \ H \qquad (4.7)$$

where the maximum rise coefficient K may be a function of wave height-to-water depth ratio (H/d), dike angle (α), and wave height-to-crown elevation ratio (H/z_0). Substitution of eq.(4.6) and (4.7) into (4.5) and by integrating results:

$$Q = \frac{4}{3} m \sqrt{2gK^3 H^3} \frac{I}{\varepsilon \lambda C} \qquad (4.8)$$

where:

Q	= overtopping volume of a solitary wave per unit dike width	[m³/sec/m]
ε, λ	= shape coefficients given in eq. (4.11)	

$$I = \int_0^{\tau*} \sqrt{\left(Sech^2\tau - \frac{z_0}{KH}\right)^3} \, d\tau$$

and $\tau* = Sech^{-1}\sqrt{\frac{z_0}{KH}}$.

It has been shown that the integral I is approximately equal to (Ozhan, 1975):

$$I = \frac{1}{2}sech^{-1}\sqrt{\left(\frac{z}{KH}\right)\left(1 - \frac{z_0}{KH}\right)^3} \qquad (4.9)$$

Then, the final result giving the overtopping volume of a solitary wave unit dike width is obtain from (4.8) and (4.9) as:

$$\frac{Q\left(1 + \frac{H}{2d}\right)}{Hd} = \frac{0.6652}{\varepsilon}\sqrt{K^3\left(1 - \frac{z_0}{KH}\right)^3 sech^{-1}\left(\frac{z_0}{KH}\right)} \qquad (4.10)$$

where m=0.611 is used.

This equation includes two empirical coefficients ε and K. Laboratory experiments were designed to investigate the values of these coefficients together with their dependence on various parameters.

The geometries of model dikes and water depths used in each experimental group are shown in figure 4.8.
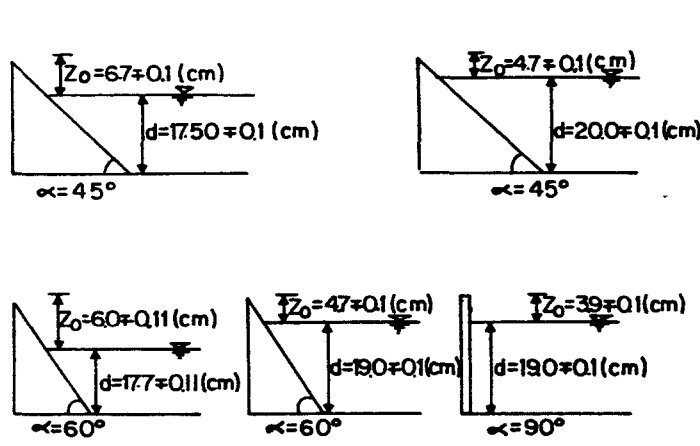
The shape coefficient, can be written as:

$$\varepsilon = \frac{Sech^{-1}\sqrt{\frac{z(t)}{z_{max}}}}{\sqrt{\frac{3H}{4d^3}Ct}} \qquad (4.11)$$

Figure 4.8. Geometries of model dikes

The values of ε for all three dike slope are plotted in figure 4.9 against H/z_0 ratio.
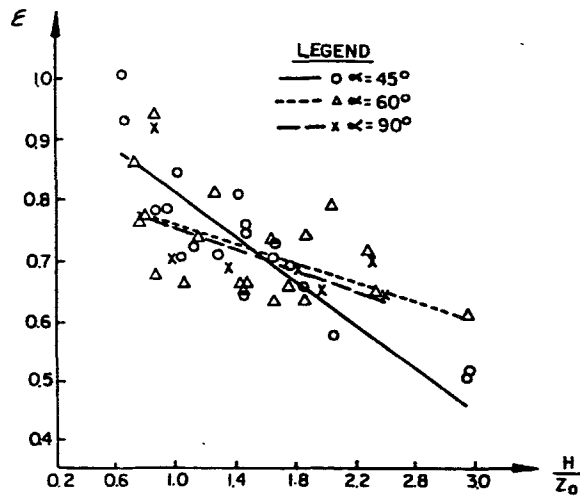
Figure 4.9. Values of shape coefficient

The maximum rise coefficient, obtained are compared with the respective K_m values corresponding to the maximum recorded level in fig. 4.10.

Figure 4.10. Comparison between theoretical and measured rise coefficient

It is observed that two values are correlated reasonably well. In line with expectations, the maximum rise coefficients computed from the theoretical model by using the measured overtopped volume are larger by 9% on the average that the respective K_m values. This is due to 3 cm distance between the measurement location and the dike crown.

The least square lines for ε and K were used in the analytical expression (Eq.4.10) to compute the dimensionless volume of overtopping as a function of $H/z_{p\,ratio}$. The resulting curves for three dike slopes tested are compared with the experimental data in figure 4.11.

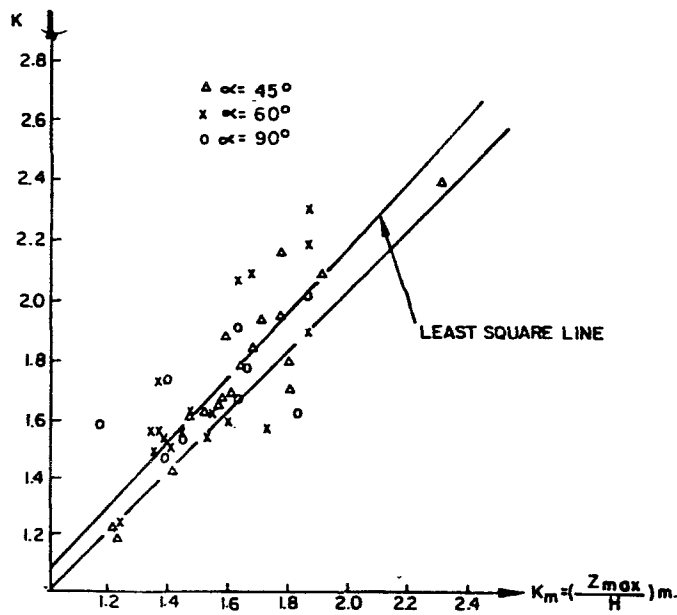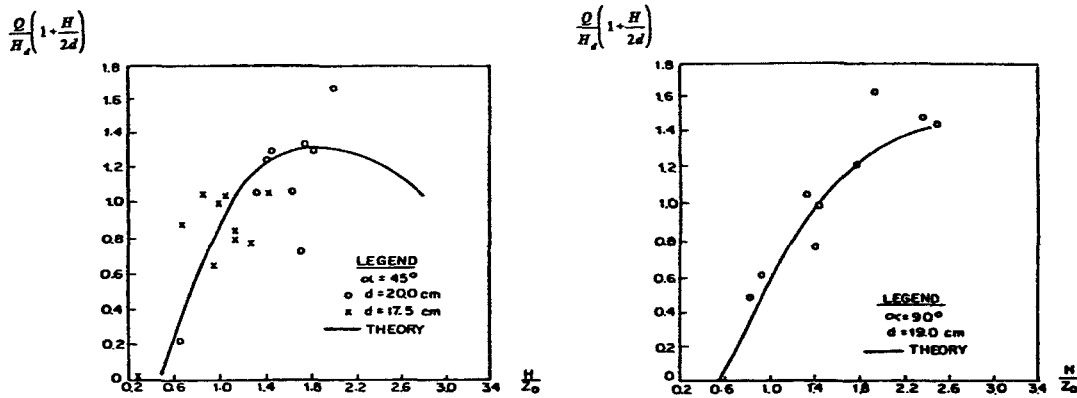*Figure 4.11.Comparison between the measured and calculated overtopping volume , α 45 and 90*

For comparison of solitary wave overtopping with that of regular waves, it is necessary to define a practical wave period for the solitary wave. This may be done as the time length over which a certain percentage of solitary wave volume passes a fixed point. The resulting expression reads as:

$$T_p = \frac{\sqrt{\dfrac{q}{d}\tanh^{-1}(\rho)}}{\dfrac{\sqrt{3}}{4}\sqrt{\dfrac{H}{d}\left(1+\dfrac{H}{2d}\right)}} \qquad (4.12)$$
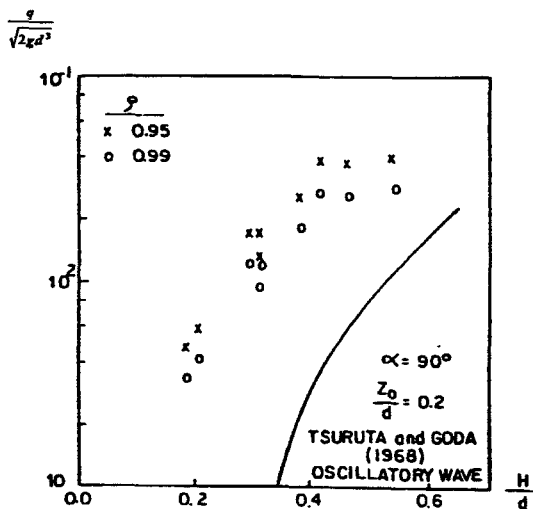
Figure 4.12. Solitary and oscillatory wave overtopping for a vertical dike

The reanalysed experimental data in this manner for the vertical dike is compared in fig.4.12 with the curve for regular oscillatory waves given by Tsuruta and Goda (1968). In this comparison, q is the average overtopping discharge over a wave period. The experimental data for solitary waves are plotted twice by using practical wave periods determined form two volume percentages, namely 95% and 99%. The presentation in figure 4.12 reveals that the solitary wave overtopping rates are significantly in excess of the respective oscillatory wave discharges.

4.4. Sekimoto experiment (1994)

The characteristics of short term overtopping rate for a deep sea block armored seawall were investigated experimentally by Sekimoto Tsunehiro. He conducted two series of experiments . One is a series that seawall has low crown height and a wave grouping effect is investigated. Another experiments is a series that it has a high crown height and slope effect of amour unit is studied. From these experiments, it has to be consider the short term wave overtopping such as an artificial island.

Experiments were conducted in a wave flume with dimension of 0.6m in width, which is partly divided from a wave basin of 5m in wide, 34m in length and 1.2m in depth. At an end of basin, rubbles banked in 1:5 slope are posed in order to reduce reflected waves. Model seawall were set up in the flume. In the frame of the experiments it is supposed that a prototype water depth in front of the seawall is 22.5m. Considering the wave flume dimensions, the model scale of series one and two are assumed to 1/85.7 and 1/87.5 respectively.

One of two experiments is a series that seawall has low crown height and a wave grouping effect is investigated. A typical model section in series-one is shown in figure 4.5. Both a vertical and a block armored seawall are used in this series. The water depth in front of a model seawall was 26.3cm. Sea bed slope in front of a seawall is 1/1000. The tetrapods (58.9g) were used as armoured bocks and the same size blocks were used in all section. A crown height was 10.5cm. It is 9m in prototype scale and the slope of amour units is 1:4/3. Irregular waves which have Wallops type spectrum were act on model seawall.
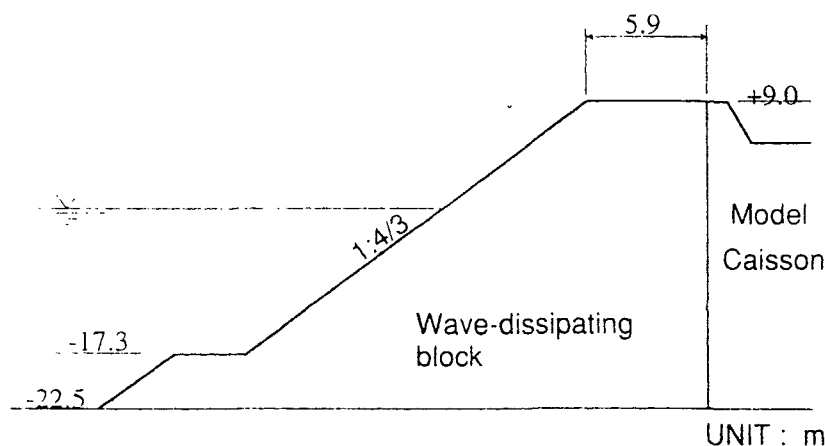

Figure 4.13.   *Typically model seawall*

Wallops type wave spectrum are of the form:

$$S(f) = \beta H^2_{1/3} T_P (T_p f)^{-m} \exp\left[-\frac{m}{4}(T_p f)^{-4}\right]$$ (4.13)

$$\beta \cong \frac{0.6238 m^{(m-2)/4}}{4^{(m-5)/4}\Gamma[(m-1)/4]}[1 + 0.7458(m+2)^{-1.057}]$$ (4.14)

$$T_p \cong T_{1/3}[1 - 0.283(m-1.5)^{-0.684}]$$ (4.15)

where:

m	= spectral shape factor	[-]
$H_{1/3}$	= significant wave height	[m]
$T_{1/3}$	= significant wave period	[sec]
T_p	= peak wave period	[sec]
Γ	= gamma function	[-]

The shape factor *m* become small, the bandwidth of wave spectrum becomes narrow, while the m is large, the band widths of wave spectra become wide. In the case that m=5 , Wallops type wave spectrum corresponds to Modified Bretschneider-Mitsuyasu type wave spectrum modified by Goda. The experimental cases are shown in Table 4.1.

Table 4.1. Experimental case for series 1

$T_{1/3}$(s)	$H_{1/3}$/hc	vertical seawall			block armored seawall		
		m=3	m=5	m=9	m=3	m=5	m=9
1.73 (16.0)	0.60	O	O	O	O	O	
	0.74	O	O	O	O	O	
	0.89	O	O	O	O	O	
	1.04	O	O	O	O	O	
	1.19	O	O		O	O	

The three types of spectral shape factor m=3.5 and 9 were selected. The wave period was 1.73 second and five kinds of wave height were used. The wave height normalized by the crown height were changed from 0.65 to 1.42.

Another experiments is a series that it has crown height and slope effect of amour unit is studied. Assuming an actual wave overtopping condition, the mean wave overtopping rate set below 0.05m³/m/s in prototype scale in the condition that the significant wave height normalized by crown height is 0.684, and significant wave period is 16s in this series.

The Wallops type wave spectra were also used in this series. In this series, the shape factor of incident wave spectra is selected m=5. The wave heights normalized by the crown height were changed from 0.46 to 0.91 and three wave periods 1.28s, 1.71s and 2.14s in experimental scale

were used, which were 12s, 16s and 20s second in prototype scale respectively. Experimental condition is shown in Table 4.2.

Table 4.2. Experimental case for series 2

$T_{1/3}$ (sec)	$H_{1/3}/h_c$	Slope of block armour units				
		1:4/3	1:1.6	1:1.8	1:2.0	1:2.5
1.28	0.456	O				
	0.548	O	O	O	O	O
	0.639	O	O	O	O	O
	0.684	O	O	O	O	O
	0.730	O				
	0.812	O	O	O	O	O
	0.913	O	O	O	O	O
1.71	0.456	O				
	0.548	O	O	O	O	O
	0.593	O				
	0.639	O	O	O	O	O
	0.684	O	O	O	O	O
	0.730	O				
	0.776	O				
	0.821	O	O	O	O	O
	0.913	O	O	O	O	O
2.14	0.456	O				
	0.548	O	O	O	O	O
	0.593	O				
	0.639	O	O	O	O	O
	0.684	O	O	O	O	O
	0.730	O				
	0.821	O	O	O	O	O
	0.913	O	O	O	O	O

In order to get the short term overtopping rate, a time dependent weight of water was measured using the measurement apparatus which was used by Sekimoto et al.(1994).
The short term wave overtopping rate measured with it is:

$$q_n(t) = \frac{1}{nT1/3} \int_{-nT_{1/3}/2}^{nT_{1/3}/2} q_i(t+\tau)d\tau, \quad n=1,3,5 \tag{4.16}$$

where:

    $q_i(t)$ = instantaneous wave overtopping quantity   [m^3/sec/m]

    $q_n(t)$ = n-wave mean overtopping rate   [m^3/sec/m]

$$q_{n-max} = Max[q_n(t)] \tag{4.17}$$

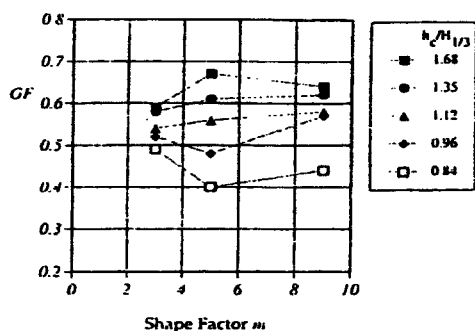 $T_{1/3}$ = significant wave period   [sec]

Figure 4.14. shows the relationship between spectral shape factor m and groupiness factor. there is no clear relationship in both. in the case of high wave height, wave breaking is occurred and groupiness factor is relatively small.

Figure 4.14. Relationship between spectral shape factor m and groupiness factor

In figure 4.15. the mean wave overtopping rate normalized by wave height is plotted against the spectral shape factor m. In this figure, the wave height is measured on the position of seawall in the condition that the model seawall dose not up. On left hand side of this figure, the results of vertical wall type seawall are shown and on the right hand side the results of block armored seawall are shown. *The mean wave overtopping rate have tendency of increase while spectral band width become narrow.*
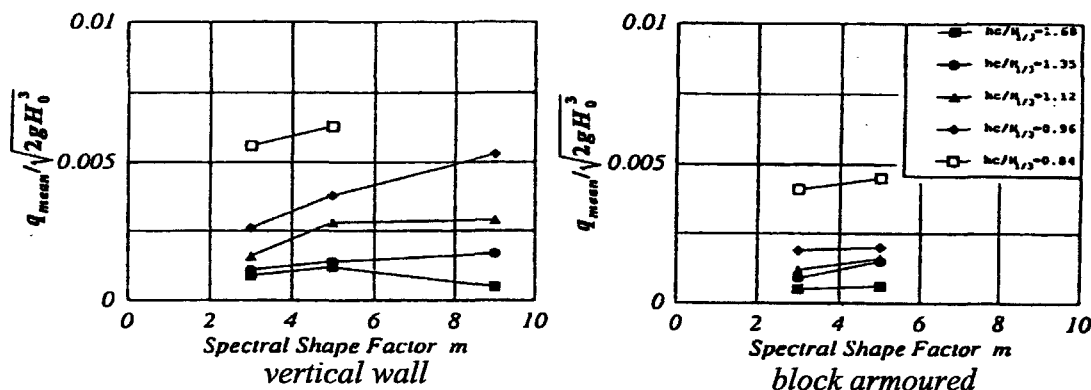
Figure 4.15. Relationship between the mean wave overtopping rate and the spectral shape factor

The relationship between wave-overtopping rate and groupiness factor is compared in figures 4.16 and 4.17. On the left hand side of this figure, the results of vertical wall type seawall are shown and the right hand side the results of block armoured seawall are shown. The results show the strong relationship between both is available. In the case of the same wave height, the wave overtopping also increase as the wave groupiness increase.
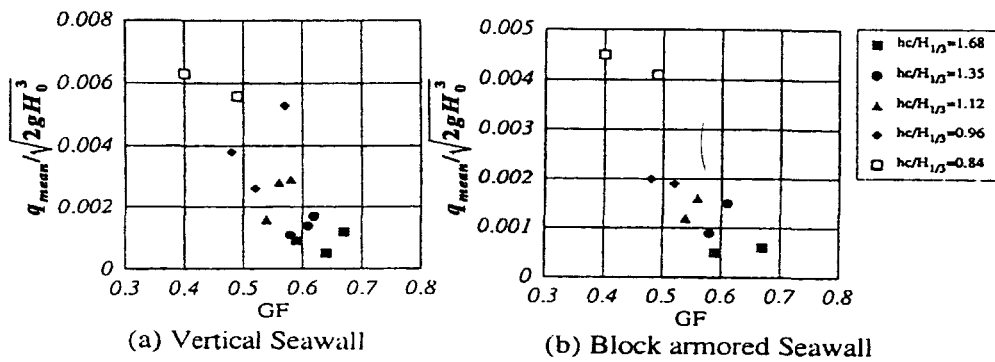
Figure 4.16. Relationship between the mean overtopping rate and the groupiness factor
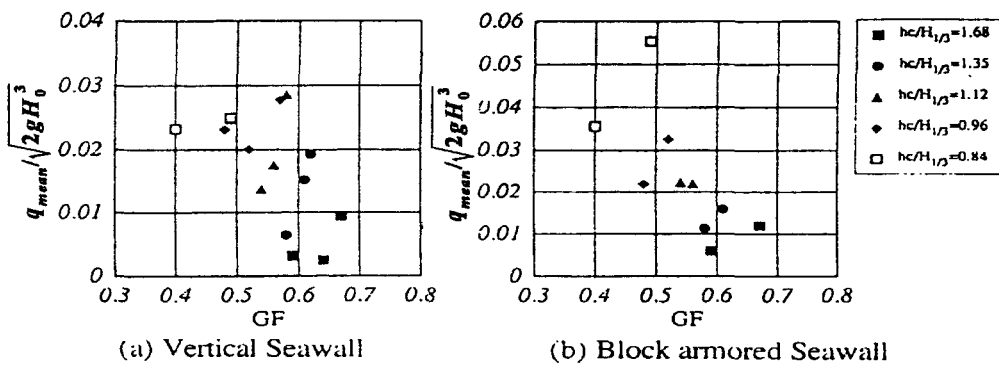
Figure 4.17. Relationship between the maximum wave overtopping rate and the groupiness factor

Figure 4.18 shows the case of mean wave overtopping rate. The mean wave overtopping rate has one to one correspond to maximum wave height. The relationship between the mean wave overtopping rate and an inverse of the slope in each wave period had investigated by Sekimoto et al. (1994). According to this study, the tendency of these relationships is similar to the results of Saville's run-up experiment (1952). That is the mean overtopping rate is small when the slope is steep. As the slope becomes mild, the mean overtopping rate becomes large. The slope further becomes mild, the mean overtopping rate decreases.

Figure 4.18. Relationship between the mean overtopping rate and the maximum wave height

4.5 Donald L. Ward experiment (1994)
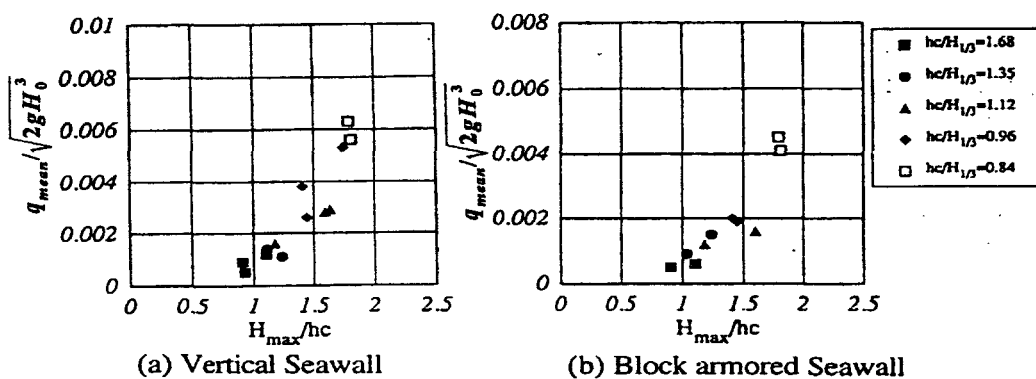
The study of D.L.Ward is evaluating effects of wind on overtopping of coastal structures through physical model studies conducted in a combined wind/wave flume .Analysis of the data should lead to a better understanding of the physical of wind effects on coastal structures.
Physical model tests have been conducted in a 36m long, 0.61m wide and 0.91m deep glass-walled wave flume equipped with a flap-type mechanical wave generator. The electrically-activated wave generator is capable of producing monochomatic wave trains as well as spectral wave trains through a computer-generated signal.

A series of tests with monochomatic wave conditions were performed to compare run-up and overtopping rates without wind to run-up and overtopping rates when wind of different intensities is added to monochromatic wave conditions. Mechanically-generated waves used in these tests had frequencies of 1.0Hz, 0.57Hz and 0.4 Hz. Waves generated by wind had a frequency of about 2.0 Hz at the toe of the test revetment. Because the mechanically generated waves had a different frequency than waves generated by wind, the result was a bi-modal spectrum comprised of a sharp, low-frequency monochromatic peak for the mechanically generated wave and a broader, high-frequency peak for wind generated waves.
Although crest of a wave from each wave train may coincide to produce a maximum wave height, it is just as likely that a wave trough from one wave train will coincide with a crest from the other wave train. The effect of the wind-generated wave train on overtopping rate, which is time-averaged, is therefore expected to be less significant that effect of wind on maximum run-up. This is illustrated in figure 4.19, which shows overtopping rates for a fixed revetment crest elevation of 60cm (10 cm above SWL).
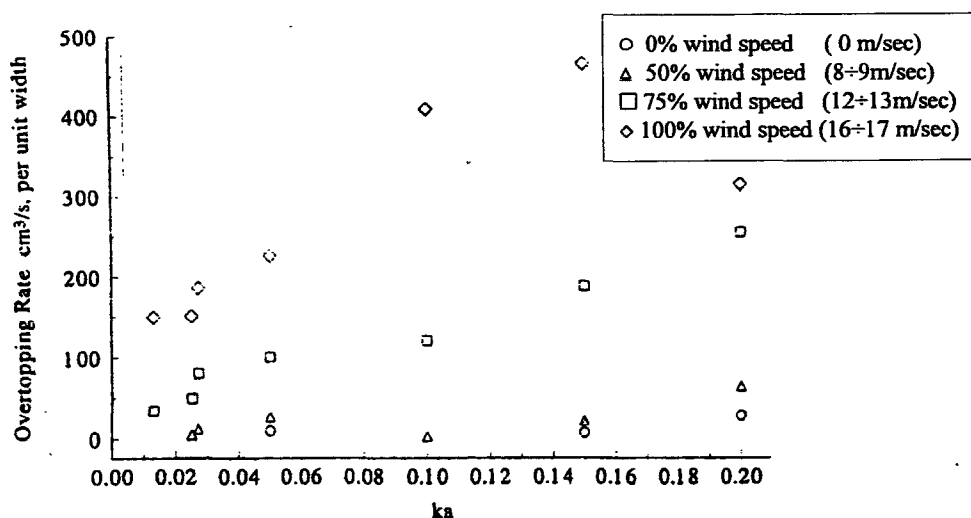

Figure 4.19. Overtopping rate for different wind speeds tested

Table 4.3. Wave steepness, period and height for each set of
test conditions

Ka	Wave period (sec)	Wave height (cm)
0.013	2.50	2.2
0.023	2.50	3.8
0.029	1.75	3.2
0.049	1.75	5.4
0.104	1.00	5.0
0.146	1.00	7.0
0.208	1.00	10.0

The 50% wind speed had little effect on overtopping rate, although larger increases were observed at 75% and 100% wind speeds. The sharp decrease in overtopping rate for maximum wind speed and wave steepness between 0.146 and 0.208 is noteworthy. The mechanically generated wave for ka=0.208 was 1.0 sec, 10cm wave (Table 4.3). At 100% wind speed, the 10cm waves broke before reaching the revetment.

It is seen in figure 4.19 that the increase in overtopping rate with wind is much greater for waves tested with a period of 1.0 sec. (0.10≤ ka ≤ 0.20) that for tests with wave periods of 1.75 sec or 2.5 sec. An explanation for this may be found in figure 4.20.
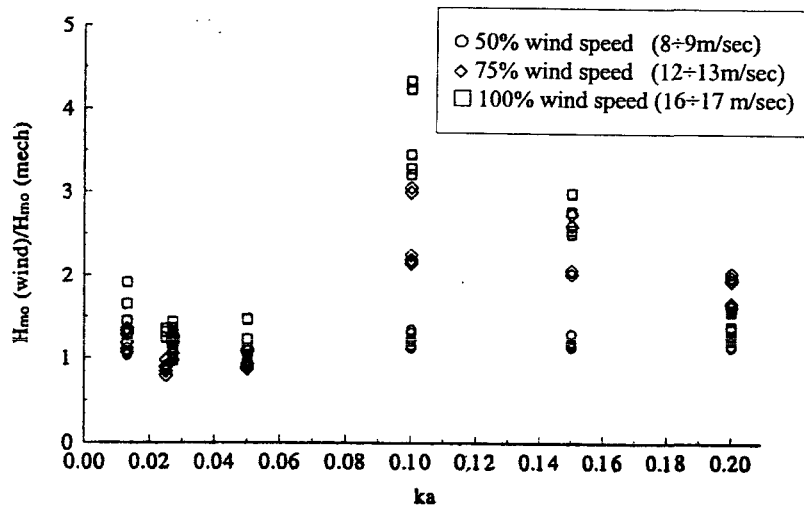
Figure 4.20. Wind effect on H_{mo} of mechanically generated wave

Figure 4.20 show the change in H_{mo} of the mechanically generated wave under the influence of wind. Because the frequency of wind waves ($\approx$2 Hz) differs significantly from frequencies of the 1.75 sec or 2.5 sec waves, wind is seen to have little effect on H_{mo}'s of the longer waves. However, the frequency of the wind waves is relatively close to the frequency of 1.0 sec waves, and wind energy is seen to have a significant effect on the H_{mo} of the 1.0 sec waves.

4.6.   Peter Sloth and Jorgen Juhl experiment (1994)

The authors has been carried out a series of flume tests at the Danish Hydraulic Institute with the aim of studying the volumes of individual wave overtopping of traditional rubble mound breakwater with an armour layer slope of 1:2.

Tests were carried out varying the crest width, the crest free board, the significant wave height and the peak wave period. For each test, the mean overtopping discharge was calculated based on the sum of the individual overtopping volumes. An expression of the mean overtopping discharge as function of the significant wave height, wave steepness, crest width and crest free board was established from these data. Subsequently, the individual overtopping data for each test were fitted to a three parameter Weibull distribution function including the mean overtopping discharge and the probability for a wave resulting in overtopping.

Physical model test have been carried out in a 22 m long and 0.6 m wide wave flume (as can be seen in figure 4.21) with the aim of measuring the overtopping volume for individual waves per unit length of the breakwater, $V(m^3/m)$.
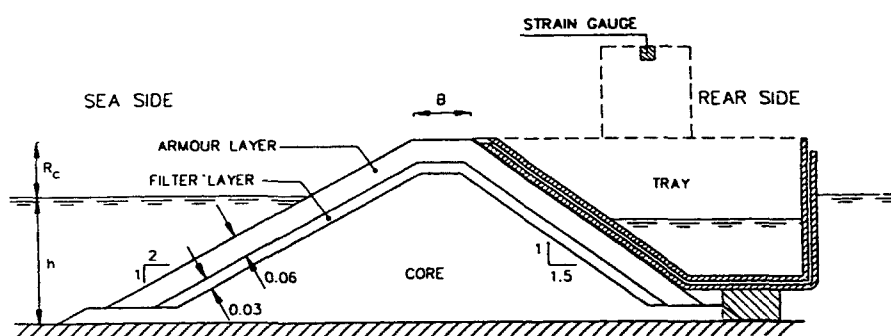
Figure 4.21. Typical cross section of breakwater used in overtopping tests

A summary of the test conditions (model measures.) for the 75 tests performed as part of the research is presented below:

Significant wave height, H_s	0.05 to0.11 m	[m]
Peak wave period, T_p	1.0 to 2.0 s	[sec]
Wave steepness, S_{op}	0.018 and 0.03	[-]
Crest free board, R_c	0.1, 0.075, 0.05 m	[m]
Width of crest, B	0.16, 0.21 and 0.26 m	[m]
Slope angle, cot(α)	2.0	[-]

The wave steepness is given by the ratio between wave height and the deep water wave length calculated on basis of the peak wave period:

$$S_{op} = \frac{H_s}{L_{op}} = \frac{2\pi}{g} \frac{H_s}{T_p^2}$$ (4.17)

The dimensionless free board, defined as R_c/H_s, varied between 0.55 and 1.30, which means that the tests were carried out with relative low-crested breakwater.

The overtopping water was collected in a o.6 m wide tay located immediately behind the breakwater in a level corresponding to the crest elevation of the breakwater. This means that the recorded wave overtopping refers to water overtopping the rear edge of the breakwater crest. Finally, the total amount of overtopping water was measured after each test and compared to the sum of all individual overtopping. Based on the total amount of wave overtopping, the mean overtopping discharge, q, was calculated.

Through the yearly overtopping results have been presented in numerous waves including dimensionless plots. The most used dimensionless parameters are the dimensionless overtopping discharge, $Q=q/\sqrt{gH_s^3}$ and the dimensionless free board, $R=R_c/H_s$.

Figures 4.22 and 4.23 show plots of data for two different wave steepnesses, and it was found that the dimensionless free board, R_c/H_s is not a proper parameter to be used as also the crest width, B, has an influence on the overtopping quantities for rubble mount breakwater. Various combinations of the crest free board and crest width have been plotted in order to describe the combined influence of these two parameters.
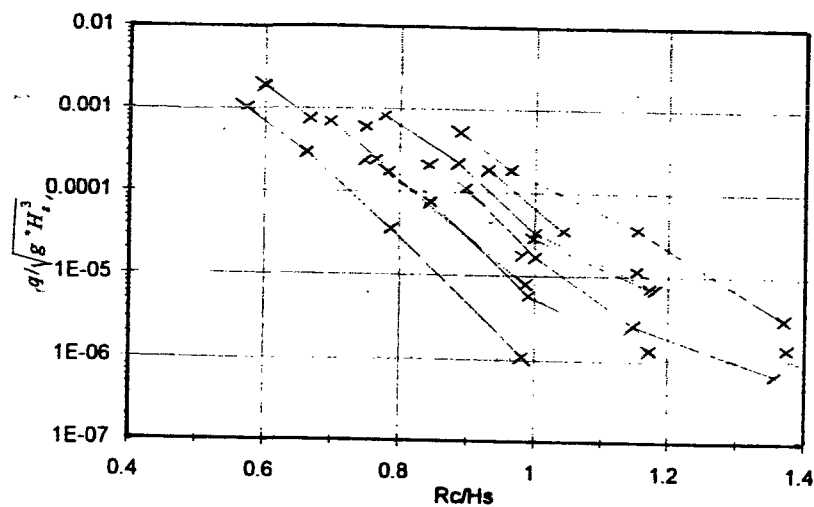
Figure 4.22. Dimensionless overtopping discharge for Sop=0.018
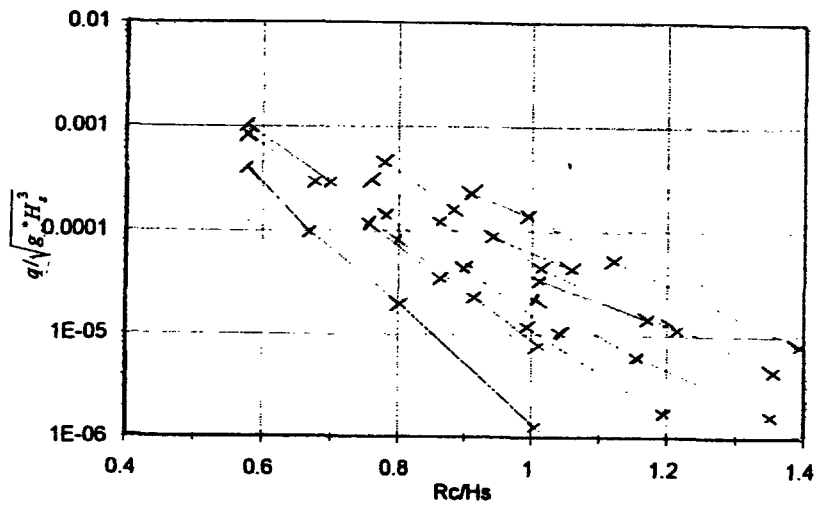
Figure 4.23. Dimensionless overtopping discharge for Sop=0.030

For a fixed wave steepness, it was found that the dimensionless mean overtopping discharge can be fitted well to an exponential function using $(2 R_c + 0.35B)/H_s$ as parameter.

Figure 4.24 show plots of the measured data for the wave steepnesses of 0.018 used in the present study.
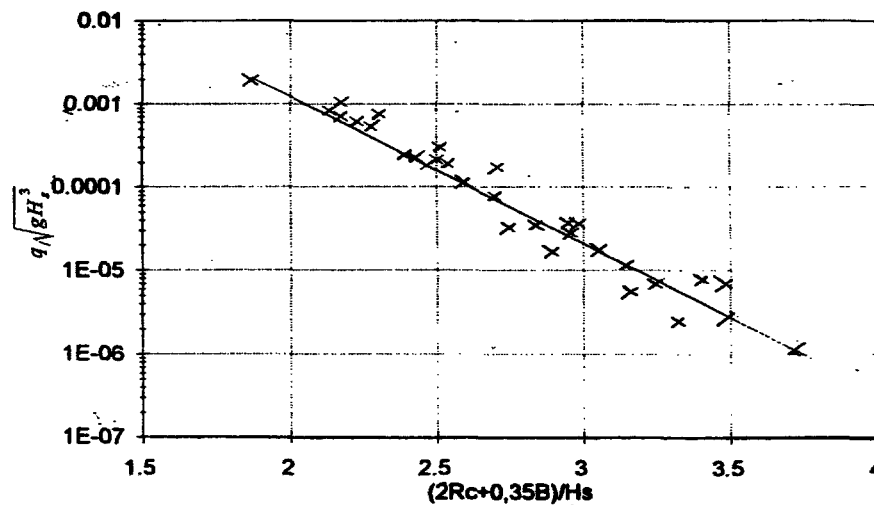
Figure 4.24. Dimensionless overtopping discharge as a function of dimensionless parameter(2Rc+0.35B)/Hs. Legend x:measured,-:calculated

Combining all the above described correlations, an expression of the mean wave overtopping discharge has been established:

$$\frac{q}{\sqrt{gH_s^3}} = \exp\left[(-17.6 - 4.74\ln\ S_{op}) + (2.96 + 1.75\ln\ S_{op})\left(\frac{2R_c + 0.35B}{H_s}\right)\right]$$ (4.18)

This equation has been plotted in fig. 4.24, and a very fine agreement was found to the measured data for both of the tested wave steepnesses. The deviations between measured and calculated values were found to be within ±50% for the major part of the data, whereas deviations up to 125% were found for the smaller overtopping discharges.

4.7. L. Franco, M. de Gerloni, J.W. van der Meer (1994-1995)

An extensive laboratory investigation on the overtopping performance of modern vertical-face breakwater has been started in Milano since 1989, With random wave flume model testing. Preliminary results were presented by de Gerloni et al. (1989, 1991).

Model tests were carried out in the 43 m long, 1,5 m deep random wave flume of ENEL SpA - Center for Hydraulic and Structural Research (CRIS) laboratory in Milano. The effects of each overtopping wave were analyzed by placing a few model cars and model persons along the center of the crown slab behind the wall, and by accurately observing the number of displacement and relative distance from the former position after each overtopping event (then repositioning the "targets"). To improve the statistical validity rather long test were used with no less than 1000 waves. Peak periode (T_p) of JONSWAP spectra (bimodal spectra were also generate) varied between 7 and 13 s, significant wave height (H_s)between 2.5 and 6 m with water depths/wave height ratios (h/H_{so}) ranging between 3 to 5. Model breakwater configuration are shown in figure (4.25). They include traditional vertical-face caissons, perforated ones (14%, 25%, 40% porosity), shifted sloping parapets and a caisson with rubble mount protection (horizontally composite) with variable elevation and width of the homogeneous porous rock berm (S_1 to S_6 in figure 4.25). All structures were designed for low overtopping conditions (i.e. high freeboard).

Additional results from model studies on similar structures designed in Italy and carried out by other European laboratories were included in the analysis, to enlarge the data set by covering a wider range of geometric and hydraulic conditions (H_s=2-8m, T_p=6-15s, h=9-18m). They were performed at Delft Hydraulics (DH) on vertical and shifted caissons and at Danish Hydraulic Institute (DHI) on perforated shifted-wall caissons. Further model test results from a research study on a simple vertical wall were supplied by CEPYC laboratory in Madrid. All these additional model test data typically only refer to the mean overtopping volumes.
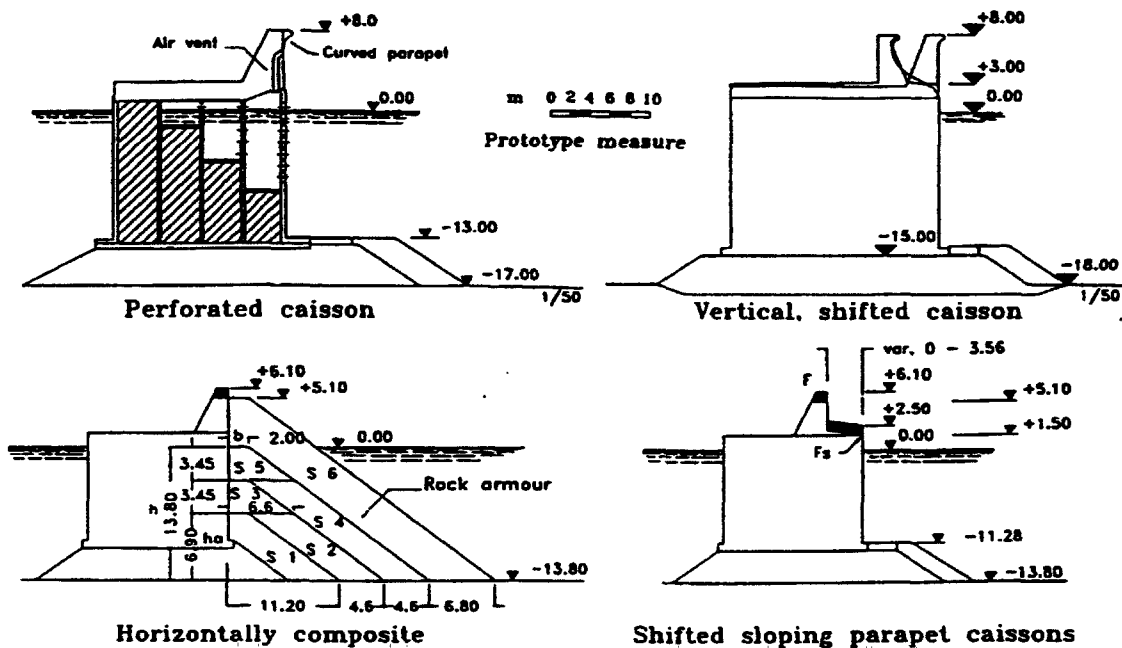
Figure 4.25. Model test sections of caissons breakwaters

For each breakwater configuration the individual overtopping volumes recorded in any tests were divided in classes of 0.1 m³/m and the corresponding effects on model cars and pedestrians were statistically evaluated for each class. Some results obtained for pedestrians are shown in figure 4.26. It is interesting to observe that the effect is dependent on the structure geometry itself. The same overtopping volume is likely to be more dangerous if the breakwater is purely vertical that in the case of perforated or shifted-parapet caissons or horizontally composite ones. This is probably due to the different overflow mechanism which produces a more concentrated and fast water jet falling down from the crest of a vertical wall in comparison with a slower, more aerated, horizontal flow over a sloping structure.
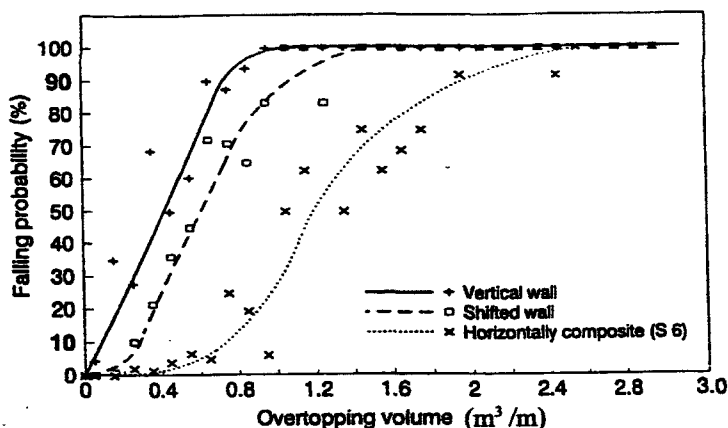
Figure 4.26. Risk curves for pedestrians on caisson breakwaters from model tests

From figure 4.27 it can be seen that the "critical bands" of overtopping volume (being dangerous above the upper limit and safe below the lower one) lie between 0.2 and 2.0 m³/m (but a concentrated jet of 0.05 m³/m on the upper body can be enough to make a person fall down as shown by the full scale calibration tests).
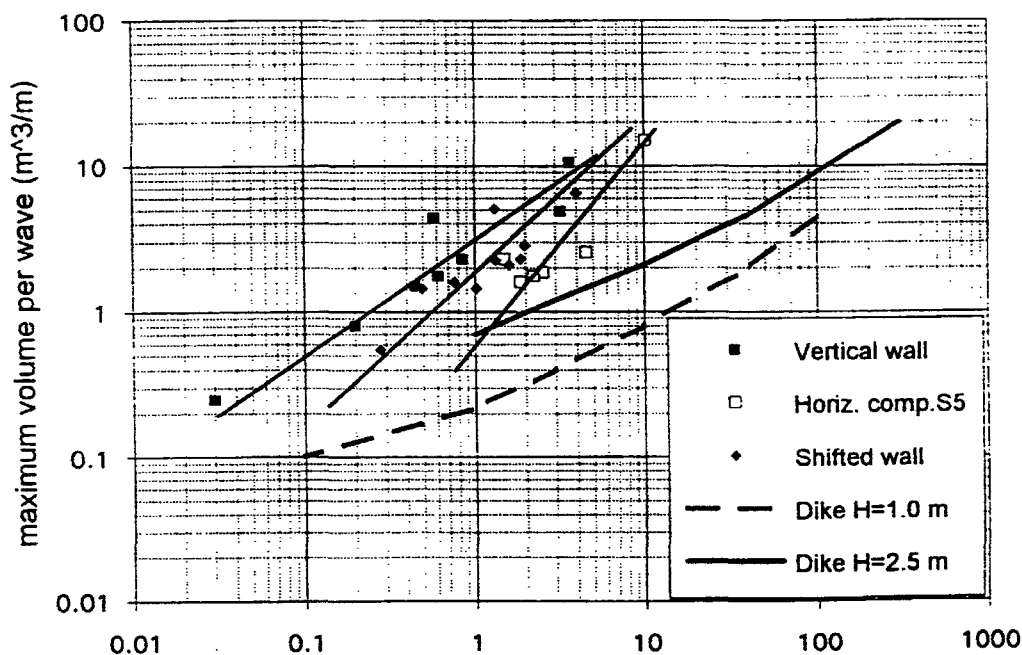
Figure 4.27. ***Relation between mean discharge and maximum overtopping volume***

It is confirmed the significant parameter for the breakwater functional safety is the overtopping volume rather than the mean discharge. A relationship exists between the two parameters but it varies with the structure geometry and wave conditions.

Figure 4.28. ***Correlation between the percentage of overtopping waves and the relative freeboard.***

The method of analysis proposed by van der Meer and de Waal (1992) to derive a general design formulas was applied to the tests results (restricted to a wave steepness range of 0.018-0.038) in terms of mean overtopping discharge allowing a direct comparison with the a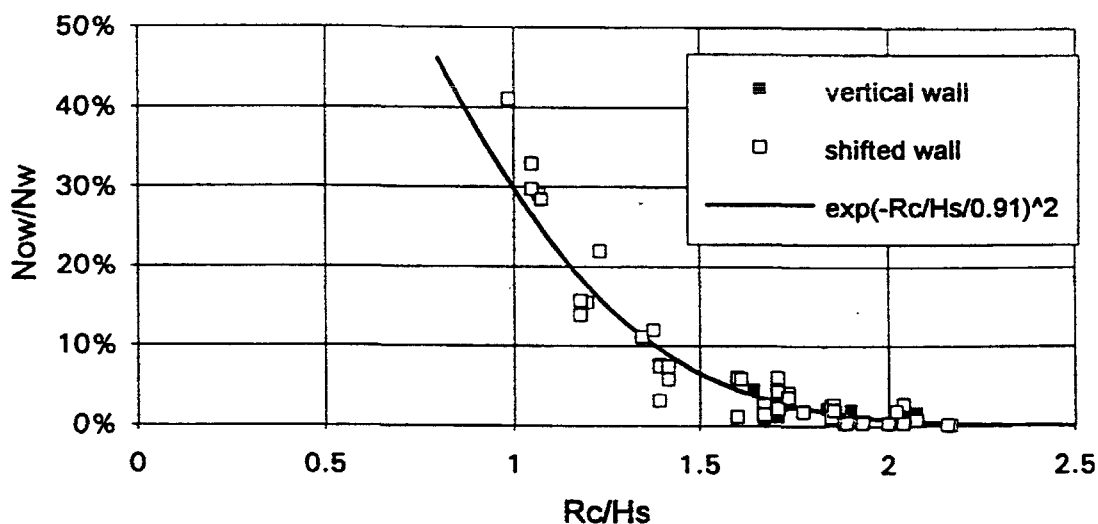bove admissible limits and an easy evaluation of the overtopping volumes per wave with eq. (4.18) and (4.19). Overtopping event occure unevently both in time and amount, often just a few waves overtopping among the thousands. The measurement of the individual overtopping volumes carried out during the model tests allowed the definition of their probability distribution. The exceedence probability of each overtopping volume is :

$$P_v = 1 - \frac{i}{N_w + 1} = C \cdot \exp\left(-\frac{V}{A}\right)^B = \exp\left(-\frac{V-C}{A}\right)^B \tag{4.18}$$

in wich:

$$A = 0.84 \cdot \overline{V} = \frac{0.84 \cdot T_m \cdot q}{\dfrac{N_{ow}}{N_w}} \tag{4.19}$$

P_v	= exceedance probability	[-]
N_w	= number of wave in the test	[-]
N_{ow}	= number of overtopping waves	[-]
V	= volume in the ith rank	[m³]
A,B,C	= fitting constants	[-]

Consistent curves have been fitted with the least square method to the experimental data representing the dimensionless mean overtopping discharge $Q = q/\sqrt{g * H_s^3}$ against the relative freeboard R_c/H_s, which is the most important parameter. Since an exponential relationship is assumed according to Owen (1980), the data should give a straight line on a log-linear plot:

$$Q = a \, \exp\left(-\frac{bR_c}{H_s}\right) \tag{4.20}$$

From figure 4.29 can be deducted that for vertical-face breakwater b=4.3 and a=0.192, which is close to the one found by van der Meer and Janssen (1994) for sloping structures (a=0.2); the value a=0.2 was then kept constant for the successive regressions with different geometries which generally showed a high correlation coefficient.

The physical interpretation of "a" is the dimensionless mean discharge when the freeboard is set at the mean water level.
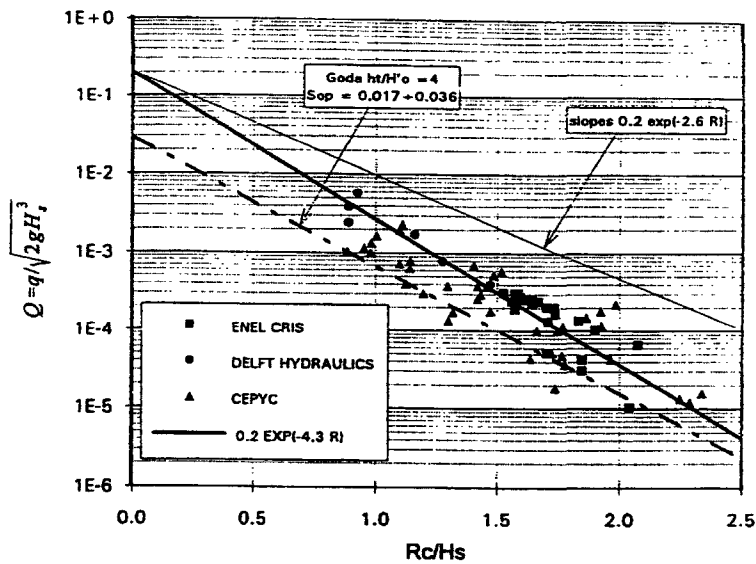
Figure 4.29. Regression of wave overtopping data for vertical wall breakwaters

Then the influence of structural modifications with reference to the vertical-face breakwater can be described by suitable freeboard reduction factors (γ), which are the ratios between the reference value b=4.3 and the various b coefficients fitted by eq.(4.20) as given in figure 4.30.
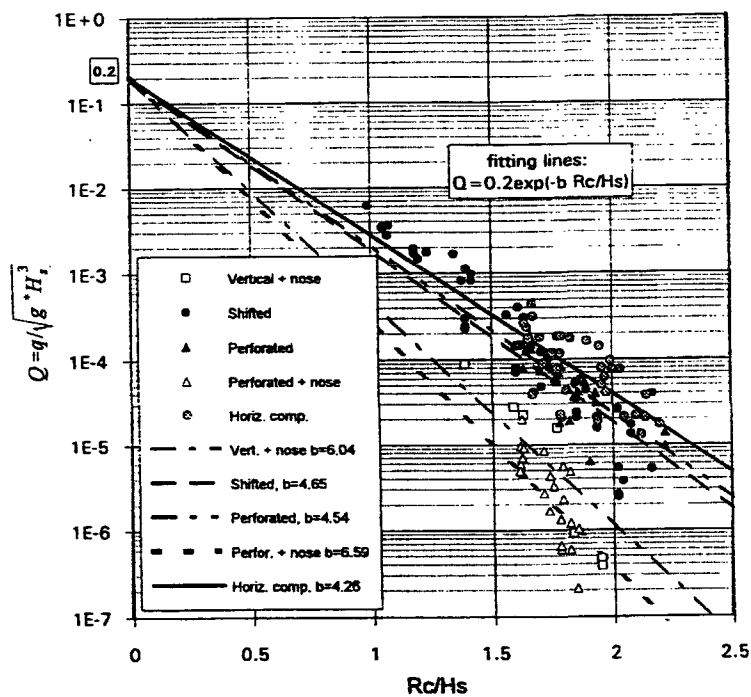
Figure 4.30. Wave overtopping data for different types of caissons breakwaters

All the data can be plotted together (figure 4.31) after correction of the R_c/H_s values for each geometry with the corresponding γ, the general equation thus becoming:

$$Q = 0.2 \ \exp\left(-\frac{4.3}{\gamma}\frac{R_c}{H_s} \right)$$

(4.20)

which can be effectively used for the preliminary design of vertical breakwater.
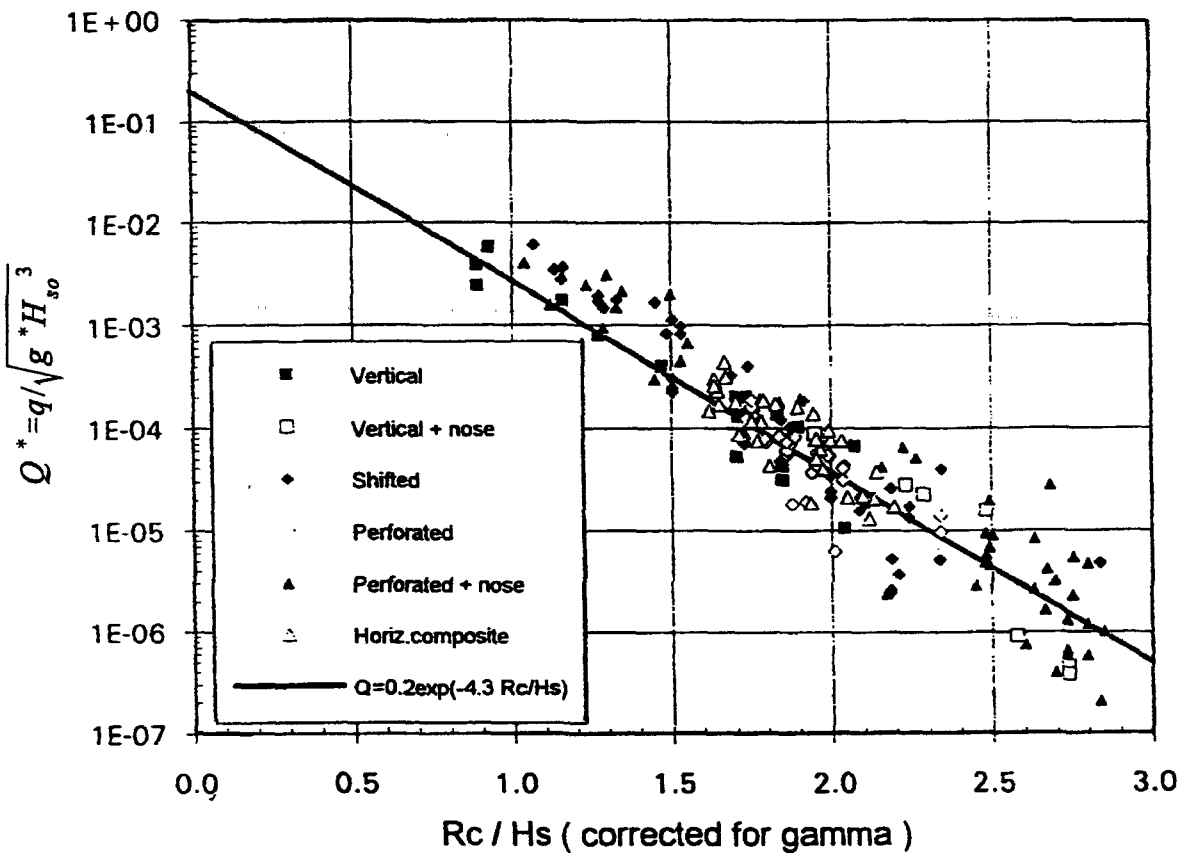
Figure. 31. Wave overtopping on vertical and composite breakwaters: conceptual design graph.

The reliability of the formula (4.21) can be given by taking the coefficient 4.3 as a normally distributed stochastic variable with a standard deviation $\sigma = 0.3$.

From the influence factors of the various caisson geometries, as compared to the plain vertical wall some useful engineering conclusions can be deduced:

- the greatest overtopping reduction can be achieved by introducing a recurved parapet (nose) at the crest of a vertical front wall: the corresponding $\gamma_n = 0.7$ means a 30% crest elevation reduction to get the same overtopping rate; this may however be limited to relatively small dischargers:

- for simply perforated or shifted caissons the freeboard saving is only 5-10%;

- if a nose is adopted at the crest of a perforated caisson, then the combined reduction factor can achieve 0.65, while its effect on a shifted parapet is negligible;

- the overtopping of horizontally composite breakwaters is influenced by porosity, slope, width and elevation of the mount. Overtopping increases if the armour crest is below or at mean sea level (max $\gamma_{s5} = 1.15$).

5. Comparison of the formulas

5.1. Generalities

As it can be seen from the previous paragraphs there are available a range of formulas for computing the overtopping discharge over a structure. Since now could not be determined a general formula for this phenomena. All the formula available are applicable in certain condition and for a specific structure. They were determined after experimental tests in empirical format. Making the following quotation:

H_s	- wave height	[m]
T	- wave period	[sec]
L_o	- wave length in deep water	[m]
h	- water depth at the structure	[m]
Q_b	- dimensionless overtopping discharge for breaking wave	[m³/sec/m]
Q_n	- dimensionless overtopping discharge for non-breaking wave	[m³/sec/m]
R_b	- dimensionless crest height for breaking wave	[-]
R_n	- dimensionless crest height for non-breaking wave	[-]
R_c	- free crest height	[-]
R_u	- run-up	[m]

The presented formulas are:

A. For dikes and vertical walls with slopping structure in front:

     - after *Dutch guidelines* (eq. 3.54):

$$Q_b = 0.06e^{-4.7R_b}$$

$$Q_n = 0.2e^{-2.3R_n}$$

$$where: \begin{cases} R_b = \dfrac{R_c \cdot \sqrt{S_{op}}}{H_s \, \tan\alpha} \cdot \dfrac{1}{\gamma_b \cdot \gamma_h \cdot \gamma_f \cdot \gamma_\beta} \\[4mm] R_n = \dfrac{R_c}{H_s} \cdot \dfrac{1}{\gamma_b \cdot \gamma_h \cdot \gamma_f \cdot \gamma_\beta} \end{cases}$$

-after *Saville* (eq.3.34)

$$Q = \frac{\sqrt{gQ_o^{*} \cdot H_0^{3}} \cdot e^{-\left(\frac{0.217}{\alpha} \cdot \tanh^{-1}\left[\frac{R_c}{R_u}\right]\right)}}{\sqrt{g \cdot H_s^{3}}}$$

where α and Q_o^{*} are read from graphs given in annexes 1-6 and run-up is depending on

$$R_u = f(H_o, h, T, k)$$

-after *Yoshimichi* (eq. 3.66):

$$Q_b = \frac{T \cdot c \cdot \left[\frac{X_o}{R_u} - \cot\alpha\right] \cdot \left[\frac{(R_u - H_s)^2}{2}\right]}{\sqrt{gH_s^{3}}}$$

$$Q_n = \frac{0.65 \cdot T \cdot (R_u - H_s)^2}{\sqrt{gH_s^{3}}}$$

in which c, X_0/R_u and H_b are computed with the following formulas:

$$R_u = \left(1 + \pi \frac{H_s}{L_o} \cdot \coth\frac{2\pi H_s}{L_o}\right) \cdot H_o$$

$$\frac{X_o}{R_u} = \cot\left[\alpha - \arctan\left(\frac{h_m \cdot \sin\alpha}{R_u}\right)\right]$$

$$c = 0.1 \cdot \left(\frac{L_o}{H_b}\right)^{1/3} \cdot \cos\alpha$$

$$H_b = (\tan\alpha)^{0.2}\left(\frac{H_o}{L_o}\right)^{-\frac{1}{4}} \cdot H_o$$

h_m = constant depending on H_b and $\cot\alpha$ is given in figure 3.17 of the report;

- after *Richard Weggel* the formulas are identically with those one deduced by Saville only that the coefficients α and Q_o^{*} are determined different;

- after *Silvester* (eq.3.91):

$$Q = \frac{\sqrt{2} \cdot \frac{2}{15} \cdot m \cdot \left(\frac{R_u}{H_s}\right)^{3/2} \cdot (1 - R)^{5/2} \cdot T}{\sqrt{gH_s^{3}}}$$

where:

m   = discharge coefficient for flow over the weir   [-]

B. For vertical walls:

-after *van der Meer* (eq. 3.97):

$$Q = c_1 \cdot e^{-c_2 \cdot R}$$

$$where \begin{cases} non-breaking \quad waves: \begin{cases} c_1 = 0.06 \cdot \sqrt{\dfrac{\tan\alpha_s}{S_{op}}} \\[3mm] c_2 = 5.2 \cdot \dfrac{\sqrt{S_{op}}}{\tan\alpha} \end{cases} \\[8mm] breaking \quad waves \begin{cases} c_1 = 0.2 \\ c_2 = 2.6 \end{cases} \end{cases}$$

- after *Goda* (eq. 3.42):

$$Q = 0.1 \cdot \beta^{3/2} \cdot \left[1 - \beta \cdot \frac{R_c}{H_o}\right]^{5/2} \cdot \sqrt{2 \cdot \left(\frac{H_o}{H_s}\right)^3}$$

$$where \quad \beta = \frac{H_o}{h_t}$$

-after *Saville, Silvester and Weggel* is the same formula as for dikes;
-after *Takada* (eq. 3.1):

$$Q = \frac{\dfrac{4}{15} \cdot \sqrt{2g} \cdot K \cdot \sqrt{(R_u - R_c)^3} \left[\left(1 - \dfrac{R_c}{R_u}\right) \cdot 0.20 + 0.125\right] \cdot T}{\sqrt{gH_s^3}}$$

K   = average coefficient of wave overtopping discharge

It should be mentioned that the term which represents the run-up R_u has specific formulas for each case. All overtopping discharges formula are dimensionless, using the same term for doing this. The term used was $\sqrt{gH_s^3}$.

5.2. Comparison for dikes and vertical walls with sloping structure in front

In order to compare how much is the difference in value for this formulas it should be processed numerical data through them. So, for a dike with the given data shown in Table 1. The obtained results are also shown in Table 5.1. and in Figure 5.1 . It can be seen that the only value which is in big difference with the others is that one given by Saville's formula.

Table 5.1.Dimensionless overtopping discharge for dikes and vertical walls with sloping structures in the front

Given data:

Hs=	3	m			
Rc=	3.5	m			
h=	6.5	m	Ho=	3.7	m
T=	8	sec	Lo=	99.8	m
Sop=	0.030				
cot theta=	3				

Dutch guidelines (eq 3.54)			U.S.A. (Saville)(eq.3.34)			Yoshimichi (eq 3.66)			Silvester (eq 3.91)		
gamma	1.000	-	h/Ho	1.750	-	Lo=	99.8	m	Hs/L	0.030	-
Rn=	1.167	m	Ho/gt^2	0.006	-	Ho=	3.7	m	Ru/Hs	1.498	-
Rb=	0.606	m	R/Ho=*	4.200	-	alpha=	0.322	rad	Ru	4.495	m
Qn=	1.37E-02	-	K=*	1.145	-	Ru=	4.922	m	Rc/Ru	0.779	-
Qb=	3.47E-03	-	Ru=	17.862	m	Hb=	6.789	m	Q=	3.19E-02	-
qn=	2.22E-01	m3/s/m	alfa=*	0.055	rad	Hb/Lo=	0.068	-	q=	5.19E-01	m3/s/m
qb=	5.65E-02	m3/s/m	Qo*=*	0.014	-	hm/Hb=*	0.210	-			
			Hs/R	0.168	-	hm=	1.426	m			
			tanh-1=*	0.169	rad	Xo=	20.982	m			
			Q=	8.37E-02	-	c=	0.232	-			
			q=	1.36E+00	m3/s/m	Q=	3.33E-02	-			
						q=	5.42E-01	m3/s/m			

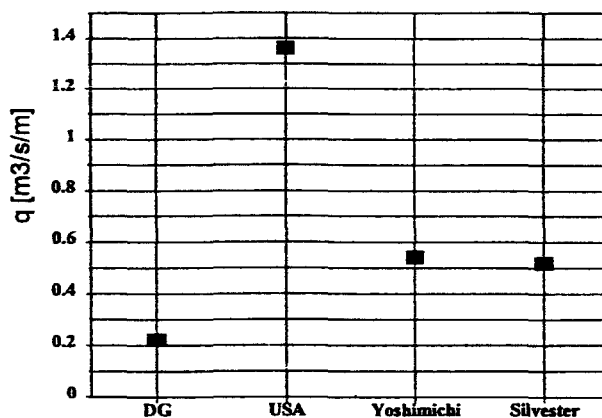*- means the values are read from graphs and tables from annex 1-9

Figure 5.1. Values for overtopping over dikes

5.3. Comparison for vertical walls

5.3.1. Between available formulas

In Table 5.2. and Figure 5.2. it is made the same comparison in the case of a vertical structure.

Table 5.2. Dimensionless overtopping discharge for vertical walls

Given data:

Hs=	3	m			
Rc=	2	m			
h=	6.5	m	Ho=	3.714286	m
T=	8	sec	Lo=	99.84	m
Sop=	0.030				
cot theta=	3				

van der Meer (eq 3.97)			U.S.A. (Saville) (eq 3.34)			Goda (eq 3.42)			Silvester (eq.3.91)		
gamma=	1.000	-	h/Ho=	1.750	-	Lo=	99.8	m	Hs/L=	0.030	-
R=	0.667	m	Ho/gt^2=	0.006	-	Ho=	3.7	m	Ru/Hs=	0.600	-
c1b=	0.200	-	R/Ho=*	2.400	-	Q=	2.47E-02	-	Ru=	2.400	m
c2b=	2.703	-	K=*	1.000	-	q=	4.02E-01	m3/s/m	Rc/Ru=	0.833	-
Qb=	3.30E-02	-	Ru=	8.914	m				Q=	3.98E-03	-
c1n=	0.2	-	alfa=*	0.068	-				q=	6.47E-02	m3/s/m
c2n=	2.6	-	Qo*=*	0.006	-						
Qn=	3.53E-02	-	Hs/R=	0.337	-						
qb=	5.37E-01	m3/s/m	tanh-1=*	0.353	rad						
qn=	5.75E-01	m3/s/m	Q=	3.49E-02	-						
			q=	5.69E-01	m3/s/m						

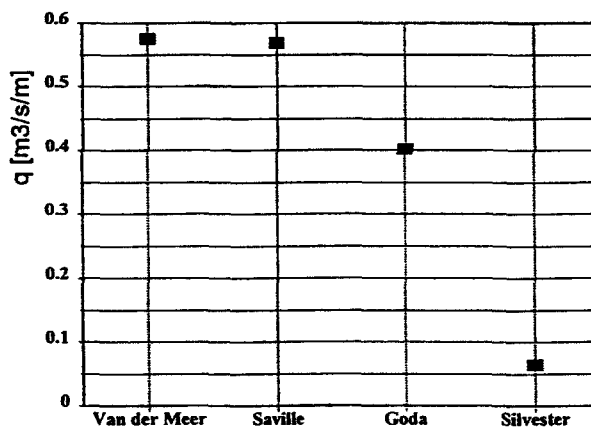*- means the values are read from graphs and tables from annex 1-9

Figure 5.2. Values for overtopping over vertical walls

5.3.2. Between Goda's graphs and Dutch Guidelines

Due to the fact that the major point of reference in the domain of overtopping over structures are Goda's graphs, underneath is presented the difference obtained between the mentioned formula and the formula used in the frame of Dutch Guidelines (section 3.7 of the report).

For the computation purpose Goda's graphs were included in a Quatro Pro spreadsheet.
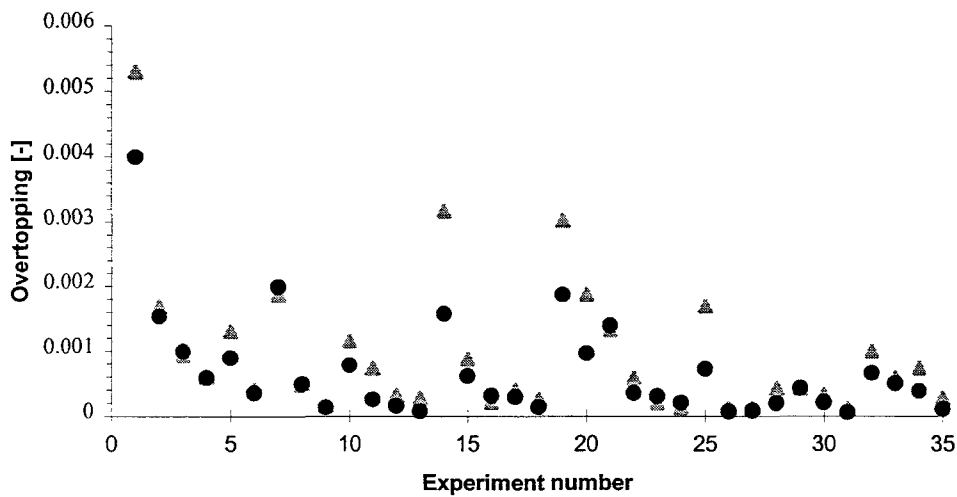

Figure 5.3. Comparison between Dutch Guidelines and Goda's graphs
Legend: ● Goda 's computed values;
▲ Dutch guidelines measurements

The results of Dutch Guidelines are obtained from reference (de Waal, TAW-A1). For this set of data the spreadsheet was use to compute overtopping values on base of Goda's graphs. Results are presented in figure 5.3. and the values in Annex 12.

From the graph it can be seen that Goda's graphs gives almost all time values smaller then those obtained with Dutch Guidelines. This is due to the fact that in Goda's graphs the slope of bottom is in the range of 1:10 to 1:30 and in the examples chosen from the above mentioned reference the bottom slope was 1:50 (which is more common in Netherlands then 1:10 or 1:30). However the results show that both formulas can be used with confidence.

With reference to the comparison presented in section 5.2 and 5.1 it can be stated that for design purposes it is good to be used Goda's graphs and Dutch Guidelines. The reason why Saville 's formulas are not very precise is the fact that it relies a lot on readings of graphs. This can lead in many cases to errors due to wrong interpretation of read data from graphs (or for example inaccurate interpolations).

6. Procedure for design of flood defence

Overtopping allowance is in direct relation with concept of risk. 100% safety is an ideal situation which is never "touched" in reality. Problem in designing is how big can be taken the risk which is equivalent with accepting a certain level of safety.
The level of safety design of a structure depends on the willingness of investing in safety and (of course) in the available budget.

The study of safety of structures concentrates on the concept of damage and collapse. Although these two terms are commonly used as having almost identical meanings, it is good to draw a clear distinction.

A structure or a structural component *fails* if it can no longer perform one of its principal functions. In the case of a flood defence structure, this function can be defined as the prevention of inundation, which means preventing a protected region from being flooded, attended by loss of human life and/or damage to property.

A structure or a structural component *collapses* if it undergoes deformations of such magnitude that the original geometry and integrity are lost. In general, collapse will be attended by a greatly increased probability of failure. It is rather conceivable that partial collapse occurs without automatically implying failure of the structure. For instance the occurrence of slip which affects a dam during a long period of low water level. The opposite may occur in the event of overtopping: the revetment of other parts of the flood defence fails, but the structure itself does not collapse.

The probability of failure multiplied by the damage or loss (eg. of life or economically due to inundation within a polder) constitutes the risk. For obtaining an optimal design, it is essential to seek a balance between the risk of inundation on one hand, against the cost of making a flood defence structure an the other.

6.1. Levels of approach

In order to determine the safety of a structure through predicting the probability of failure due to a particular mechanism, the following approaches can be followed:

-   deterministic approach (level O-approach): The design is based on average situations and an appropriate safety factor is included to obtain a safe structure;
-   semiprobabilistic approach(level I approach); A characteristic value is used in the design, like the load which is not exceeded in 95 % of the cases.
-   probabilistic approach (level II and III-approaches): The probabilistic approach considers the full statistical distribution of all parameters.

Presently, scientific developments are ongoing in the probabilistic techniques, for which a lot of research is done. In practice, the design follows in general the semi-probabilistic methods.

6.1.1. Deterministic approach

The traditional design is based upon the deterministic approach. In this approach a limit state condition is chosen with respect to the accepted loading state of the structure (eg. water lever + wave height). This limit state usually corresponds to a certain strength value (eg. crest level) or the characteristic strength. Exceedance of the limit state condition ("failure") is not accepted.

6.1.2. Probabilistic approach

Within the probabilistic approach, the mechanisms are described by means of a formula or a computational model. On the basis of such a model, a so-called reliability function Z can be defined, which regards the limit state in such a way that negative values of Z correspond to failure, and positive values to non-failure. In general form, the Z-function can be written as:

$$Z = \text{Strength - Load} \qquad\qquad (6.1)$$

By using this Z-function, the probability of failure can be defined by $P\{Z<O\}$. For simple failures (like the collapse of an overloaded plank over a ditch) the Z-function can be described easily. For the collapse and failure of a dyke, however, this Z-function may be very complicated, mainly because of the complicated interaction between water (supplying the loadings), soil, revetment (mainly at the strength side), etc. These interactions involve a number of failure mechanisms.

In this report failure is associated with overtopping being a leading mechanism.

6.2. Daily computation of probability

The application of the probability theory to the assessment of structural reliability may lead to the question whether the calculated probability of failure corresponds to reality. It is supposed that a probabilistic safety analysis is only fruitful when it is based on accurate computational models and on sufficient statistical data. However, in practice these requirements are seldomly fulfilled. In most cases, it is just the lack of (statistical) data and the absence of an adequate computational model that are important features of the reliability problem. In other words, the uncertainties associated with them are often even greater than the uncertainties due to the intrinsically (by nature) stochastic character of load and strength.

These uncertainties must be taken into account in determining the margins of safety. Theoretically, the best procedure consists in first translating all the uncertainties into probabilistic terms (especially into the coefficients of variation), followed by the determination of the required safety factors. Of course, in the case of "model uncertainties" and "statistical uncertainties", the coefficients of variation can only be estimated subjectively. As a consequence, a calculated probability of failure can be interpreted as a "measure of confidence in a particular design".

The accepted probabilities of exceedance for loadings and prescribed safety coefficients applied in established codes of practice or design rules reflect the collective opinion of a large number of professionals rather than the subjective opinion of one expert. Hence, the probabilities and parameters have the character of design quantities. For this reason the designation "notional probabilities" is sometimes used in literature. Besides, in most cases it will suffice just to have an approximate idea of the order of magnitude of the failure probabilities.

It is very important that a sound and balanced design can be produced with the available information. For instance, a difference of one order of magnitude or a factor of 10 in the failure probability of a dike corresponds to a difference of merely a few centimetres in its design height only (J.K.Vrijling, 1996).

6.3. Design procedure

6.3.1. Design criteria

The determination of the probability of failure of a flood defence system inevitably starts with the question as to which probability of failure is acceptable. Even though the calculated failure probability can only to a limited extent be conceived as a "frequentistic" probability in the sense of an inundation occurring once in N years, such a relation nevertheless has to be established.

Hence it is advisable to adjust the calculation of failure probability as much as possible to the assumptions made in the predesign stage and, in addition, to conceive a standard or norm for the acceptable probability, so that a framework serviceable for discussion in the social context is available.

Risk is regarded as the expectation of the consequences of inundation (mathematically: probability x consequence). In this context, two points of view should be examined: that of the individual, who considers the acceptance of a particular risk; and that of society, which judges the probability of a particular accident.

Personal acceptable risk

The personal assessment of risks by an individual can be considered the smallest component of the socially accepted level of risk. In the individual sphere, the appraisal (i.e., the balancing process of the desired benefits against the accompanying risk) is often accomplished quickly and intuitively. Furthermore, a correction can be quickly made if the appraisal turns out to be incorrect.

Social acceptable risk

In principle, the acceptance level of risks of a democratic society consists of the aggregate, or the summed total, of all individual appraisals. Although it can be said that, at social level, for every project in the widest sense the social benefits are balanced against the social costs (including risk), this process of appraisal can not be made explicit. Actually, the social optimization process is accomplished in a tentative way, by trial and error, in which governing bodies make a choice. The further course of events shows how wise this choice was.

If a socially acceptable risk level must be determined for a particular project, a solution can be reached only through a considerable simplification of the problem. One way to achieve this is to schematize the problem to a mathematical economic decision problem by expressing all consequences of the disaster in- monetary terms. A second approach consists of deducting an acceptable level of risk from accident statistics, while limiting the consequence of the disaster to the number of deaths.

6.3.2. Height of the crest of the structure

The mathematical decision problem has been formulated by Van Danzig (1955) for the inundation of central part of The Netherlands in the Delta Commission's report . To simplify the problem, the height of a dyke is assumed to be a deterministic quantity. Furthermore, the only failure mechanism considered is overtopping, which means that inundation of a polder only occurs when the storm tide level rises above the crest level of the dyke. These simplifications allow for establishing the probability of inundation directly from the high water exceedance line:

$$P(S_v > h_0) = F_{S_v}(h_0) = e^{-\frac{h_0 - \alpha}{\beta}}$$ (6.2)

where:

S_v- storm tide level	[m];
h_0-height of dyke	[m]
α,β -constants	[-];

Let S denotes the total damage (on buildings, stocks, cattle and loss of production) which occurs upon inundation of the polder. The mathematical expectation of this loss per year is the product of the inundation probability and the loss S. In a first approximation some losses (like loss of income and loss of human lives) are not considered. The monetary value of the expected loss over the service life of a structure (N years) is a measure for the total loss. In this model description, the risk of failure can be reduced by heightening the structure. The cost of this safety measure consists of a partly constant and a partly approximate proportion to the increase in height. The total cost consists of the sum of the cost of heightening the structure and the monetary value of the expected losses.

The optimal height of the structure can be determined by a differentiation with respect to the decision variable h, as to arrive at the minimum total cost. In practice, when a dike is constructed an additional height is included, which give a higher crest level. This is done to account for water level oscillations and overtopping due to wind waves.

6.3.3. Inundation depth and inundation speed

In general, inundation can occur as a result of overflowing and/or wave overtopping of a flood defence structure or as a result of flow through a gap due to collapse of the structure. The flow rate depends on the length of the structure (in the case of overtopping), the behaviour (variation) of the river water level, the ground level or the water level in the polder protected by the dyke, and the size and shape of the gap in the dyke. The size and shape of the gap will in turn depend on the velocity of the inflowing water, the inflow duration, and the composition of the subsoil and the body of the dyke.

Water flows over the crest of the structure and, river water is discharged laterally into the polder. Let $Q(\tau)$ be the lateral discharge, where Q represents the rate of flow and T represents time. The total volume of river water that has been flowed into the polder at the instant t is then:

$$V(t)_{it} = \int_{t_0}^{t} Q(\tau) \, d\tau \tag{6.3}$$

where t_0 is the instant at which the lateral discharge commences. Furthermore, let $A(\zeta)$ be the area of the endangered polder at level ζ (see figure 7.3), $h_p(t)$ the inundation depth at time t and h_{po} be the lowest point in the polder. Then the mass balance for the water that has flowed into the polder is:

$$\int_{t_0}^{t} Q(\tau) \, d\tau = \int_{h_{po}}^{h_p(t)} \int A(\xi) \, d\xi \tag{6.4}$$

Equation (6.4) determines the inundation depth. The greatest inundation depth at the instant t is $\{h_p(t)-h_{po}\}$. The inundation speed is obtained by differentiation of equation (6.4) with respect to time:

$$\frac{dh_p}{d} = \frac{Q(t)}{A(h_p(t))} \tag{6.5}$$

The unknown quantity in these equations is the lateral discharge of river water Q(t).
The level of the river bottom will be taken as the zero reference plane for height or levels. (figure 7.3.)

7. Computer programs

In this chapter are presented the following computer programs:

-vert_ovr	-	Pascal programme which computes the values of overtopping over vertical structure;
-goda.wb2,cmp.wb2	-	Quatro Pro spreadsheets which gives the output as the Pascal programme;
-cress modules	-	the modules which are needed for the extension with IHE coastal structures computation program CREES.

7.1. Pascal programme -vert_ovr

Based on the formulas presented on previous chapters a Pascal programme was developed. The programme is organized in menus as follows:

(A) - The main menu with four options (figure 7.1.)
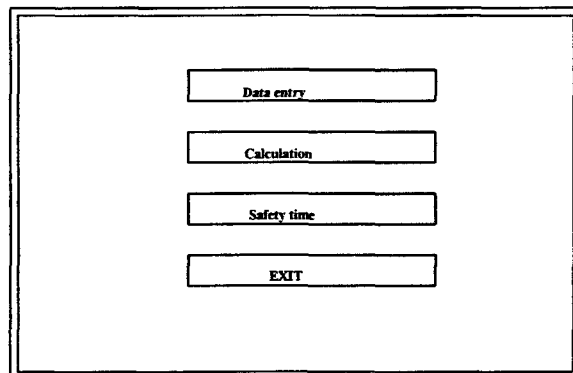
Figure 7.1. Main menu

*Option **Data entry** for input data .*

This option has three alternatives for input the data (figure 7.2.) : from a file, case in which the name of file with input data   is required; from the keyboard and create data file. This last option allows the user to create a file of data. In the last two options of this menu input values for the data will be required.

The required input data are:

   1 - Structure characteristics as they are quoted in chapter 5 of the report:

      - front of structure: vertical or with a sloping structure in front;

      - structure with or without berm;

      - slope of the bottom in front of structure;

      - height of the water in front of structure   h;

      - height of the crest R_c.

In case that the front of the structure has a slope in the front additional data are required in this section:

      - slope of the structure in front of berm;

      - slope of berm;

      - slope of structure after berm.

   2 - Wave characteristics:

      - height of the wave H_s;

      - period of a wave   T;

      - significant wave height in deep water H_{os}.
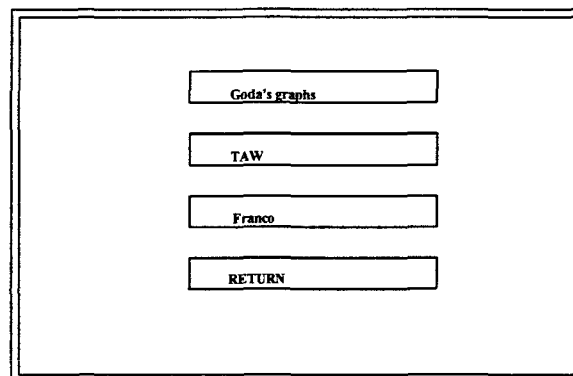
Figure 7.2. Data entry menu

Option **Calculation** in which there is a secondary menu which gives the choice of computation wave overtopping with different formulas.

However, there are some restrictions. In case of Franco formula if the input values for geometric and hydraulic conditions are not in the range of:

      - wave height $H_s=2\div8$ [m]

      -period of the wave $T_p=6\div8$ [sec]

      -height of water in front of structure h=9÷18   [m]

the program will not perform any computation and will give a sound message.

Option Safety time which computes the time for filling a certain volume. Requires the following data (figure 7.3)

- geometric dimensions of the area: B,L   [m]
- existent height of water: h_e [m]
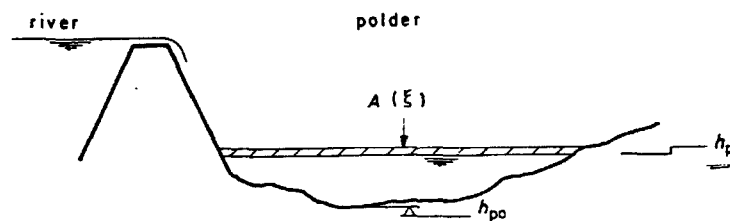- allowable water height: h_a [m]

Fig. 32.   Diagram defining a polder.

Figure 7.3.   Geometric definition of the flooded area

Option EXIT as the name saying for existing the program. Output is located in text file "results" and on the screen.

(B) - The **secondary menu** in correspondence with option Calculation of the main menu
         (figure 7.4)
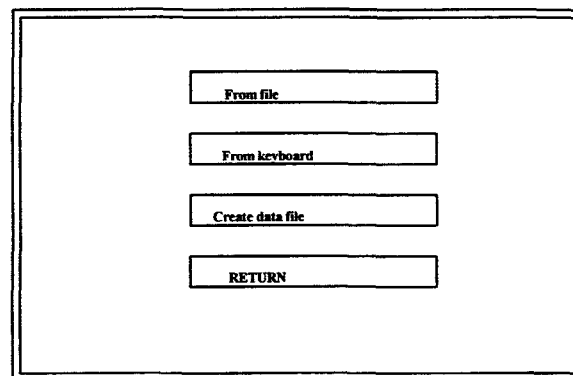
Figure 7.4.   Secondary menu

*Option **Goda's graphs*** is computing the overtopping by using interpolation in the 12 Goda's graphs presented in Annex

*Option **TAW*** is computing the overtopping using the formulas from Dutch Guidelines (1989).

*Option **Franco*** compute overtopping with Franco's formula only if the requirements for the input data are fulfilled.

*Option **RETURN*** go back in the main menu.

Remark: Only one computation formula can be used for one set of input data. If the same set needs to be done with another formula the programme should be ran again with the same input data.

In order to run the programm needs the following files to be located with it in the same directory:

        -discl;
        -grv1_12, grv1_17, grv1_36, grv3_12, grv3_17, grv3_36;
        -grs1_12, grs1_17, grs1_36, grs3_12,grs3_17,grs3_36.

7.2. Spreadsheet

For the purpose of computation at once between different formulas, Quatro Pro spreadsheets for computation the dimensionless overtopping was done.

7.3. Link towards CRESS

Modules were added to CRESS with the purpose that in path

Coastal Hydraulics\Run-up, overflow and overtopping\Overtopping over a vertical wall

the volume of overtopping over vertical structures to be computed.

References

*****-Costal Engineering Research Center - 1984. Shore Protection Manual. U.S. Army Corps of Engineers.

*****-Wave Run-up on Sea Dykes in Consideration of Overtopping Security by Using Benchmarks of Flotsam - Fourth International Conference an Coastal and Port Engineering in Developing Countries - Rio de Janeiro - Brazil - 25-29 September 1995.

Archetti , R., Franco, L.& con. - "Large Scale Model Tests on Wave Overtopping on Rubble-mount Breakwaters"-Fourth International Conference an Coastal and Port Engineering in Developing Countries - Rio de Janeiro - Brazil - 25-29 September 1995.

Battjes , J.A.- "Computation of Set-up, Longshore Currents, Run-up and Overtopping Due to Wind-generated Waves." - Communications on Hydraulics Department of Civil Engineering Delft University of Technology - Report no. 74-2.

de Waal, J.P., van der Meer,J.W. - "Wave Run-up and Overtopping on Coastal Structures - 23nd. International Conference on Coastal Engineering 4-9 October 1992 Venice Italy.

de Waal,J.P. - TAW-A1-"Wave overtopping of vertical coastal structures",Report on Physical model tests and study - Delft Hydraulics, February 1994

Goda, Y. - Random Seas and Design of Maritime Structures, Univ of Tokyo press, 323 pp. 1985.

Goda, Y., Kishira, Y., Kamiyama, Y. - Laboratory Investigation on the Overtopping Rate of Seawalls by Irregular Waves. Report of the Port and Harbour Research Institute, Vol. 14, No 4.,1975

Inoue, M., Shimada,H., Tonomo,K. - Quantitative Study on Overtopping of Irregular Waves, Proc. Coastal Engineering, JSCE, vol 36, pp 618-622, 1989.

Jayewardene, I.F.W., Haradasa,D.K.C., Tainsh,J. - "Model Study on Water Levels Due to Irregular Wave Overtopping of Sea Defences" - Fourth International Conference an Coastal and Port Engineering in Developing Countries - Rio de Janeiro - Brazil - 25-29 September 1995.

Jensen,J., Juhl, J. - "Wave overtopping on breakwater and Sea Dykes" - 20nd. International Conference on Coastal Engineering 1986.

Juang,J-T - "Effect on Wind Speed to Wave Run -up"- 23nd. International Conference on Coastal Engineering 4-9 October 1992 Venice Italy.

Juhl, J., Jensen,J. - "Features of Berm Breakwaters and Practical Experience" - Fourth International Conference an Coastal and Port Engineering in Developing Countries - Rio de Janeiro - Brazil - 25-29 September 1995.

Kimura, A. ,Seyama, A. - Statistical Proprieties of Short-Term Overtopping, Proc. 19th ICCE, pp 532-546, 1984.

Klopman, G. , Breteler, M.K.- TAW-A1, Unie van Waterschappen en Waterschap Friesland - "Overslag en golfkrachten op verticale waterkeringsconstructies" H 2014 Waterloopkunding Laboratorium/wl Augustus 1995

Mizuguchi , M. - "Breaking of Irregular Wave on a Slope"- 23nd. International Conference on Coastal Engineering 4-9 October 1992 Venice Italy.

Muraca,A., Rossi,V. -"Field Analysis of Wave Action on Breakwater" - 23nd. International Conference on Coastal Engineering 4-9 October 1992 Venice Italy.

Nagai, S. , Takada, A. - Relations Between the Run-up and Overtopping of Waves - 13nd. International Conference on Coastal Engineering July 10-14, 1972 Vancouver, Canada.

Niemeyer , H.D., Gartner, J., Kaiser,R., Peters,K., Schneider, O. - "The Estimation of Design

Ozhan, E., Yalciner,A.C. -"Overtopping of Waves at Model Sea Dikes" - 22nd. International Conference on Coastal Engineering 2-6 July 1990 Delft

Paape, A. - "Experimental Data on The Overtopping of Seawalls by Waves" - Hydraulics Laboratory Delft Publication No.23 September 1960.

Prins, J.E. - "Model Investigations of Wind Wave Forces"- Hydraulics Laboratory Delft Publication No.24 September 1960.

Shiigai, H., Kono, T. - Analitical Approach On Wave Overtopping On Levees - Proc. The 12th. Coastal Engineering Conference Vol. 1, pp. 563~573, Sep. 1970.

Sloth, P., Juhl, J. - "Individual Wave Overtopping Volumes For a Rubble Mound Breakwater"- Fourth International Conference an Coastal and Port Engineering in Developing Countries - Rio de Janeiro - Brazil - 25-29 September 1995.

Takada , A. - Wave Overtopping Quantity Correlated To the Surface Elevation of Finite Amplitude Clapotis - Proc. The Japan Society Of Civil Engineering, No. 201, pp. 61~76, May, 1972.

Takada, A. - On Relations Wave Run-up, Overtopping and Reflection - Proc. The Japan Society of Civil Engineering No. 182, pp.18~30, Oct. 1970.

TAW, (1974). Wave run-up and overtopping. Technical Advisory Committee on protection against inundation. Government publishing office, The Hague, The Netherlands.

Tominaga, Y., Hashimoto, H., Sakuma , N.- Wave Run-up and Overtopping on Coastal Dikes - Proceedings of Tenth Conference on Coastal Engineering September, 1966 Tokio, Japan.

van der Meer, J.W. , Angremond, K. - "Wave Transmission at Low-crested Structures" - Coastal Structures and Breakwaters - Proceeding of the Conference Organized by the

Institution of Civil Engineering and Held in London on 6-8 November 1991.

van der Meer, J.W., Franco, L. - "Vertical Breakwaters" - Delft Hydraulics - Publication No. 487 February 1995.

van der Meer,J.W. - TAW -"Wave Run-up on And Overtopping of Dikes"-Delft Hydraulics -Report H 638 - July 1994

van der Meer , J.W. , Vis, F.C. - "Conceptual Design of Berm Breakwater" - Fourth International Conference an Coastal and Port Engineering in Developing Countries - Rio de Janeiro - Brazil - 25-29 September 1995.

van der Meer, J.W. ,Stam ,C.-J.M.- "Wave Run-up on Smooth and Rock slopes"- Delft Hydraulics - Publication No. 454 May 1991.

Verhagen,H.J - "Revetments, Sea-dikes and River-levees"- Handout IHE-Delft 1996

Wang , Z., Grune, J. - "Influence of Berms On Wave Run-up on Sloping Seadykes" - Fourth International Conference an Coastal and Port Engineering in Developing Countries - Rio de Janeiro - Brazil - 25-29 September 1995.

Wouters, J. - "Hamburg Harbour - Integrated Numerical and Physical Model Investigation on Wave Overtopping During High-water Condition" Delft Hydraulics Report H828 - 1989.

Yamamoto, Y. , Horikawa,K. - "New Methods to Evaluate Wave Run -up Height and Wave Overtopping Rate"- 23nd. International Conference on Coastal Engineering 4-9 October 1992 Venice Italy.
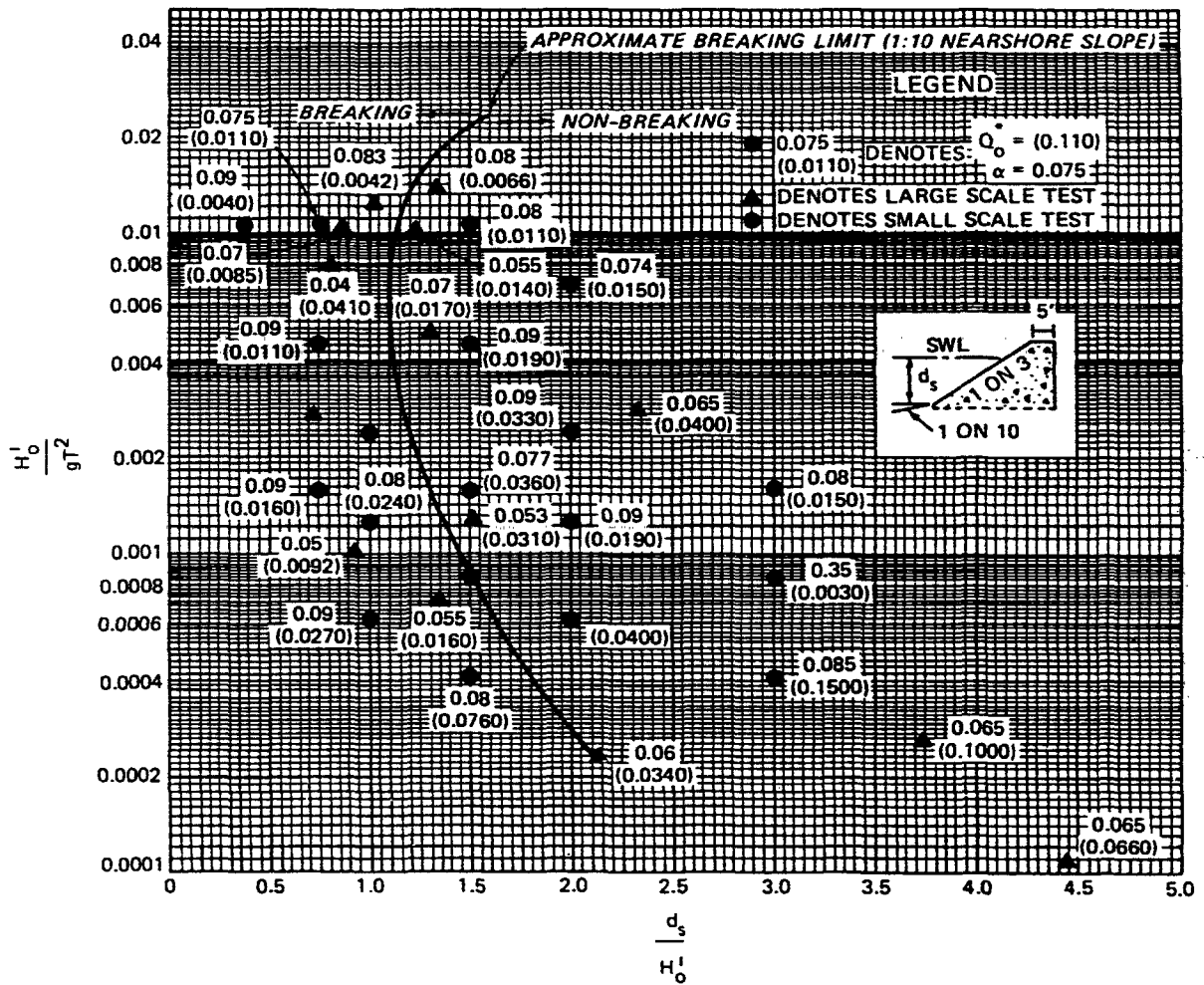
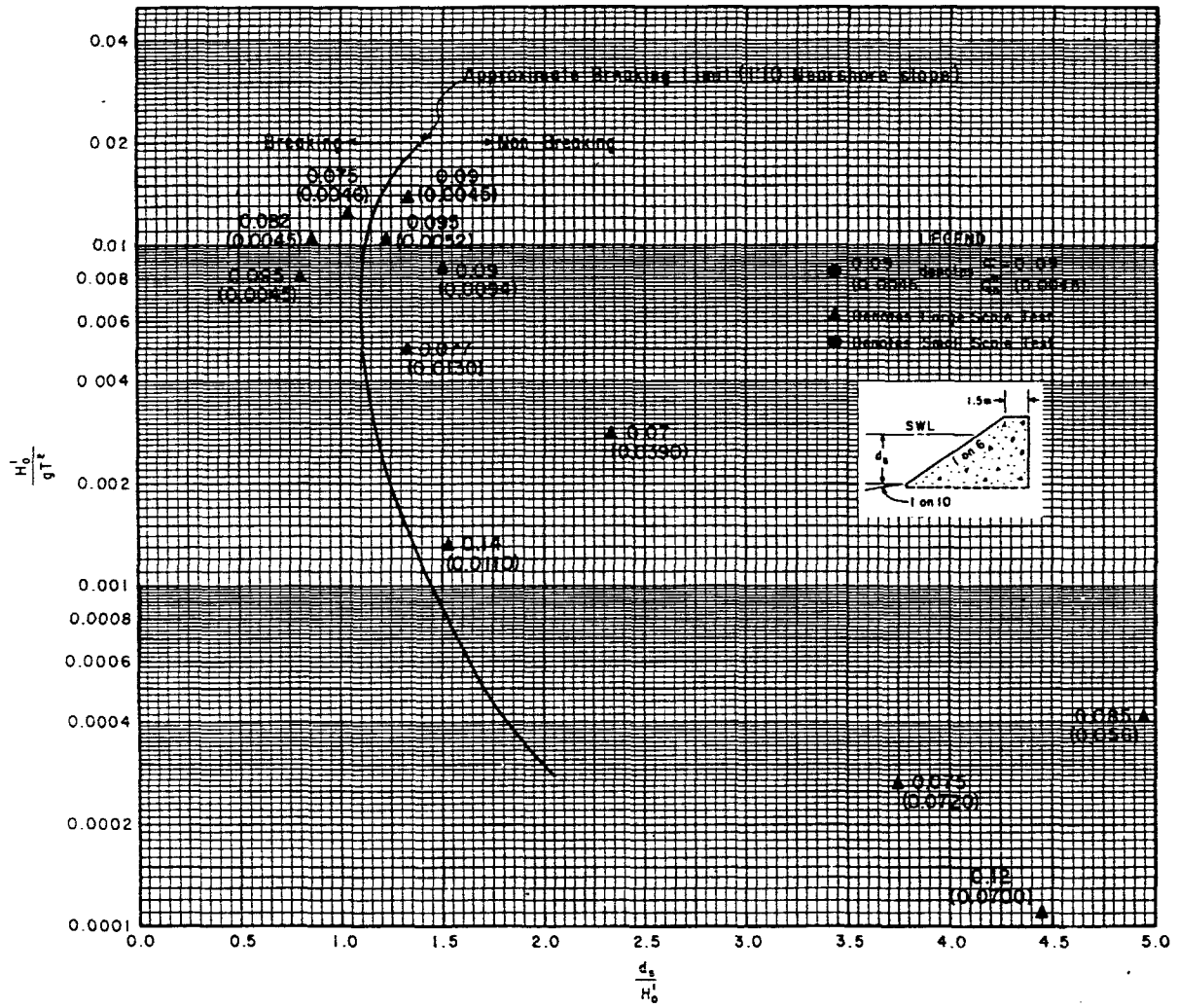**Annex** *1.Overtopping parameters α and Q*o (smooth vertical wall on a 1:10 nearshore slope)*
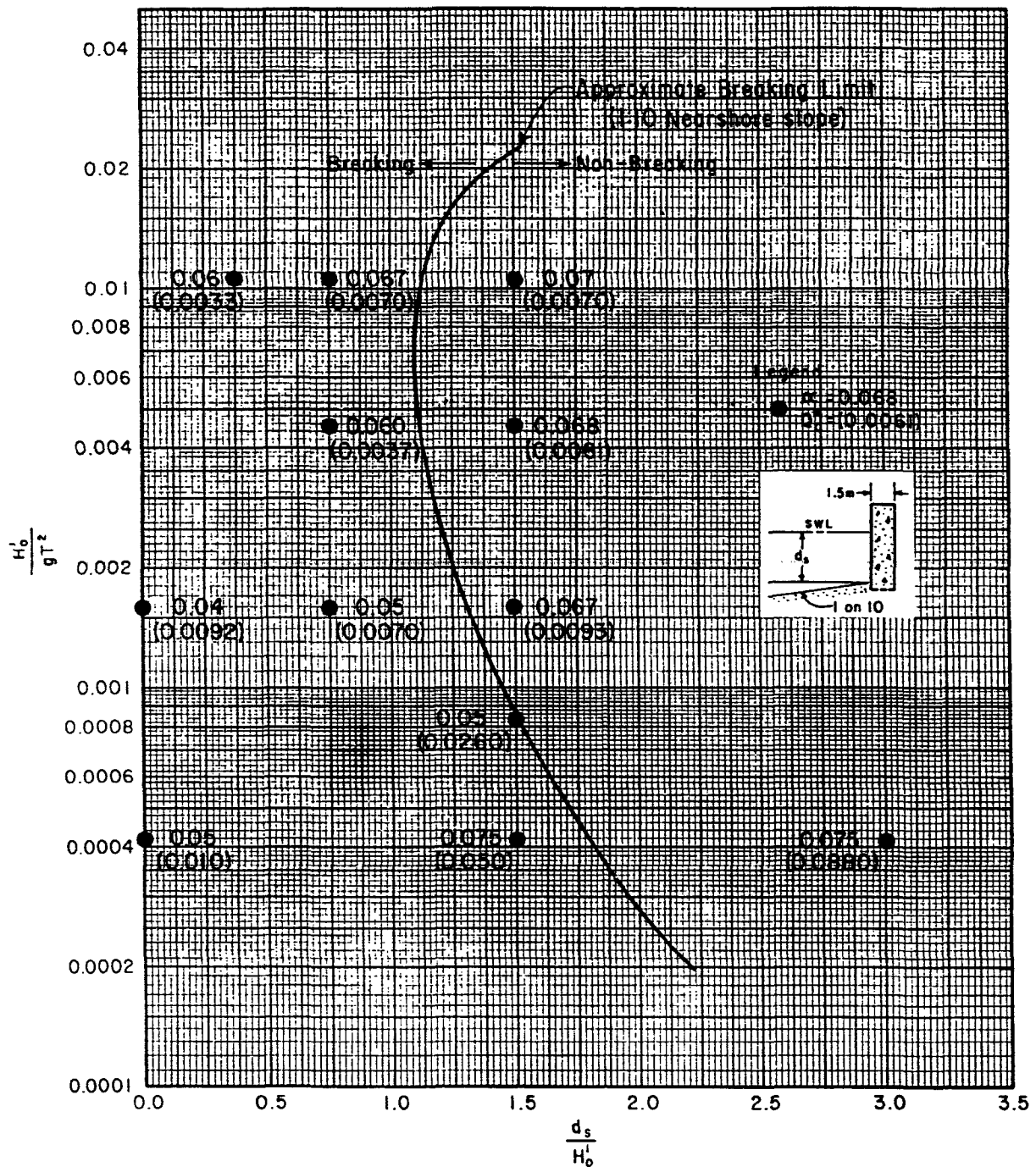
Annex 2.*Overtopping parameters* α *and Q*o (smooth 1:1.5 structure slope on a 1:10 nearshore slope)*
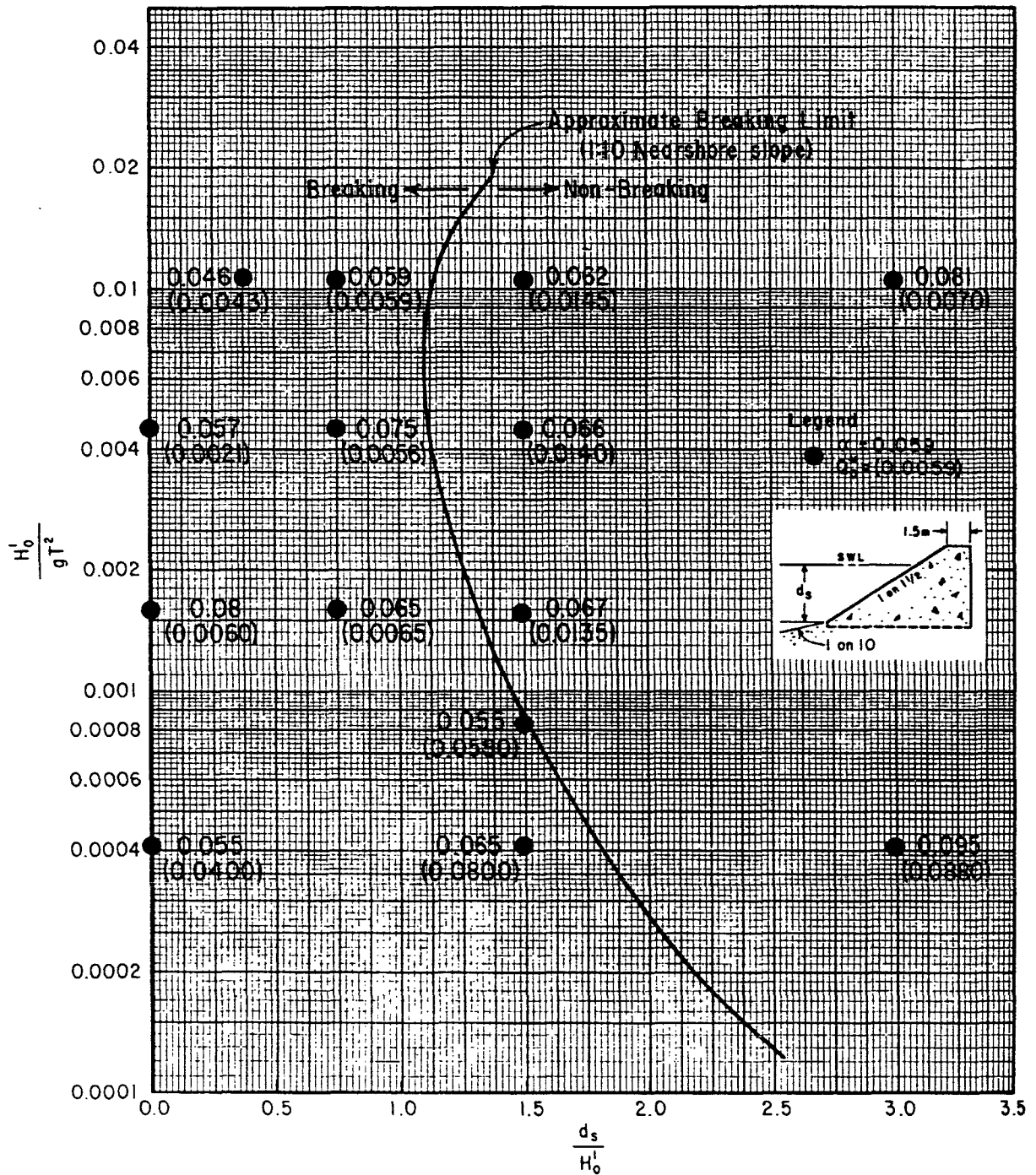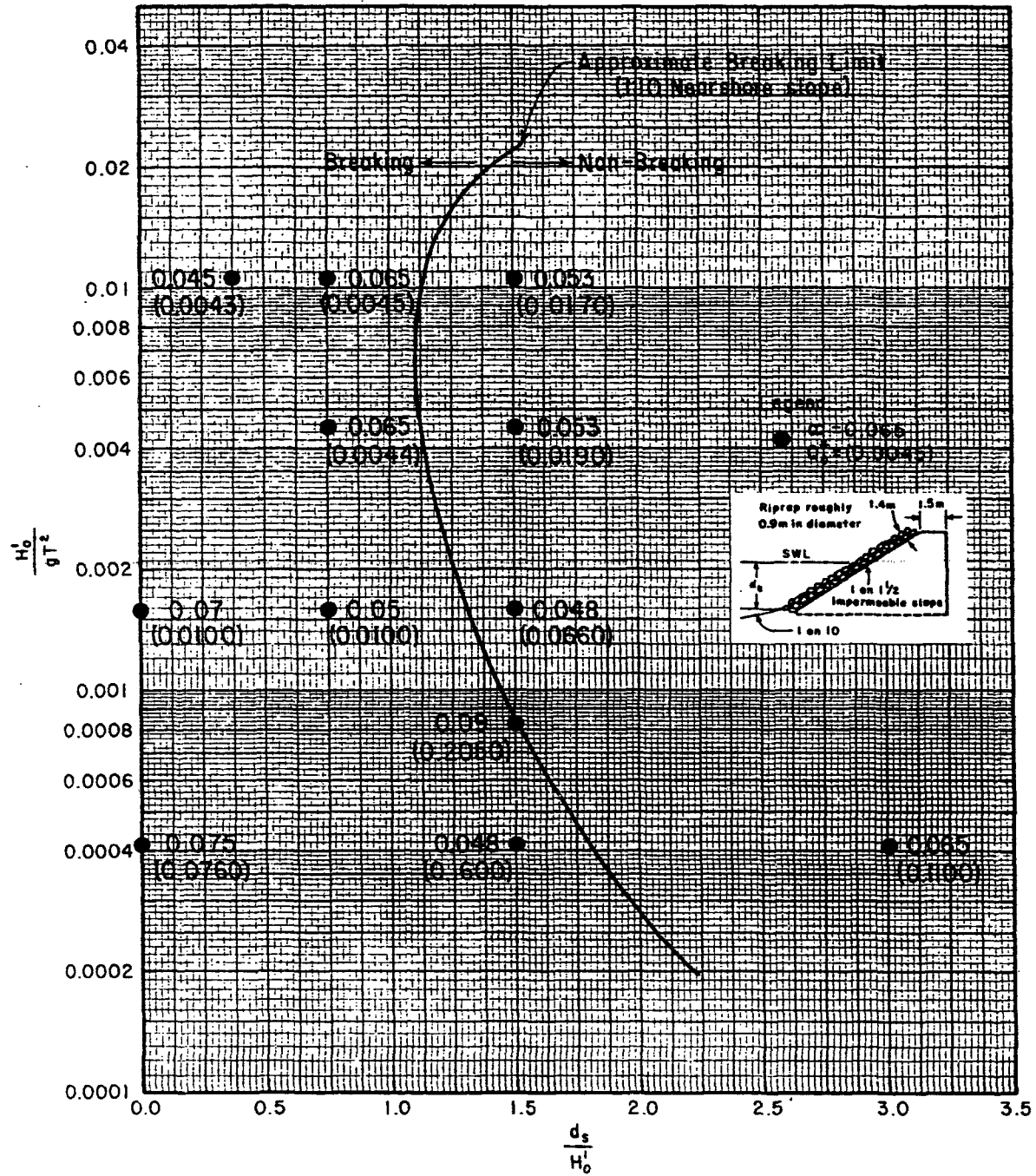
**Annex** *3.Overtopping parameters α and Q*o (smooth 1:3 structure slope on a 1:10 nearshore slope)*

Annex *4.Overtopping parameters* α *and Q*o (smooth 1:6 structure slope on a 1:10 nearshore slope)*
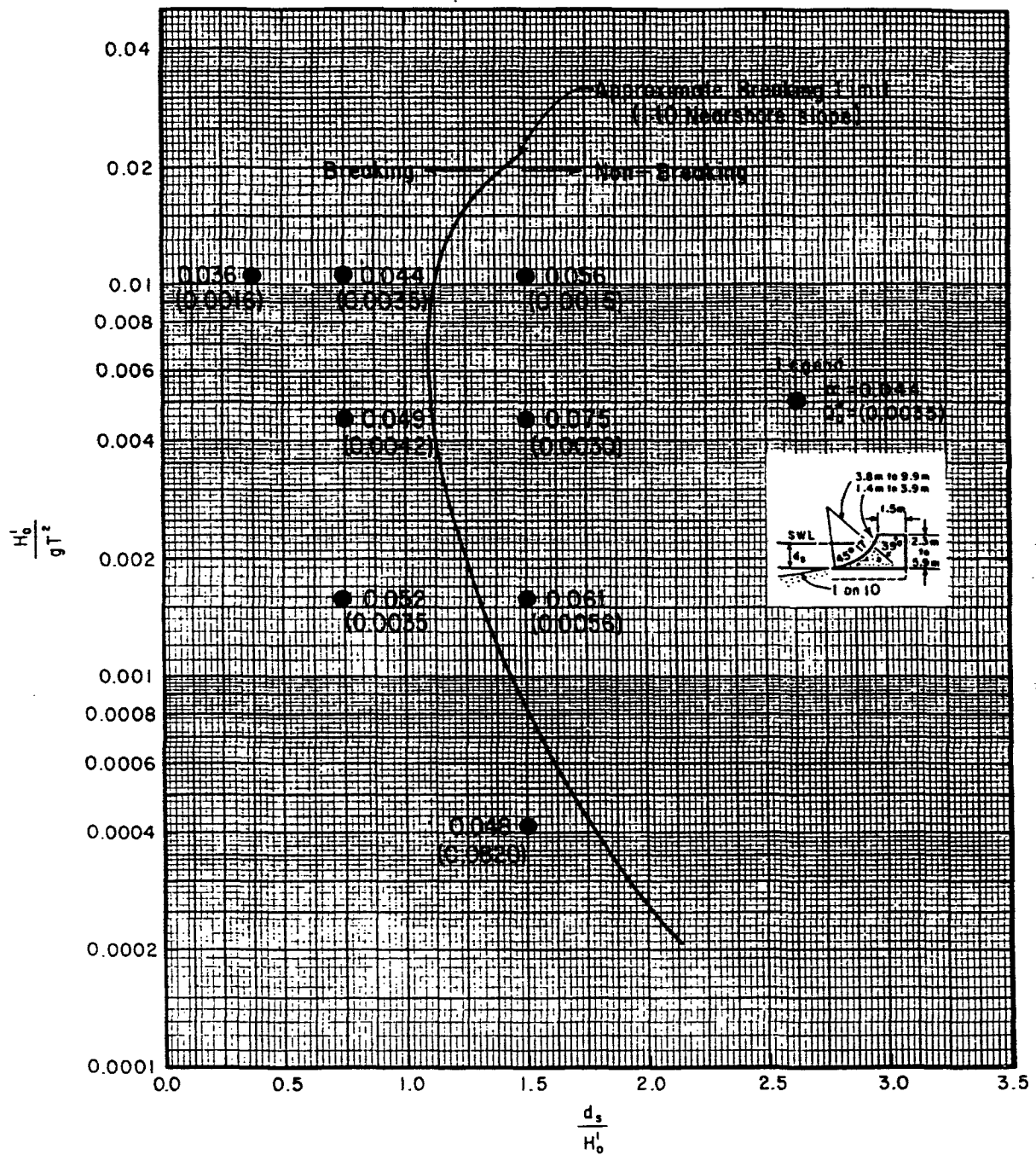
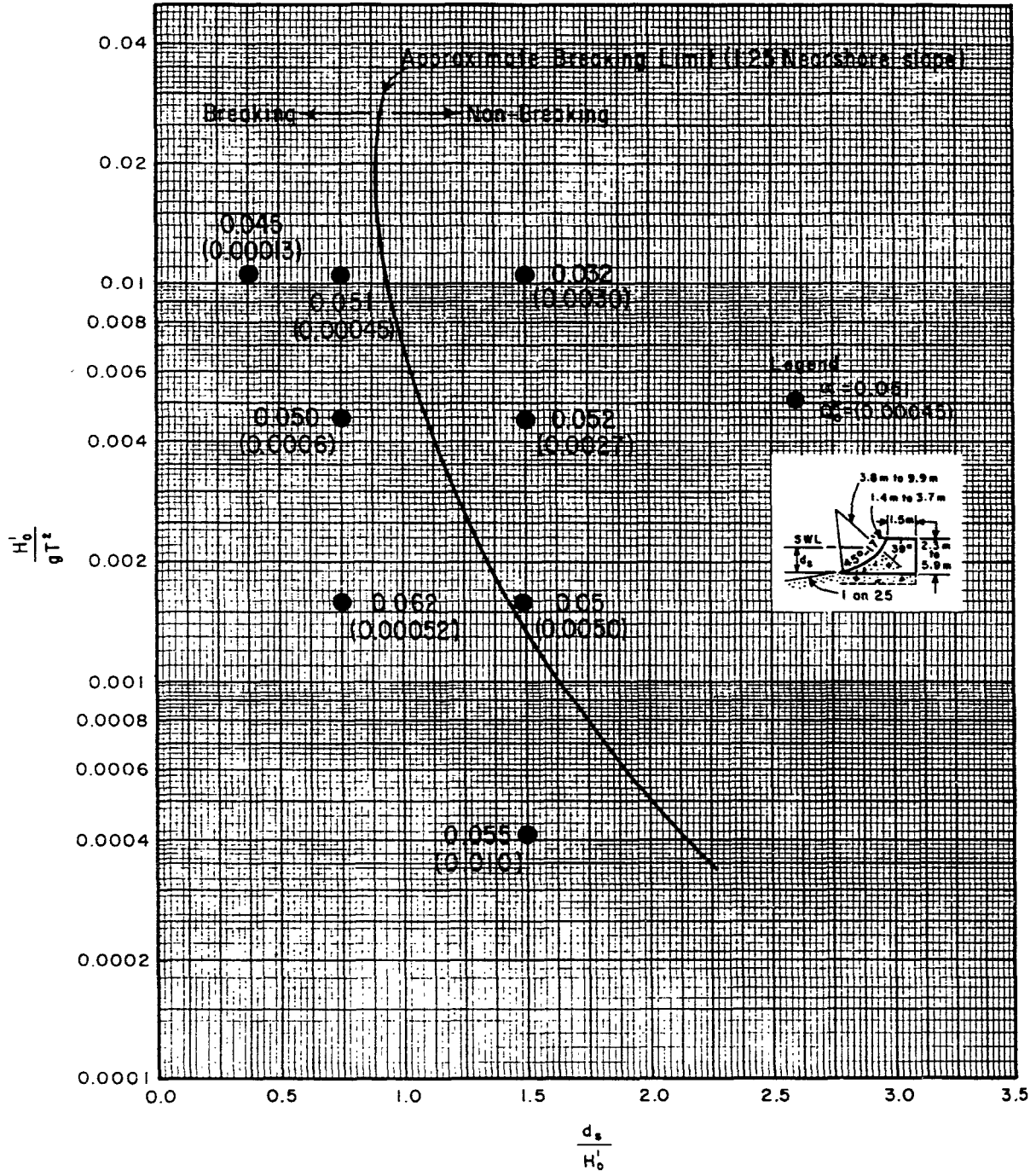**Annex 5.**   *Overtopping parameters α and Q*o (riprapped 1:1.5 structure slope on a   1:10 nearshore slope)*

Annex 6.*Overtopping parameters α and Q*o (stepped 1:1.5 structure slope on a 1:10 nearshore slope)*
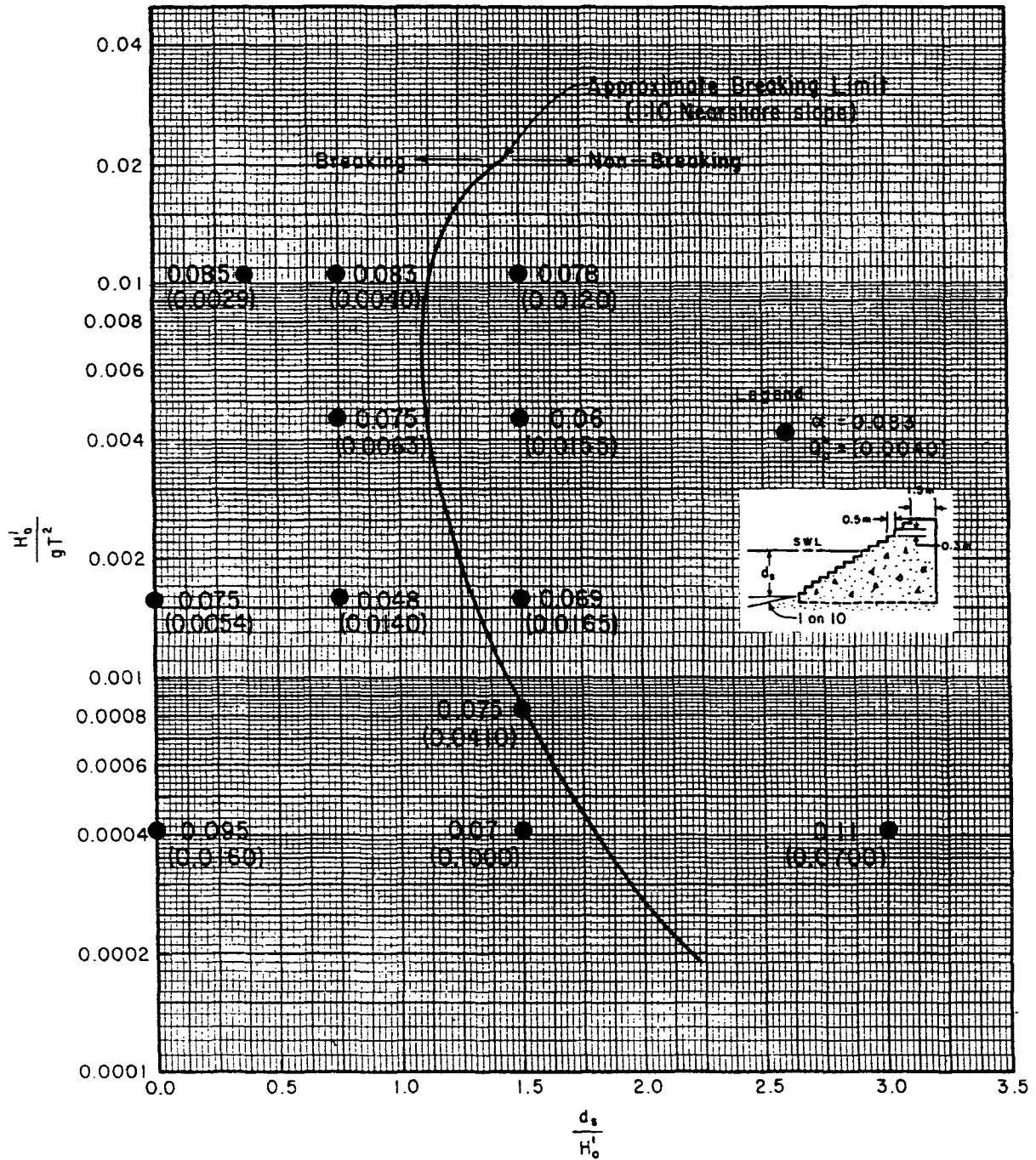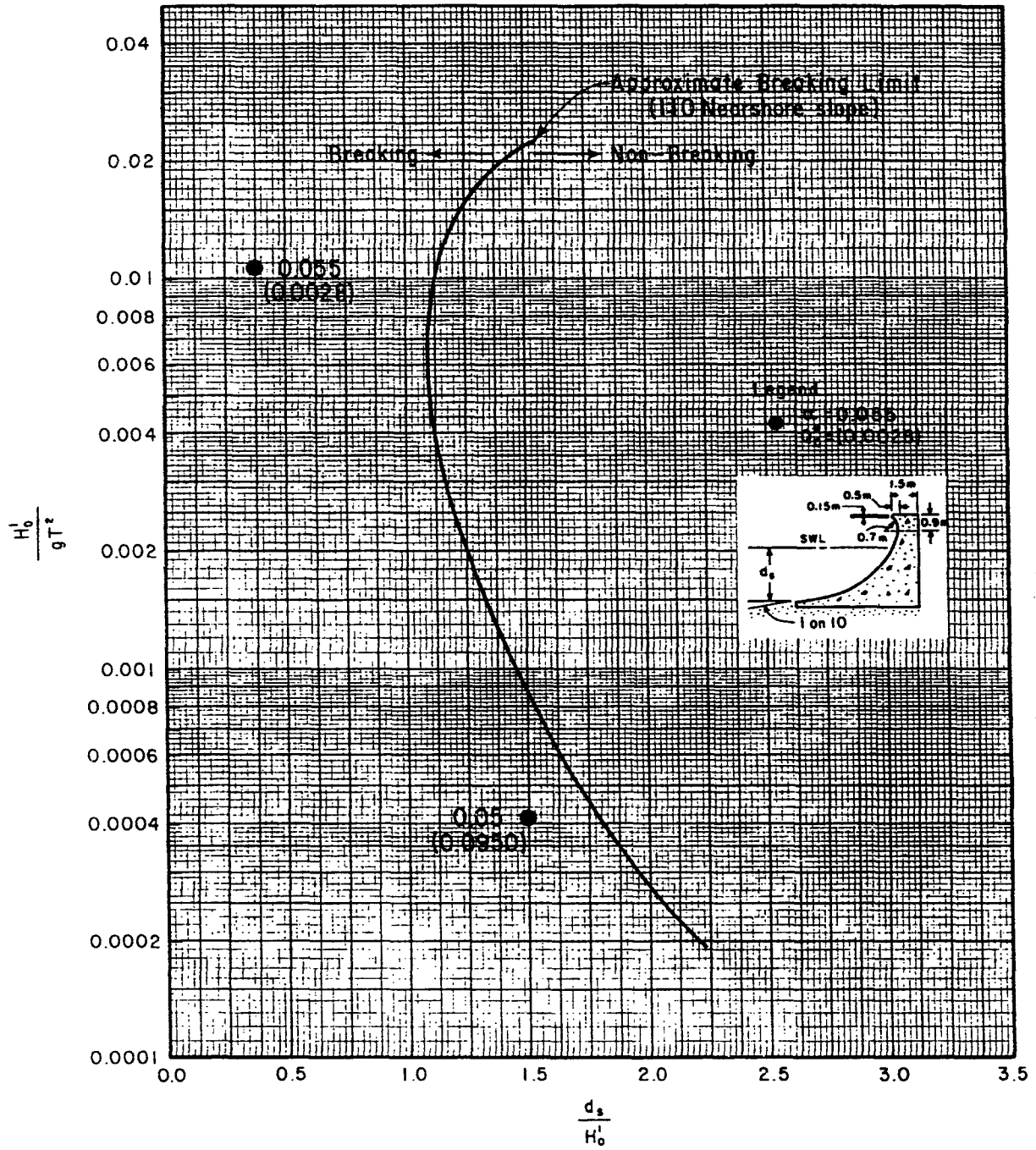
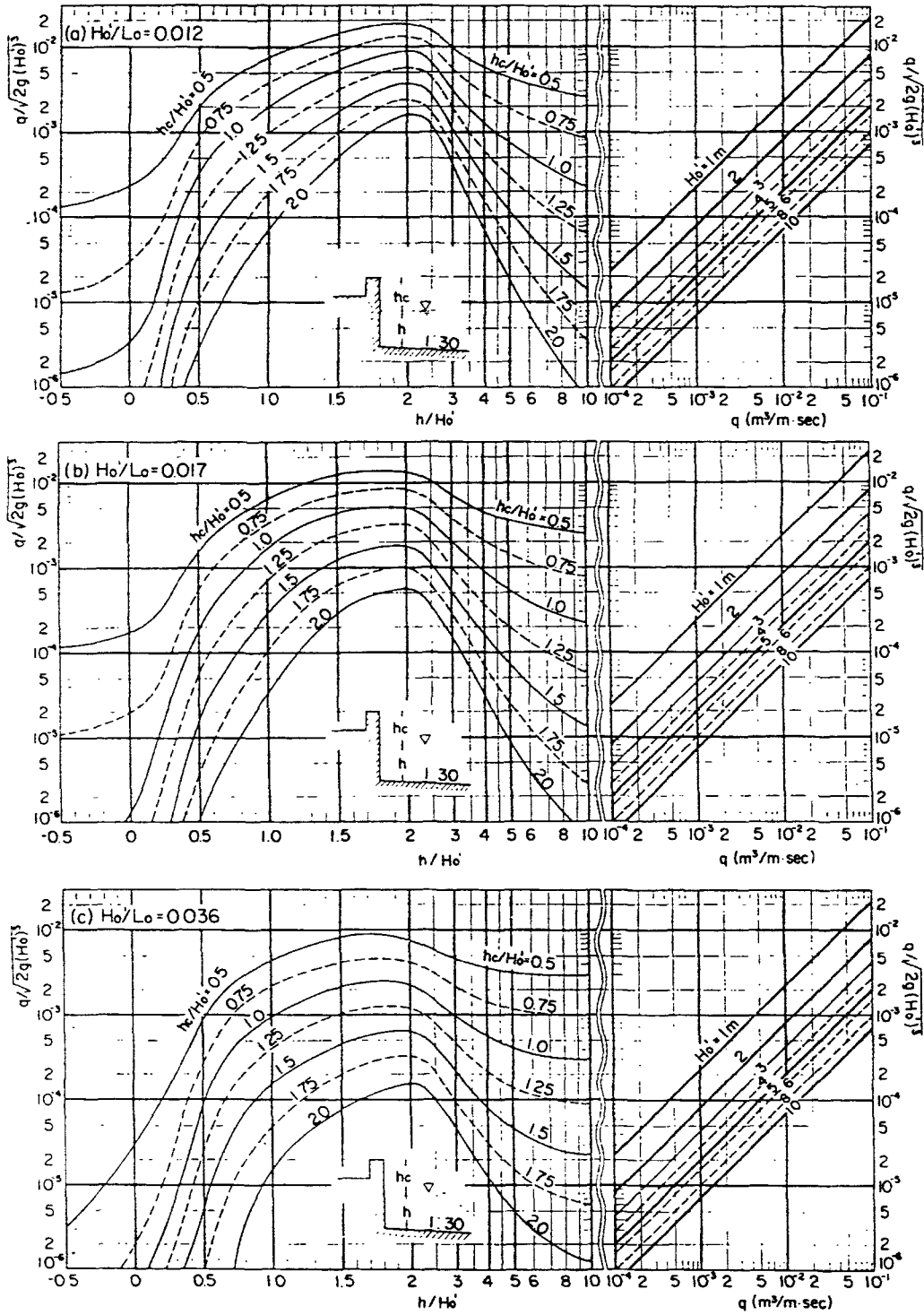**Annex** 7.*Overtopping parameters α and Q*o (curved wall on a 1:10 nearshore slope)*

Annex 8.*Overtopping parameters* α *and* Q^*o *(curved wall on a 1:25 nearshore slope)*
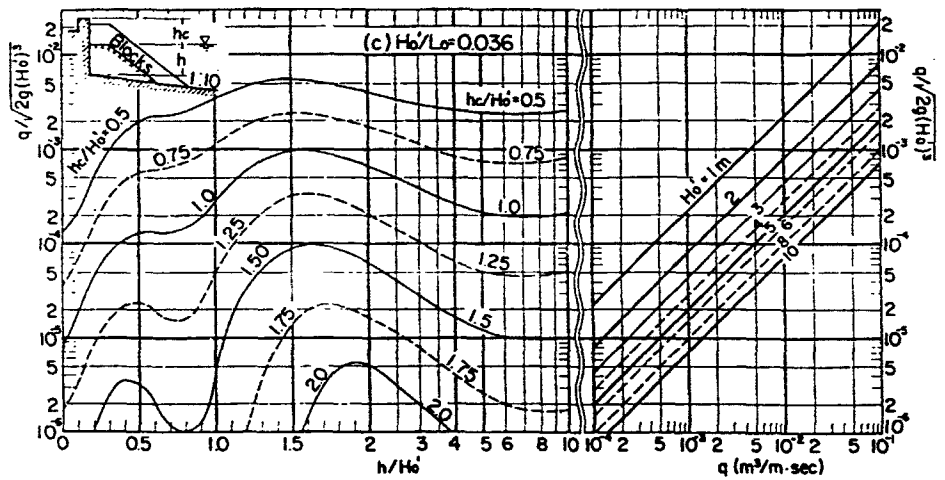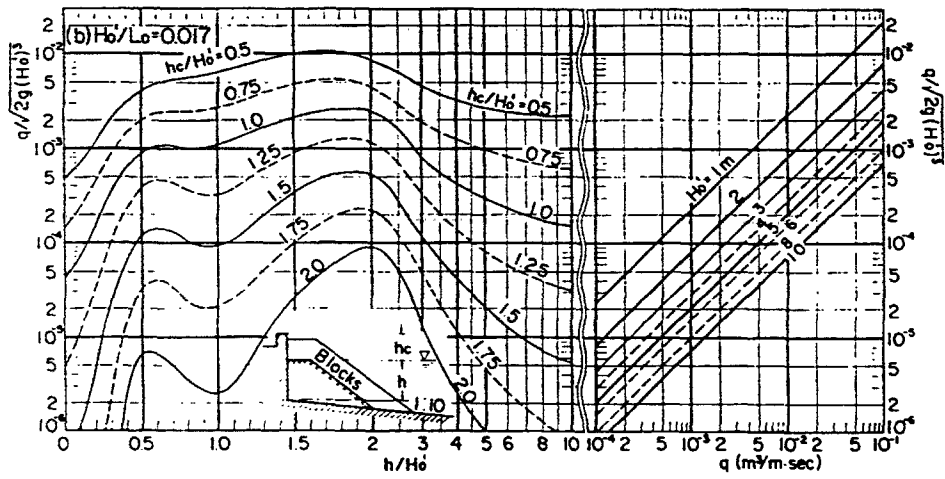
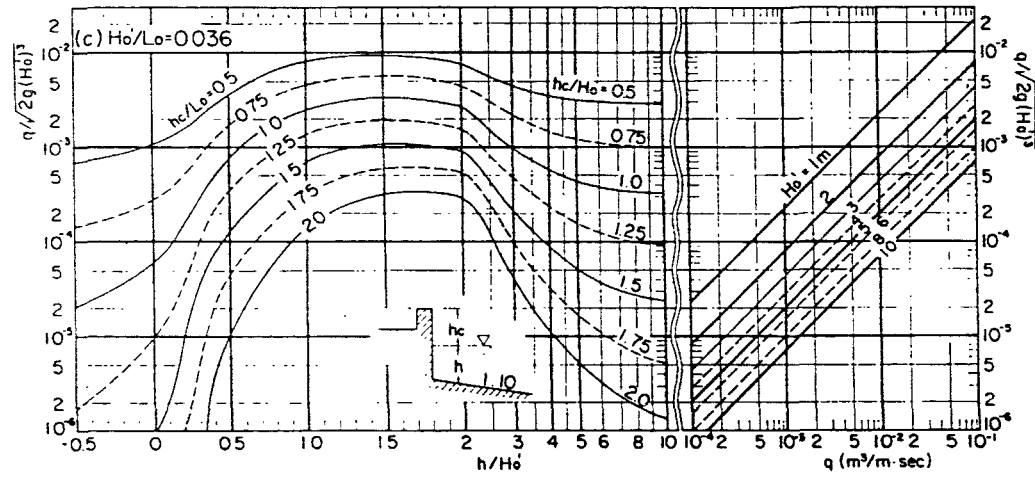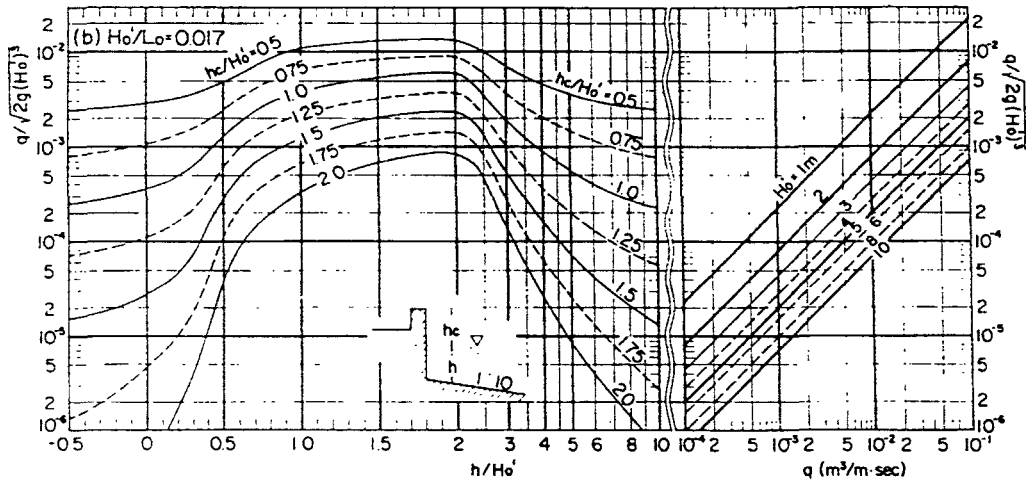**Annex 9.***Overtopping parameters* α *and* Q^*o *(recurved wall on a 1:10 nearshore slope)*
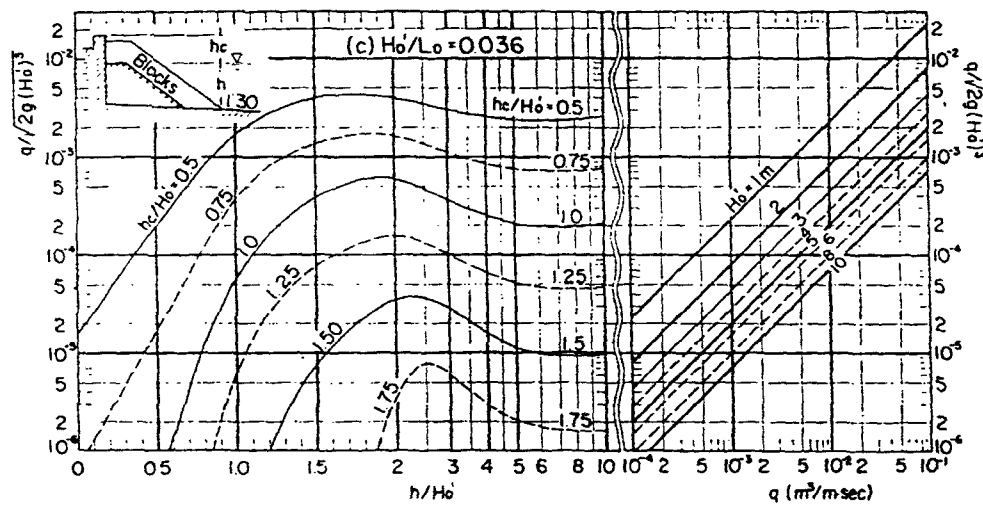
Annex 10. a Goda's graphs

Annex 10 d.

Annex 10.b
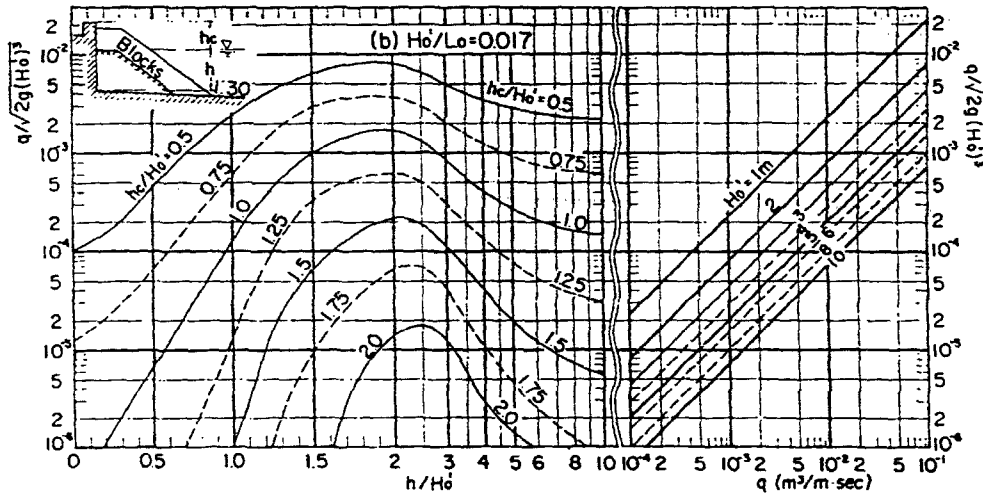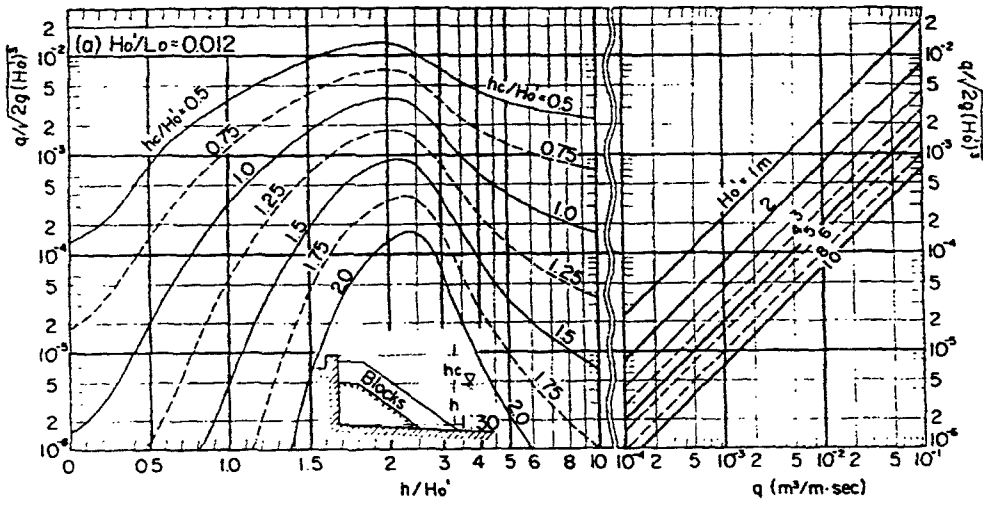

(a) $Ho'/Lo = 0.012$

(b) $Ho'/Lo = 0.017$

(c) $Ho'/Lo = 0.036$
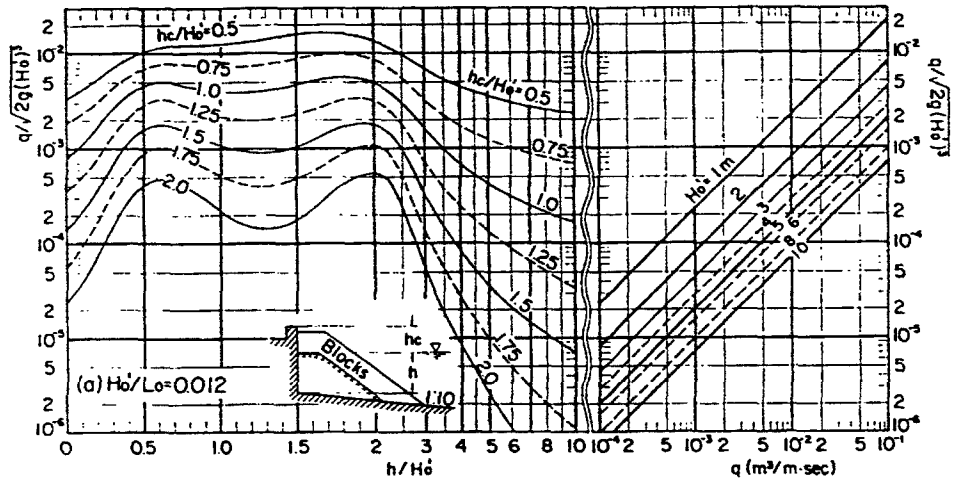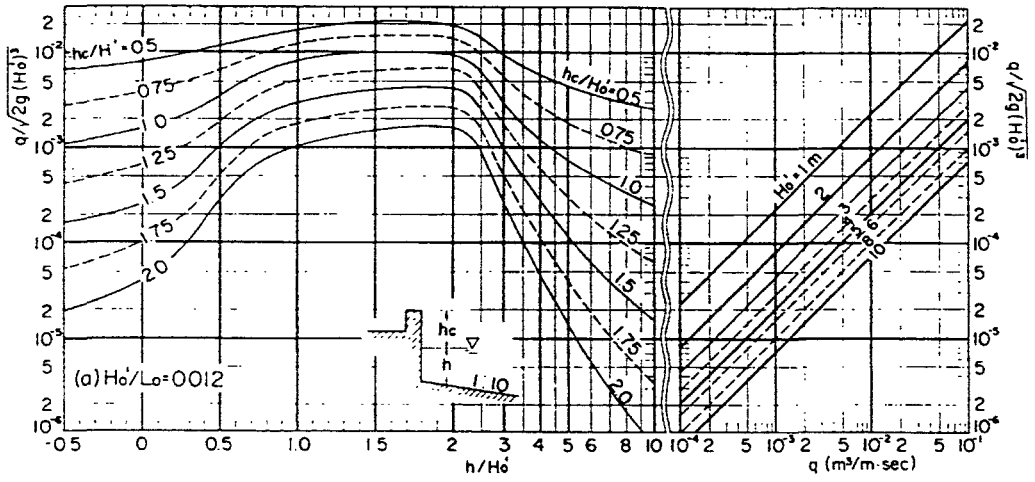
Annex 10.c

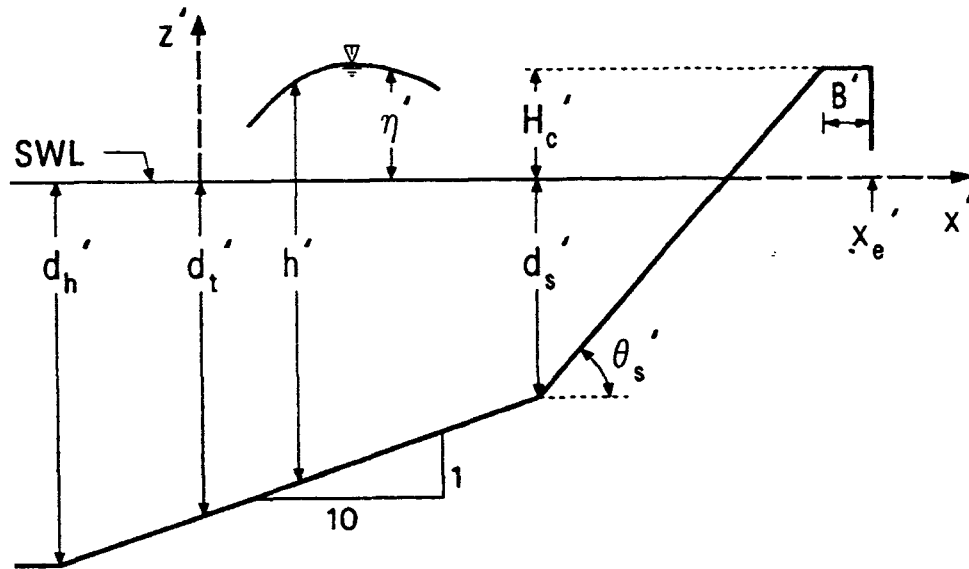## Annex 11. *Kobayashi mathematical model (/numerical model)*

Figure 3.24. Definition sketch for numerical model and comparison with data

The two-dimensional coordinate system (x', z') used in that paper is defined in figure 3.24 in which the prime indicates the physical variables. Fig 3.24 also shows the slope geometry for the tests of Saville (1955) with which the modified numerical model will later be compared. in the following, the problem is formulate in a general manner. the x' - coordinate is taken to be positive in the landward direction with x'=0 at the water depth d_t' below the stillwater level (SWL) where the incident train is specified as input. The z' - coordinate is taken to be positive upward with z'=0 at SWL. the water depth d_t' and the variation of the local slope angle θ' with respect to x' are used to specify any slope geometry in the computation domain $0 \le x' \le x_e$', where x_e' is the x' - coordinate of the landward edge of the slope which is assumed to be located above SWL.

In figure 3.24, tan θ' is equal to 0.1 in front of the structure and tan θ_e' on the structure slope while it is zero on the crest of the structure. assuming that the pressure is hydrostatic below the instantaneous free surface located at z' =η', Kobayashi et al. (1987) used the following equation for mass and x' - momentum integrated from the assumed impermeable bottom to the free surface.

$$\partial \frac{h'}{\partial t'} \quad \frac{\partial}{\partial x'}(h'u') \quad 0 \tag{3.76}$$

$$\frac{\partial}{\partial t'}(h'u') \quad \frac{\partial}{\partial x'}(h'u'^2) \quad g h' \frac{\partial \eta'}{\partial x'} \quad \frac{\tau'b}{\rho} \tag{3.77}$$

in which :

    t'   = time

    h'   = instantaneous water depth;

u'   = instantaneous depth-averaged horizontal velocity;

g   = gravitational acceleration;

η   = instantaneous free surface elevation above SWL;

τ'_b = bottom shear stress;

ρ   = fluid density, which is assumed constant.

The bottom shear stress is expected as:

$$\tau'_b \; \frac{1}{2} \rho f' u' u' \tag{3.78}$$

in which f' is the bottom friction factor which is assumed to be constant for given slope roughness characteristics neglecting the effect of viscosity.

Kobayashi and Watson (1987) compared the numerical model with the empirical formulas for wave run-up and reflection proposed by Ahrens and Martin (1985) and Seelig (1983), respectively. Their limited calibration indicated that f'=0.05 or less for small-scale smooth slopes, although the computed results were not very sensitive to the value of f'. consequently, f'=0.05 is used for the subsequent computation.

Denoting the characteristic wave period and height by T' and H'_0, respectively, the following dimensionless variables are introduced:

$$t \; \frac{t'}{T'}; \quad x \; \frac{x'}{T'\sqrt{gH'_0}}; \quad x_e \; \frac{x'_e}{T'\sqrt{gH'_0}}; \quad u \; \frac{u'}{\sqrt{gH'_0}}; \tag{3.79}$$

$$z \; \frac{z'}{H'_0}; \quad h \; \frac{h'}{H'_0}; \quad \eta \; \frac{\eta'}{H'_0}; \quad d_t \; \frac{d'_t}{H'_0}; \tag{3.81}$$

$$\sigma \; T' \sqrt{\frac{g}{H'_0}}; \quad \theta \; \sigma\tan \theta'; \quad f \; \frac{1}{2}\sigma f'; \tag{3.80}$$

in which:

σ   = dimensionless parameter related to wave steepness;

θ   = normalized gradient of the slope;

f   = normalized friction factor.

In terms of normalized coordinate system, the slope geometry in the computation domain is given by:

$$z \; \int_0^x \theta dx \; d_\rho \quad \text{for} \quad 0 \le x \le x_e \tag{3.82}$$

For normally incident monochromatic waves, the characteristic period and height used for the normalization are taken to be the period and height of the monochromatic wave. since the wave

height varies due to wave schooling, it is required to specify the location where the value of H'_0 is given. for a coastal structure located on the horizontal seabed, Kobayashi et al. (1987) used the wave height at the toe of the structure, which was tacked to be located at x=0, so that the normalized wave height at x=0 was unity. for the monochomatic wave overtopping tests of Saville (1955), the deep water wave height was given. As a result, the wave height H'_0 used for the normalization is taken to be the deep-water wave height in the following substitution of eq 3.82 into eq. 3.76 and 3.78 yields:

$$\frac{\partial h}{\partial t} \quad \frac{\partial m}{\partial x} \quad 0 \tag{3.83}$$

$$\frac{\partial m}{\partial t} \quad \frac{\partial}{\partial x}\left(m^2 h^{-1} \quad \frac{1}{2}h^2 \right) \quad \theta h \quad f|u|u \tag{3.84}$$

in which m=uh is the normalized volume flux per unit width. Eq. (3.83) and (3.84) expressed in the conservation-law form of the mass and momentum equations except for the two terms on the right hand side of eq (3.84) are solved numerically in the time domain using the explicit dissipative Lax-Wendroff finite difference method based on a finite-difference grid of constant space size Δx and constant time step Δt as explained by Kobayashi et al. (1987).

For the subsequent computation for smooth slope, the number of spatial grid points in the computation domain $0 \le x \le x_e$ is typically taken to be about 130. The number of time steps per wave period is taken to be on the order of 6000.

The initial time t=0 for the computation marching forward in time is taken to be the time when the specific incident wave train arrives at the seaward boundary located at x=0 and no wave action is present in the computation domain $0 \le x \le x_e$. In order to derive appropriate seaward and landward boundary conditions, Eq (3.84) and (3.85) are rewritten in terms of the characteristic

$$\frac{\partial \alpha}{\partial t} \quad (u \quad c)\frac{\partial \alpha}{\partial x} \quad \theta \quad \frac{f|u|u}{h}; \quad\quad dog \quad \frac{dx}{d} \quad u \quad c \tag{3.85}$$

$$\frac{\partial \beta}{\partial t} \quad (u \quad c)\frac{\partial \beta}{\partial x} \quad \theta \quad \frac{f|u|u}{h}; \quad\quad dog \quad \frac{dx}{d} \quad u \quad c \tag{3.86}$$

with:

$$c \quad \sqrt{h}; \quad \alpha \quad u \quad 2c; \quad \beta \quad u \quad 2c. \tag{3.87}$$

The seaward boundary is taken to be located seaward of the breakpoint so that the flow at x=0 is subcritical and satisfies the condition u,c at x=0, which is normally satisfied seaward of the breakpoint.

Then α and β represent the characteristics advancing landward and seaward, respectively, in the vicinity of the seaward boundary. Kobayashi et al. (1987) expressed the total water depth at the

seawater boundary in the form:

$$h \quad d_t \quad \eta_i(t) \quad \eta r(t); \quad a \quad x \quad 0 \tag{3.88}$$

in which η_i and η_r are the free surface variations at x-0 normalized by the deep-water wave height H'_0. It is convenient to introduce the following dimensionless parameters:

$$K_s \quad \frac{H'}{H'_0}; \quad L \quad \frac{L'}{d'_t}; \quad U_r \quad \frac{H'(L')^2}{(d'_t)^3} \quad \frac{K_s L^2}{d_t}; \tag{3.89}$$

in which:

K_s	= schooling coefficient at x=0;
H'	= wave height at x=0;
H'_0	= deep-water wave height used for the normalization;
L	= normalized wavelength at x=0;
L'	= wavelength at x=0;
d'_t	= water depth below SWL at x=0;
U_r	= ursell parameter at x=0.

The landward boundary on the structure is located at the moving waterline where the water depth is essentially zero unless wave overtopping occurs at the landward edge located at $x-x_e$. For the actual computation, the waterline is defined as the location where the normalized water depth h equals an infinitesimal value, δ, where $\delta = 10^{-3}$ is used on the basis of the previous computation for smooth slope (Kobayashi and Watson 1987). Wave overtopping is assumed to occur even the normalized water depth h at $x=x_e$ becomes greater than δ. The computation procedure for the case of wave overtopping at $x-x_e$ essentially follows the procedure used by Packwood (1980) to examine the effect of wave overtopping on the measured wave transformation in the surf zone on the gentle slope whose height was less than wave run-up. It is assumed that water flows over the landward edge freely since a different boundary condition is required for a vertical wall (Greenspan and Young 1978). The flow approaching the landward edge can be supercritical as well as subcritical since the associated water depth is relatively small.

An additional relationship required to find the values of u and h at $x=x_e$ is obtained from the value of α $(u \quad 2\sqrt{h})$ at $x=x_e$ computed using eq.(3.86) with f=0 which is approximated by a simple first-order finite difference equation. On the other hand, if $u>\sqrt{h}$ at the grid point next to the landward edge, the flow approaching the the landward edge is supercritical, and both characteristics α and β given by eq.(3.86) and (3.87) advance to the landward edge from the computation domain. Since eq.(3.86) and (3.87) are equivalent to eq (3.84) and (3.85), the values of u and h at $x=x_e$ are obtained directly from eq. (3.44) and (3.85) with f-0, which are approximated by simple first-order finite difference equations (Wurjanto 1988). If the value of h at $x=x_e$ becomes less that or equal to δ, the wave overtopping at $x=x_e$ is assumed to cease and the composition of the *waterline movement is resumed.*

Annex 12. Dutch Guidelines measurements and Goda's computed values for overtopping

no	D.G.	Goda
1	0.00503	0.004
2	0.001686	0.00154
3	0.0009307	0.001
4	0.0006047	0.00059
5	0.001307	0.0009
6	12/30	0.00036
7	0.001872	0.002
8	0.0004756	0.0005
9	0.0001586	0.000144
10	0.001158	0.000786
11	0.0007405	0.00026
12	0.000324	0.000162
13	0.00028	8.1E-05
14	0.00317	0.00158
15	0.00088	0.00062
16	0.000216	0.00032
17	12/30	0.0003
18	0.0002685	0.000142
19	0.00302	0.00187
20	0.00187	0.00097
21	0.00133	0.00104
22	0.000586	0.00036
23	0.000203	3.1E-05
24	0.000129	0.00021
25	0.00169	0.00073
26	0.000116	7.7E-05
27	0.000116	9.3E-05
28	0.000427	0.000204
29	0.000427	0.000433
30	0.000329	0.000215
31	0.000111	6.2E-05
32	0.000997	0.000663
33	0.000586	0.000509
34	0.00074	0.00039
35	0.000277	1.1E-05